2012

The functional morphology of the intermandibulo-cervical envelope of the American alligator (Alligator mississippiensis)

Brooke Hopkins Dubansky
Louisiana State University and Agricultural and Mechanical College, bhopki1@tigers.lsu.edu

Follow this and additional works at: https://digitalcommons.lsu.edu/gradschool_dissertations

THE FUNCTIONAL MORPHOLOGY OF THE
INTERMANDIBULO-CERVICAL ENVELOPE OF THE
AMERICAN ALLIGATOR (*ALLIGATOR MISSISSIPPIENSIS*)

A Dissertation

Submitted to the Graduate Faculty of the
Louisiana State University and
Agricultural and Mechanical College
in partial fulfillment of the
requirements for the degree of
Doctor of Philosophy

in

The Department of Biological Sciences

by
Brooke Hopkins Dubansky
B.Sc., Louisiana State University, 2004
May, 2012

Dedication

For my parents Jess and Kathy, and my sisters Ashley and Morgan.

This is the end-result of all of the time we've been apart.

For my husband Ben,

whose love and encouragement keeps me going.

For Michelle,

who has been sitting next to me for the last six and a half years.

Acknowledgments

I will always be grateful to my advisor Dr. Dominique G. Homberger for convincing me to get my Ph.D. in biology, and introducing me to new ways of thinking about anatomy, evolution and the process of science. Without her I would not be on the path I am on today.

I thank my current committee members Drs. Hermann H. Bragulla, Mark S. Hafner, Ryoichi Teruyama and John P. Hawke for all of their technical support, advice and critiques throughout my graduate program.

Dr. Ruth M. Elsey and Phillip "Scooter" Trosclair at Rockefeller Wildlife Refuge (Grand Chenier, LA) were instrumental in providing me with specimens for my research. I especially thank Dr. Elsey for her feedback and encouragement for my research presentations at various national conferences. Drs. Javier G. Nevarez, Daniel J. Hillmann, and Hermann H. Bragulla at the LSU School of Veterinary Medicine provided feedback and assistance for my IACUC protocol and procedures. Dr. Lorrie Gaschen and Mark Hunter acquired the CT data of the alligator specimen, and Drs. Jinghua Je and Leslie G. Butler taught me how to use the Avizo® 3D analysis software.

I am especially grateful to Dr. Fernando Galvez and his lab members Dr. Charlotte M. Bodinier, and Benjamin D. Dubansky, who provided advice, technical assistance, lab space, equipment, and materials for the histological aspects of my research. Dr. Ryoichi Teruyama provided advice and access to his equipment for the microscopic imaging of my histological slides. Dr. Matthew L. Brown and Ying Xiao of the Socolofsky Micrscopy Center at LSU provided assistance in preparing frozen sections, and Dr. Brown was a reliable source of advice on any subject that dealt with a camera, microscope, or imaging software.

Various faculty members at LSU have been a source of support and advice, and have influenced my research and teaching: Kathy S. Thompson, Dr. William B. Stickle, Dr. Miles E. Richardson, Dr. Daniel J. Hillmann, Dr. Kirsten Prüfer-Stone, Dr. Mark A. Mitchell, and Dr. William H. Worger.

Several members of the Homberger Lab helped me to prepare the materials for this dissertation. Elizabeth A. Cook provided invaluable expertise in scientific illustration. Michelle L. Osborn, Jonathan A. Bonin, Elise R. Orellana, Roy "Deuce" J. Andermann, Jr., and Bradley M. Wood graciously lent their assistance on various aspects of my research project and several oral and poster presentations. Amanda N. Cooper, Dominique A. Diggs, Elizabeth E. Cooper,

Table of Contents

List of Tables

List of Figures

Abstract

Alligators appear to swallow prey items that are large relative to their head size. Therefore, the intermandibulo-cervical envelope (i.e., the skin, *Fascia superficialis*, and constrictor musculature) was expected to be expandable. The three main layers of the intermandibulo-cervical envelope expand and recoil *in tandem*, but through different mechanisms. In the skin, which consists of hard-cornified scales and soft-cornified interscale skin segments, only the latter are expandable. Therefore, the width and orientation of the interscale skin segments determine the extent and direction of expansion of the skin. Whereas the intermandibular skin region is very expandable and enables the manipulation and crushing of large prey items in the mouth cavity, the gular and cervical skin regions can expand longitudinally, but have very limited circumferential expansibility. Elastic fibers in the dermis and *Fascia superficialis* provide the resilience needed to return the skin to its resting condition. The trilaminate *Fascia superficialis* expands by changing the orientation of its helically arranged collagen fibers. The three main skin regions, which are also characterized by particular scale and interscale skin patterns, are in congruence with the three parts of the underlying constrictor musculature. The expansibility of the constrictor muscles is determined by their proportion of muscle length to tendon length, because muscle fibers can lengthen passively, whereas collagenous tendon fibers resist lengthening. The expansibility of the constrictor muscles diminishes from rostral to caudal. Whereas the longitudinal expansibility of the intermandibulo-cervical envelope allows lateral and dorso-ventral movements of the head and neck, the limited circumferential expansibility of the gular and cervical regions constrains the size of prey items that can pass through the throat and matches the narrow isthmus of the thoracic inlet. Hence, the functional-morphological data of the intermandibulo-cervical envelope require a reinterpretation of feeding mechanics and prey choice of alligators.

Chapter 1
Introduction: Reptile Skin

1.1. General Morphology and Histology of the Reptilian Integument

1.1.1. Epidermis

The reptilian epidermis is composed of tough, non-compressible and non-stretchable scales with limited flexibility, which are separated by soft, pliable interscale skin (Mercer 1961; Maderson 1964; Spearman 1973; von Düring & Miller 1979; Banerjee & Mittal 1980; Lillywhite & Maderson 1982; Landmann 1986; Alibardi 2003; Alibardi *et al.* 2007). The scales provide mechanical protection against abrasion, while the interscale skin allows passive movement of the scales relative to one another during locomotion and feeding, and to accommodate the movement of underlying structures, such as bulging muscles or moving skeletal elements (Mercer 1961; Gans 1974; Spearman 1973; Banerjee & Mittal 1980; Maderson & Alibardi 2000; Alibardi *et al.* 2007; Homberger & de Silva 2000). Hence, different mechanical demands on different parts of the body are correlated with regional variants of scale patterns (Maderson 1984; Alibardi & Thompson 2000; Maderson & Alibardi 2000; Homberger & de Silva 2003; Dubansky & Homberger see Chapter 2), although some authors attribute varying scale sizes and patterns to environmental factors (Spearman 1973; Regal 1975; Lillywhite & Maderson 1982). Scale patterns have also been used for taxonomic purposes, especially of squamates i.e., lizards and snakes (Lange 1931; Maderson, 1964; Soulé & Kerfoot 1972; Spearman 1973; Landmann 1986; Jayne 1988; Arnold *et al.* 2002); crocodilians (Brazaitis 1987; Richardson *et al.* 2002); and dinosaurs and other fossil reptiles (Arnold *et al.* 2002; Kim 2010). Reptilian scales are either imbricating or non-imbricating (von Geldern 1921; Maderson 1964, 1984; Spearman 1966, 1973; Soulé & Kerfoot 1972; Regal 1975; Banerjee & Mittal 1980; Lillywhite & Maderson 1982; Landmann 1986; Alibardi & Thompson 2000; Homberger & de Silva 2000; Maderson & Alibardi 2000; Alibardi 2004; Coria & Chiappe 2007), although Dubansky & Homberger (see Chapter 2) identified a third scale configuration in crocodilians, namely overlapping.

- **Imbricating Scales**

Many squamates have imbricating scales, in which the cranial edge of one scale is overlapped by the free projecting edge of the more cranial scale. The caudally projecting edge of a scale has an external surface as well as an internal surface that faces the caudally adjacent interscale skin segment and scale (Maderson 1964, 1985; Spearman 1966, 1973; Sengel 1976; Banerjee & Mittal 1980; Lillywhite & Maderson 1982; Landmann 1986).

2

The scaly skin can be moved passively relative to the underlying body through the stretching of the interscale skin between them, and it returns to its resting position through the resilience of the underlying dermal and subcutaneous connective tissue (Hoffmann 1890; Lange 1931; Maderson & Alibardi 2000) or by dermal or cutaneous muscles (Lange 1931; Lissmann 1950; Gans 1974; Jayne 1988). Squamates with dermal or cutaneous muscles can move their skin actively, as has been observed in snakes during rectilinear locomotion (Lissmann 1950; Gans 1974; Jayne 1988).

- **Non-imbricating Scales**

Some squamates i.e., geckos and chameleons (Maderson 1964; Coria *et al.* 2007); the black tegu (Lillywhite & Maderson 1982); and helodermatids (Coria *et al.* 2007); and members of the Crocodylia and Chelonia, also have non-imbricating scales (Alibardi & Thompson 2000; Richardson *et al.* 2002). Non-imbricating scales can be either flat and plate-like or raised and tuberculate. Among the non-imbricating scales of reptiles, only the ones of Crocodylia have been positively identified as not associated with dermal muscles (Homberger & de Silva 2000; see Chapter 2.). In crocodilians, displaced scales are returned to their resting position solely by the resilience and elasticity of their underlying dermal and subcutaneous tissues (see Chapter 2).

- **Overlapping Scales of Crocodilians**

According to Alibardi & Thompson (2000), the scales in the ventral gular and cervical regions of the skin of alligators appear to be imbricated, similar to the condition in squamates. However, the overlapping scales of crocodilians differ from truly imbricating scales, in that they are flat and have no projecting edge; instead, the interscale skin and underlying dermis are folded in such a way that the caudal edge of the cranial scale is slightly pushed over the cranial edge of the caudal scale. Like the non-overlapping scales of crocodilians, the overlapping scales are not associated with dermal musculature, and return to their resting position after displacement by the resilience of the elastic fiber networks located in the dermis and superficial fascia (Homberger & de Silva 2000; see Chapter 2).

- **Epidermal Glands and Skin Appendages**

   Unlike mammalian and amphibian integument, the reptilian integument is mostly devoid of epidermal glands, except for a few localized glands, such as the gular musk glands and dorsal integumentary glands in crocodilians (Bell 1827; Reese 1915; von Eggeling 1931; Spearman 1973; Dunker 1982; Park 2002) and the femoral glands in some lizards (von Eggeling 1931; Spearman 1973; Dunker 1982; Alberts 1990). Most glandular secretions in reptiles have been considered to have a pheromonal function (von Eggeling 1931; Dunker 1982). The slitlike orifices of the gular glands in crocodilians open into a longitudinal folds of the interscale skin along the mandible, and the expansion and compression of the skin in this region massages the lipid-rich secretion along the interscale folds and conditions the expandable interscale skin segments (Dubansky & Homberger, see Chapter 2). The reptilian integument lacks appendages, such as hair or feathers, but reptiles have hard-cornified claws and some reptiles (e.g. some geckos) have subdigital lamellae used for climbing (Spearman 1966; Maderson & Alibardi 2000).

- **General Histology and Biochemistry**

   The reptilian epidermis is a stratified keratinized and cornified epithelium. The basal layer of the epidermis contains stem cells, which divide. As the epidermal cells differentiate, they are pushed toward the surface by the dividing cells of the deeper layers. The epidermis of reptiles synthesizes two types of keratin, namely alpha-keratin and beta-keratin (Mercer 1961; Spearman 1966; von Düring & Miller 1979; Landmann 1986; Alibardi & Thompson 2000; Richardson *et al.* 2002; Sawyer & Knapp 2003; Alibardi *et al.* 2007; Bragulla & Homberger 2009). The secondary structure of beta-keratins is a beta-sheet, while that of alpha-keratins is an alpha-helix (Spearman 1966; Landmann 1986; Sawyer & Knapp 2003; Bragulla & Homberger 2009). Most reptilian scales are rigid, non-compressible, and non-stretchable, because they are composed mostly of beta-keratins, and the interscale epidermis is composed mostly of alpha-keratins, which are soft and pliable (Mercer 1961; von Düring & Miller 1979; Alibardi & Thompson 2000; Alibardi 2003; Alibardi *et al.* 2007).

   Alpha-keratins in reptiles are associated with soft-cornified interscale skin segments. Alpha-keratins are found in the stratified epithelia of all vertebrates (Bragulla & Homberger 2009). In both birds and reptiles, the flexible alpha-keratinzed portions of the integument are

4

associated with intra- and intercellular lipids, which help to maintain the water barrier (Lucas & Stettenheim 1972; Matoltsy & Huszar 1972; Menon & Menon 2000; Stettenheim 2000; Alibardi & Thompson 2001), and keep it conditioned (Stettenheim 2000; see Chapter 2).

Beta-keratins in reptiles and birds are associated with hard-cornified structures such as scales, claws and feathers (Spearman 1966; Sawyer & Knapp 2003; Alibardi *et al.* 2007; Bragulla & Homberger 2009; Ye *et al.* 2010). There are different types of beta-keratins and the types and combinations expressed vary in different species, in different tissues within an individual, and even within the same tissue of an individual, depending on the mechanical role of the specific tissue (Spearman 1966; Sawyer & Knapp 2003; Alibard *et al.* 2007). In light of this observation, Sawyer & Knapp (2003) suggest that beta-keratins might have evolved from a gene that coded for both alpha- and beta-keratin proteins. This is further supported by the fact that alpha-keratin filaments can convert to beta-pleated sheets in response to certain mechanical forces, such as stretching (Bragulla & Homberger 2009) and steam treatment (Spearman 1966). Indeed, hard-cornified and beta-keratinized structures are found where resistance to mechanical abrasion is required (e.g., scales).

> Squamates and *Sphenodon*

The distribution of alpha- and beta-keratin varies among different reptilian orders. Squamates and *Sphenodon* have a vertical keratin layering, in which the epidermis synthesizes a deep layer of alpha-keratin and a superficial layer of beta-keratin (Spearman 1966, 1973; Baden & Maderson 1970; Parakkal & Alexander 1972; Lillywhite & Maderson 1982; Landmann 1986; Alibardi 2003; Alibardi *et al.* 2007). Nevertheless, the amount of beta-keratins varies between the scales and interscale skin segments, and the interscale skin synthesizes mostly alpha-keratins, resulting in flexibility and protection against excessive water loss (Baden & Maderson 1970; Spearman 1973; Banerjee & Mittal 1980; Landmann 1986). The vertical layering of alpha- and beta-keratin is a key aspect of the shedding mechanism characteristic of lepidosaurs (Spearman 1966; Parakkal & Alexander 1972; Banerjee & Mittal 1980; Lillywhite & Maderson 1982; Maderson 1984; Maderson & Alibardi 2000; Alibardi 2003), which is based on a chronological alternation of alpha- and beta-keratinization and creates histologically distinct layers that differ from the epidermal layers in other vertebrates (Spearman 1966, 1973; Baden & Maderson 1970; Parakkal & Alexander 1972; Banerjee & Mittal 1980; Maderson 1984; Maderson & Alibardi 2000).

> Crocodilians and Turtles

It is has been assumed that the epidermis of Crocodilians and Chelonians has a horizontal keratin distribution, in which the scale epidermis contains hard-cornifying beta-keratins and the epidermis of the interscale skin segments contains soft-cornifying alpha-keratins without any overlap or transition between the two epidermal and keratin types (Spearman 1966; Baden & Maderson 1970; Lillywhite & Maderson 1982; Landmann 1986; Richardson *et al.* 2002; Alibardi 2003). However, more recent studies of the crocodilian epidermis describe a condition in which the basal and suprabasal cells of the hard-cornified scale epidermis produce alpha-keratins, whereas the upper pre-corneous and corneous cells produce beta-keratins (Alibardi & Toni 2007; Alibardi *et al.* 2007). This means that the entire epidermis (scales and interscale portions) produces alpha-keratins in its deeper layers, whereas beta-keratin synthesis is restricted to the upper layers of the epidermis of the hard-cornified scales. These newer findings cast some doubt on past studies (Baden & Maderson 1970; Maderson 1985; Landmann 1986) that drew conclusions about archosaurian relationships based on the supposed horizontal distribution of the alpha- and beta-keratins in the epidermis of birds and crocodilians.

1.1.2. Dermis

- **Morphology and Histology of the Dermis of Reptiles**

The reptilian dermis is divided into a superficial *Stratum laxum*, which is composed of loosely arranged thin collagen fiber bundles with many capillaries, and a deep *Stratum compactum*, which is composed of densely packed thick collagen fiber bundles that are often highly organized (Krause 1921; Lange 1931; Maderson 1964; Moss 1972; von Düring & Miller 1979; Jayne 1988; Landmann 1986; Maderson & Alibardi 2000; Richardson *et al.* 2002; Vickaryous & Hall 2008). Both strata contain elastic fibers that are responsible for returning the integument to its resting position after being stretched (Krause 1921; Lange 1931; Moss 1972; see Chapter 2). The thickness of the *Stratum compactum*, as well as the organization of its collagen fibers and its anchoring to underlying subcutaneous structures varies regionally within an individual, depending on the local mechanical demands on specific body regions (Moss 1972; Jayne 1988; see Chapter 2).

Krause (1921) and Alibardi and Thompson (2000) describe differences in the arrangement of collagen fibers under the scale and interscale epidermis of snakes and alligators. In these

reptiles, the dermis that supports the scale epidermis is loose and becomes dense with highly organized fibers under the interscale epidermis. Whereas Krause (1921) does not offer a functional explanation for these differences in the dermis, Alibardi (1994) and Alibardi and Thompson (2000) hypothesize that some fiber bundles form anchoring complexes, perhaps similar to the anchoring complexes of hair and feather follicles, which pull on the scale edges and contribute to the final shape of the scale after development is completed. However, it is more likely that the arrangement of collagen fiber bundles in the dermis is already initiated at the earliest stages of embryonic development (Homberger & de Silva 2003) and are involved in the proper folding of the interscale skin as the developing embryo starts to move and thereby generates a force regime that determines the arrangement of connective tissue fibers. Alibardi and Thompson (2000) also claim that the different scale types are histologically uniform, but this is unlikely given the fact that the collagen fibers of the dermis form an integral part of the stretch and return mechanism (see Chapter 2). An elastic membrane is known to be present in the dermis of some snakes (Lange 1931, Close & Cundall 2012), lizards (Lange 1931; personal observations), and birds (Lange 1931; Homberger & de Silva 2000; Homberger 2002; Orellana *et al.* 2012)

- **Osteoderms**

Osteoderms (i.e., bony plates found in the dermis under some scales), are found in *Sphenodon* and some squamates, as well as in all members of the Crocodylia. They are formed by the direct ossification of connective tissue (Maderson 1964; Moss 1972; Spearman 1973; Seidel 1979; Landmann 1986; Vickaryous 2008). The functional significance of osteoderms is still unclear (Seidel 1972; Richardson *et al.* 2002). Some of the hypothesized functions of the osteoderms in crocodilians include thermoregulation, mineral storage, protection from predators, and attachment sites for constrictor muscles (Seidel 1979; Richardson *et al.* 2002). The latter explanation is the most compelling, as cervical and gular constrictor muscles and the superficial fascia are anchored to the osteoderms in the alligator, except just behind the head where osteoderms are absent presumably to allow movement of the head and where, as a consequence, the *Fascia superficialis* and constrictor musculature attach to the cervical vertebrae (see Chapter 3).

7

1.2. References

Alberts, A. 1990. Chemical properties of femoral gland secretions in the desert iguana, *Dipsosaurus dorsalis*. Journal of Chemical Ecology 16(1): 13-25.

Alibardi, L. 1994. Modifications of the dermis during scale regeneration in the lizard tail. Histology & Histopathology 9: 733-745.

Alibardi, L. & Thompson, M.B. 2000. Scale morphogenesis and ulstrastructure of the dermis during embryonic development in the alligator (*Alligator mississippiensis*, Crocodilia, Reptilia). Acta Zoological (Stockholm) 81: 325-338.

Alibardi, L. & Thompson, M.B. 2001. Fine structure of the developing epidermis in the embryo of the American alligator (*Alligator mississippiensis*, Crocodilia, Reptilia). Journal of Anatomy 198: 265-282.

Alibardi, L. 2003. Adaptation to the land: The skin of reptiles in comparison to that of amphibians and endotherm amniotes. Journal of Experimental Zoology (Mol Dev Evol) 298B: 12-41.

Alibardi, L. 2004. Dermo-epidermal interactions in reptilian scales: Speculations on the evolution of scales, feathers, and hairs. Journal of Experimental Zoology (Mol Dev Evol) 302B: 365-383.

Alibardi, L. & Toni, M. 2007. Characterization of keratins and associated proteins involved in the corneification of crocodilian epidermis. Tissue & Cell 39: 311-323.

Alibardi, L. Toni, M. & Dalla Valle, L. 2007. Hard cornification in reptilian epidermis in comparison to cornification in mammalian epidermis. Experimental Dermatology 16: 961-976.

Arnold, E.N., Azar, D., Ineich, I. & Nel, A. 2002. The oldest reptile in amber: A 120 million year old lizard from Lebanon. Journal of Zoology, London 258: 7-10.

Baden, H.P. & Maderson, P.F.A. 1970. Morphological and biophysical identification of fibrous proteins in the amniote epidermis. Journal of Experimental Zoology 174: 225-232.

Banerjee, T.K. & Mittal, A.K. 1980. Histochemistry of snake epidermis. Pp. 23-34 *in* The Skin of Vertebrates (Spearman, R.I.C. & Riley, P.I., eds.). Academic Press, London.

Bell, T. 1827. On the structure and use of the submaxillary odoriferous gland in the genus *Crocodilus*. Philosophical Transactions of the Royal Society of London 117(1): 132-139.

Bragulla, H.H. & Homberger, D.G. 2009. Structure and functions of keratin proteins in simple, stratified, keratinized and cornified epithelia. Journal of Anatomy 214: 516-559.

Brazaitis, P. 1987. The identification of crocodilian skins and products. Pp. 373-386 *in* Wildlife Management: Crocodiles and Alligators (Web, G.J.W., Manolis, S.C. & Whitehead, P.J., eds). Surrey Beatty & Sons Pty, Chipping Norton, New South Wales.

Caldwell, M.W. & Dal Sasso, C. 2004. Soft-tissue preservation in a 95 million year old marine lizard: Form, function, and aquatic adaptation. Journal of Vertebrate Paleontology 24(4): 980-985.

Close, M. and Cundall, D. Extensible tissues and their contribution to macrostomy in snakes. Integrative and Comparative Biology abstract 89.1

Coria, R.A. & Chiappe, L.M. 2007. Embryonic skin from late Cretaceous sauropods (Dinosauria) of Auca Mahuevo, Patagonia, Argentina. Journal of Paleontology 81(6): 1528-1532.

Evans, S.E. & Wang, Y. 2007. A juvenile lizard specimen with well-preserved skin impressions from the Upper Jurassic/Lower Cretaceous of Daohugou, Inner Mongolia, China. Naturwissenschaften 94: 431-439.

Evans, S.E. & Wang, Y. 2010. A new lizard (Reptilia: Squamta) with exquisite preservation of soft tissue from the Lower Cretaceous of Inner Mongolia, China. Journal of Systematic Palaeontology 8(1): 81-95.

Frolich, L.M. 1997. The role of the skin in the origin of amniotes: Permeability barrier, protective covering and mechanical support. Pp. 327-352 *in*: Amniote Origins: Completing the Transition to Land (Sumida, S.S. & Martin, K.L.M., eds.). Academic Press, San Diego.

Gans, C. 1962. Terrestrial locomotion without limbs. American Zoologist 2: 167-182.

Gans, C. 1974. Biomechanics: An Approach to Vertebrate Biology. The University of Michigan Press, Ann Arbor. Pp. 22-71.

Hoffmann, C.K. 1890. Schlangen. I. Integument. Pp. 1401-1420 *in* Klassen und Ordnungen des Thier-Reichs wissenschaftlich dargestellt in Wort und Bild, Band 6, Abhteilung 3 (Bronn, H.G., ed). C.F. Winter'sche Verlagshandlung, Leipzig.

Homberger, D.G. & de Silva, K.N. 2000. Functional microanatomy of the feather-bearing integument: Implications for the evolution of birds and avian flight. American Zoologist 40: 553-574.

Homberger, D.G. & de Silva, K.N. 2003. The role of mechanical forces on the patterning of the avian feather-bearing skin: A biomechanical analysis of the integumentary musculature in birds. Journal of Experimental Zoology (Mol Dev Evol) 298B: 123-139.

Jayne, B.C. 1988. Mechanical behavior of snake skin. Journal of Zoology, London 214: 125-140.

Kim, J.Y, Kim, k.S., Lockley, M.G. & Seo, S.J. 2010. Dinosaur skin impressions from the Cretaceous of Korea: New insights into modes of preservation. Palaeoecology 293: 167-174.

Krause, R. 1921. Mikroskopische Anatomie der Wirbeltiere in Einzeldarstellungen. II. Vögel und Reptilien. Walter de Gruyter & Co., Berlin & Leipzig, Pp. 319-323.

Landmann, L. 1986. Epidermis and Dermis. Ch.9 *in* Biology of the Integument, Vol. 2J. (Bereiter-Hahn, J., Matoltsy, A.G. & Richards, K.S., eds.). Springer Verlag, Berlin.

Lange, B. 1931. Integument der Sauropsiden. Pp. 375-448 *in* Handbuch der vergleichenden Anatomie der Wirbeltiere, Band 1 (Bolk, L., Göppert, E., Kallius, E. & Lubosch, W., eds.). Urban & Schwarzenberg, Berlin.

Lillywhite, H.B. & Maderson, P.F.A. 1977. Histological changes in the epidermis of the subdigital lamellae of *Anolis carolinensis* during the shedding cycle. Journal of Morphology 125: 379-402.

Lillywhite, H.B. & Maderson, P.F.A. 1982. Skin structure and permeability. Pp. 397-442 *in* Biology of the Reptilia, Vol. 12, Physiology C, Physiological Ecology (Gans, C. & Pough, F.H., eds.). Academic Press, London.

Lissmann, H.W. 1950. Rectilinear locomotion in a snake. Journal of Experimental Biology 26: 368-379.

Lucas, A.M. & Stettenheim, P.R. 1972. Avian anatomy: Integument. Part II. Agricultural Handbook 362. United States Department of Agriculture, Washington, D.C.

Maderson, P.F.A. 1964. The skin of lizards and snakes. British Journal of Herpetology 3(6): 151-154.

Maderson, P.F.A. 1968. Observations on the epidermis of the tuatara (*Sphenodon punctatus*). Journal of Anatomy 103(2): 311-320.

Maderson, P.F.A. 1984. The squamate epidermis: A new light has been shed. Pp. 111-124 *in* The structure, Development, and Evolution of Reptiles (Ferguson, M.W., ed.). Academic Press, London.

Maderson, P.F.A. 1985. Some developmental problems of the reptilian integument. Pp. 523-598 *in* Biology of the Reptilia, Vol. 14, Development A. (Gans, C., ed.). John Wiley & sons, New York.

Maderson, P.F.A. & Alibardi, L. 2000. The development of the Sauropsid integument: A contribution to the problem of the origin and evolution of feathers. American Zoologist 40: 513-529.

Matoltsy, A.G. & Huszar, T. 1972. Keratinization of the reptilian epidermis: An ultrastructural study of the turtle skin. Ultrastructure Research 38: 87-101.

Menon, G.K. & Menon, J. 2000. Avian epidermal lipids: Functional considerations and relationship to feathering. American Zoologist 40:540-552.

Mercer, E.H. 1961. Keratin and Keratinization. Pergamon Press, New York.

Moss, M.L. 1972. The vertebrate dermis and the integumental skeleton. American Zoologist 12: 27-34.

Parakkal, P.F. & Alexander, N.J. 1972. Keratinization: A Survey of Vertebrate Epithelia. Academic Press, New York, Ch.4.

Park, J-Y. 2002. Integumentary Glands. Pp. 38-39 *in* Crocodiles: Inside Out. A Guide to the Crocodilians and their Functional Morphology (Richardson,K.C., Webb, G.J.W. & Manolis, S.C., eds.). Surrey Beatty & Sons, Chipping Norton.

Reese, A.M. 1915. The Alligators and its Allies. G.P. Putnam's Sons, New York.

Regal, P.J. 1975. The evolutionary origin of feathers. The Quarterly Review of Biology 50(1): 35-66.

Richardson, K.C., Webb, G.J.W., & Manolis, S.C. 2002. Crocodiles: Inside Out. A Guide to the Crocodilians and their Functional Morphology. Surrey Beatty & Sons, Chipping Norton.

Sawyer, R.H. & Knapp, L.W. 2003. Avian skin development and the evolutionary origin of feathers. Journal of Experimental Zoology (Mol Dev Evol) 298B: 57-72.

Schmidt, W.J. 1914. Studien am Integument der Reptilien VI. Über die Knochenschuppen der Crocodile. Zoologische Jahrbücher Abteilung für Anatomie und Ontogenie der Tiere 38: 643-672.

Seidel, M.R. 1979. The osteoderms of the American Alligator and their functional significance. Herpetologica 35(4): 375-380.

Sengel, P. 1976. Morphogenesis of Skin. Cambridge University Press, London. Pp. 54-57.

Soulé, M. & Kerfoot, W.C. 1972. On the climatic determination of scale size in a lizard. Systematic Zoology 21(1): 97-105.

Spearman, R.I.C. 1966. The keratinization of epidermal scales, feathers, and hairs. Biological Review 41: 59-96.

Spearman, R.I.C. 1973. The skin of reptiles. Pp. 83-90 *In* The Integument: A Textbook of Skin Biology. Cambridge University Press, London.

Soulé, M. & Kerfoot, W.C. 1972. On the climatic determination of scale size in a lizard. Systematic Zoology 21(1): 97-105.

Stettenheim, P.R. 2000. The integumentary morphology of modern birds—An overview. American Zoologist 40: 461-477.

Vickaryous, M.K. & Hall, B.K. 2008. Development of the dermal skeleton in *Alligator mississippiensis* (Archosauria, Crocodylia) with comments on the homology of osteoderms. Journal of Morphology 269: 398-422.

von Düring, M. & Miller, M.R. 1979. Sensory nerve endings of the skin and deeper structures of reptiles. Pp. 407-441 *in* Biology of the Reptilia, Vol. 9, Neurobiology A. (Gans, C., ed.). Academic Press, London.

von Eggeling, V. 1931. Hautdrüsen. Pp. 633-692 *in* Handbuch der vergleichenden Anatomie der Wirbeltiere, Band 1 (Bolk, L., Göppert, E., Kallius, E. & Lubosch, W., eds). Urban & Schwarzenberg, Berlin.

von Geldern, Charles E. 1921. Color changes and structure of the skin of *Anolis carolinensis*. Proceedings of the California Academy of Sciences, 4th Series 10 (10): 77-117.

Ye, C., Wu, X., Yan, P., Amato, G. 2010. Beta-keratins in crocodiles reveal amino acid homology with avian keratins. Molecular Biology Report 37: 1169-1174.

Chapter 2

The Intermandibulo-cervical Integument of the American Alligator (*Alligator mississippiensis*)

2.1. Introduction

Reptiles and birds use either cranio-inertial or lingual feeding to transport a food item through the oral cavity and into the pharynx to be swallowed. Lingual feeding requires a fleshy, mobile tongue with a papillose friction surface, and sometimes glands that increase adherence of the food bolus to the tongue (Schwenk 2000). The movements of the tongue are coupled with movements of the hyolaryngeal apparatus, and the food is moved from the anterior part of the oral cavity backwards to the pharynx as the hyolingual apparatus is protracted and retracted (Schwenk 2000). This feeding behavior is seen in all squamates and birds that swallow relatively small food items (Zweers 1982; Homberger 1999; Schwenk 2000).

In order to transport a large food item with the tongue, its surface area would also have to increase proportionately for the food item to adhere to its surface; however, a large tongue would obstruct the entrance into the pharynx (Cleuren & De Vree 2000). Some reptiles and birds with diets consisting of both small and large food items [e.g. pigeons (*Columba livia*) and tegus (*Tupinambis* spp.)] solve this conundrum by switching to cranio-inertial feeding (Zweers 1982; Elias *et al.* 2000; Reilly *et al.* 2001; Metzger & Herrel 2004; Montuelle *et al.* 2009), in which the large food item is tossed into the air and falls into the open mouth and pharynx by gravity and concurrent forward movements of the head and neck (Gans 1969; Zweers 1982; Smith 1986; Busbey 1989; Cleuren & De Vree 1992, 2000; De Vree & Gans 1994; Elias *et al.* 2000; Schwenk 2000; Reilly *et al.* 2001; Metzger & Herrel 2004; Montuelle *et al.* 2009).

The Komodo dragon (*Varanus komodoensis*) is the only obligate cranio-inertial feeder among squamates (Smith 1985, 1986; Schwenk 2000). Its tongue is highly mobile, yet reduced in width throughout its length (i.e., surface area-to-volume) as a specialization for chemoreception and, therefore, cannot be used to move food items through the oral cavity into the pharynx and esophagus (Smith 1985, 1986; Schwenk 2000). Several authors have shown that this feeding behavior in Komodo dragons, who are large prey specialists, is associated with the large size of the prey (Smith 1986; Pianka 1995; Elias *et al.* 2000; Montuelle *et al*. 2009).

Herons and egrets (Ardeidae) are also obligate cranio-inertial feeders and often swallow enormous prey items (Cummins 1986; Cummins & Homberger 1986; Homberger 1999; Reilly *et al.* 2001; Westneat 2007; Montuelle *et al*. 2009), whose passing through the oral cavity, pharynx, and esophagus is facilitated by the expandable skin of the floor of their mouths, gullet, and neck,

14

respectively; long-fibered constrictor muscles; and a hyoid skeleton that is built into the connective tissue of the throat (Cummins 1986; Cummins & Homberger 1986).

Like ardeid birds, Crocodilians are also obligate cranio-inertial feeders and are said to have the capacity to swallow relatively large prey items whole (Diefenbach 1975; Neill 1975; Cleuren & De Vree 1992, 2000; Grigg & Gans 1993; Bonner 2010), but the functional morphology of the skin and subcutaneous structures of their throat and neck to accommodate the required expansion have not yet been analyzed, as it has in ardeid birds (Cummins 1986; Cummins & Homberger 1986. This lack of information precludes a meaningful comparison and evolutionary interpretation of the cervical envelope of birds and reptiles that manage to swallow large prey items whole.

The reptilian epidermis in general is composed of tough, non-compressible and non-stretchable scales, which are separated by soft, pliable interscale skin (Mercer 1961; Maderson 1964; Spearman 1973; Gans 1974; Banerjee & Mittal 1980; Lillywhite & Maderson 1982; Landmann 1986; Cundall & Greene 2000; Alibardi 2003; Alibardi *et al.* 2007). The scales provide mechanical protection against abrasion, while the pliable interscale skin allows the scales to be moved passively relative to one another, thereby enabling the skin to stretch during movements of the body and to accommodate the movements of underlying structures, such as bulging muscles and moving skeletal elements (Mercer 1961; Spearman 1973; Banerjee & Mittal 1980; Maderson & Alibardi 2000; Alibardi *et al.* 2007; Homberger & de Silva 2000). Hence, different mechanical demands on different parts of the body are correlated with regional variants of scale patterns (Gans 1974; Maderson 1984; Alibardi & Thompson 2000; Maderson & Alibardi 2000; Homberger & de Silva 2003).

This study investigates the regional variation in scale and interscale skin patterns as it relates to variations in the micro-architecture of the dermis and subcutaneous layers of the intermandibulo-cervical envelope, and how these regional morphological differences are adjusted to the overall structural system that allow expansion for the swallowing of prey items that are large relative to the size of the head and neck. This data will contribute to a better understanding of the structural and functional interplay between the head and neck during feeding.

2.2. Materials and Methods

2.2.1. Materials

Three alligator specimens (DGH-AL-019, DGH-AL-021, and DGH-AL-024; see Table 2.1) were obtained from Rockefeller Wildlife Refuge (Grand Chenier, Louisiana) and euthanized by injection of a Beuthanasia-D solution (1.5 ml/kg) into the supravertebral sinus under an Institutional Animal Care and Use Committee (IACUC) protocol (#08-105) granted by the Division of Laboratory Animal Medicine at the School of Veterinary Medicine, Louisiana State University, Baton Rouge. These specimens were fixed by perfusion with a 4% buffered formaldehyde solution through the right aorta, as well as by injection of formaldehyde directly into the subcutaneous tissues.

Table 2.1: Alligator Specimens and Techniques used to Analyze the Functional Morphology of the Intermandibulo-cervical Envelope

Specimen ID	Snout-to-Tail Length	Sex	Wild or Farmed at Rockefeller Wildlife Refuge	Techniques	IACUC Protocols and Wildlife Permits
DGH-AL-002	101.60 cm	Female	Farm-raised	Microdissections of the skin, *Fascia superficialis*, and constrictor musculature	N.A. (from the Comparative Anatomy Teaching Collection)
DGH-AL-019	91.44 cm	Female	Wild-caught	Histology of relaxed and stretched skin from the paralingual intermandibular and post-hyoid gular subregions*	IACUC protocol # 08-105; Louisiana Wildlife & Fisheries Special Alligator Permit (Nov 29, 2008)
DGH-AL-021	115.60 cm	Female	Wild-caught	Histology of the gular glands and surrounding skin and musculature	IACUC protocol # 08-105; Louisiana Wildlife & Fisheries Special Alligator Permit (Nov 29, 2008)
DGH-AL-022	160.02 cm	Female	Wild-caught	Histology of relaxed and stretched skin from the intermandibular, gular and cervical regions*	Carcass donated after unrelated field study under Louisiana Wildlife & Fisheries Special Alligator Permit (Dec 16, 2010)
DGH-AL-023	134.62 cm	Male	Wild-caught	Histology of relaxed and unstretched skin from the sublingual intermandibular and gular subregions*	Carcass donated after unrelated field study under Louisiana Wildlife & Fisheries Special Alligator Permit (Dec 16, 2010)
DGH-AL-024	127.00 cm	Female	Wild-caught	CT-scanning and 3D imaging	IACUC protocol # 08-105; Louisiana Wildlife & Fisheries Special Alligator Permit (Jan 12, 2011)
DGH-AL-025	91.40 cm	Female	Undetermined	Mesoscopic imaging of relaxed and stretched fresh skins from all subregions	Carcass donated after unrelated field study under Louisiana Wildlife & Fisheries Special Alligator Permit (Dec 16, 2010)

* The subregions studied for each specimen are listed; those that are not listed were excluded for that particular specimen.

Three fresh carcasses (heads-*cum*-thoraces) of three alligators (DGH-AL-022, DGH-AL-023, and DGH-AL-025; see Table 2.1) were donated under a Louisiana Wildlife and Fisheries Special Alligator Permit after an unrelated field study at Rockefeller Wildlife Refuge. These specimens

were fixed by submersion in 4% buffered formaldehyde solution and injection of formaldehyde directly into the subcutaneous tissues.

One alligator specimen (DGH-AL-002; see Table 2.1) was part of the Comparative Anatomy Teaching Collection at the Department of Biological Sciences, Louisiana State University, Baton Rouge. It had been obtained from Rockefeller Wildlife Refuge in 1999 by a former student, euthanized at the School of Veterinary Medicine, Louisiana State University, Baton Rouge, and perfused with 4% buffered formaldehyde solution through the left carotid artery.

2.2.2. Methods

- **Anatomical Techniques**
  - Microdissection

Specimens were dissected under stereomicroscopes (Wild Heerbrugg M3, Leica Microsystems Ltd., Switzerland), one of which was fitted with a dual ocular discussion tube (Wild Bridge Type 355110). Illumination was provided through a fiber-optic ring-light fitted with a polarizing filter and connected to a lightbox (Intralux 6000 or HCL 150, Volpi USA, Auburn, NY). Dissection tools included two pairs of fine stainless steel forceps (Dumoxel non-magnetic #5, Fine Science Tools, Inc., Foster City, CA; and SS Pakistan, Carolina Biological Supply Company, Burlington, NC), and a pair of stainless steel iridectomy microdissecting scissors (SS Pakistan, Carolina Biological Supply Company, Burlington, NC). The forceps were honed by hand under high magnification (16×) using a natural black Arkansas novaculite stone (Fine Science Tools, Foster City, CA).

The cutaneous and subcutaneous layers were dissected layer by layer under high magnification (64× and 160×). Adhesions between two tissue layers were marked by first separating them around the adhesion and then sewing a colored thread into the lower tissue layer around the base of the adhesion. The two tissue layers were then separated from each other by bisecting the adhesion above the threaded marker. In this way, the adhesions between two tissue layers could later be correlated with structures above and below the two tissue layers (see below).

17

➢ Preparation of Skin Specimens for Histology (Table 2.2 and Figure 2.1)

Skin pieces (~15 mm x 15 mm; Fig. 2.1A) that included both scales and interscale skin segments and any underlying cutaneous musculature were excised from each skin subregion from preserved specimens (DGH-AL-019, DGH-AL-022, and DGH-AL-23; see Table 2.1). These skin pieces were left in their relaxed state and stored in a 1% 2-phenoxyethanol solution prior to being processed for histological sectioning. Comparable skin pieces (~15 mm x 15 mm; see Fig. 2.1B) were excised from freshly euthanized specimens (DGH-AL-019 and DGH-AL-022; see Table 2.1). The skin pieces were stretched maximally along their sagittal or transverse body axes, or along both axes if possible, and pinned with the epidermis on the outside to felt-covered vulcanized rubber balls with a diameter of 48.26 mm (Kong Co., Golden, CO), which had been wrapped in cheesecloth to prevent felt fibers from adhering to the subcutaneous tissues. The mounted skin pieces were submerged in 4% buffered formaldehyde to fix them in the stretched state.   After fixation, the stretched skin pieces were stored in a 1% 2-Phenoxyethanol solution prior to being processed for histological sectioning.

Table 2.2 Biomechanical preparation of skin specimens

1. Skin regions are divided into skin subregions.
2. Skin subregions are cut into pieces that include rows of scales and the circumferential and longitudinal interscale segments between them.
3. Skin pieces from each subregion are cut into two skin samples.
4. Skin samples embedded in Paraplast® embedding medium
   - One sample is oriented so that the circumferential interscale segment was sectioned by the microtome blade.
   - The second sample is oriented so that the longitudinal interscale segment was sectioned by the microtome blade.
5. Skin sections are stained and photographed.

➢ Histology

Tissue embedding and orientation: The relaxed skin pieces were divided into two smaller skin samples (~5 mm x 5 mm) comprising a complete interscale skin segment flanked by portions of its adjacent scales (see Fig. 2.1). The skin samples were dehydrated in a series of ascending concentrations of histology-grade ethanol (70%, 95%, and 100%) and then placed into 99.9% t-butanol. The samples were cleared in Histochoice® clearing agent (Amresco, Solon, OH).   Each dehydrated and cleared skin sample was embedded in Paraplast X-tra® tissue embedding medium (Sigma-Aldrich Co., LLC, St. Louis, MO). One of the two skin samples

18

was oriented in the melted Paraplast® so that the longitudinal interscale skin segment, which parallels the sagittal axis of the body, was cross-sectioned. The other skin sample was oriented so that the transverse or circumferential interscale skin segment, which is perpendicular to the sagittal axis of the body, was cross-sectioned. The melted Paraplast® within the plastic molds containing the specially oriented skin samples was allowed to solidify overnight in a refrigerator.
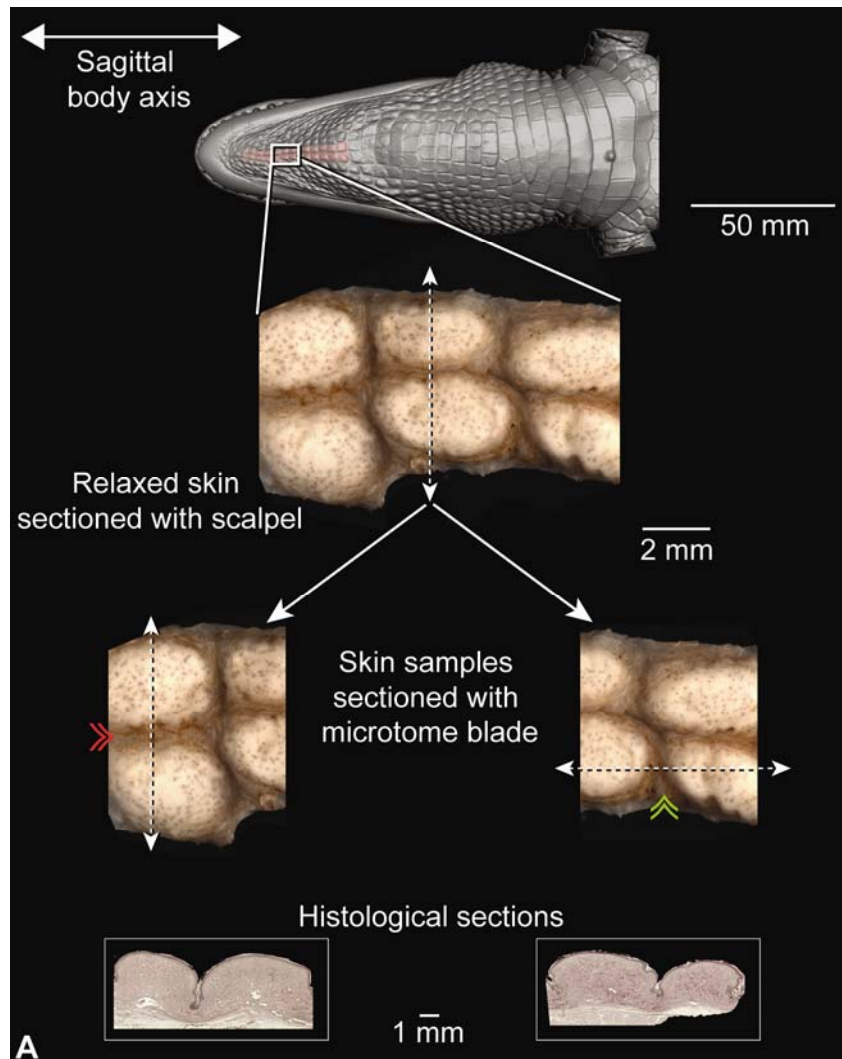
Figure 2.1 Diagram of the histological preparation method of the skin of an American Alligator (Alligator mississippiensis), using skin from the sublingual skin subregion as an example. (**A**) Relaxed skin sample; (**B**) Stretched skin sample. Symbols: Red double arrowheads = interscale skin segment oriented along the sagittal body axis (i.e., the longitudinal interscale skin segment); green double arrowheads = interscale skin segment oriented along the transverse body axis (i.e., the transverse or circumferential interscale skin segment); dashed arrow = location where the skin was sectioned with a scalpel or microtome blade.

19

Figure 2.1 (cont'd)
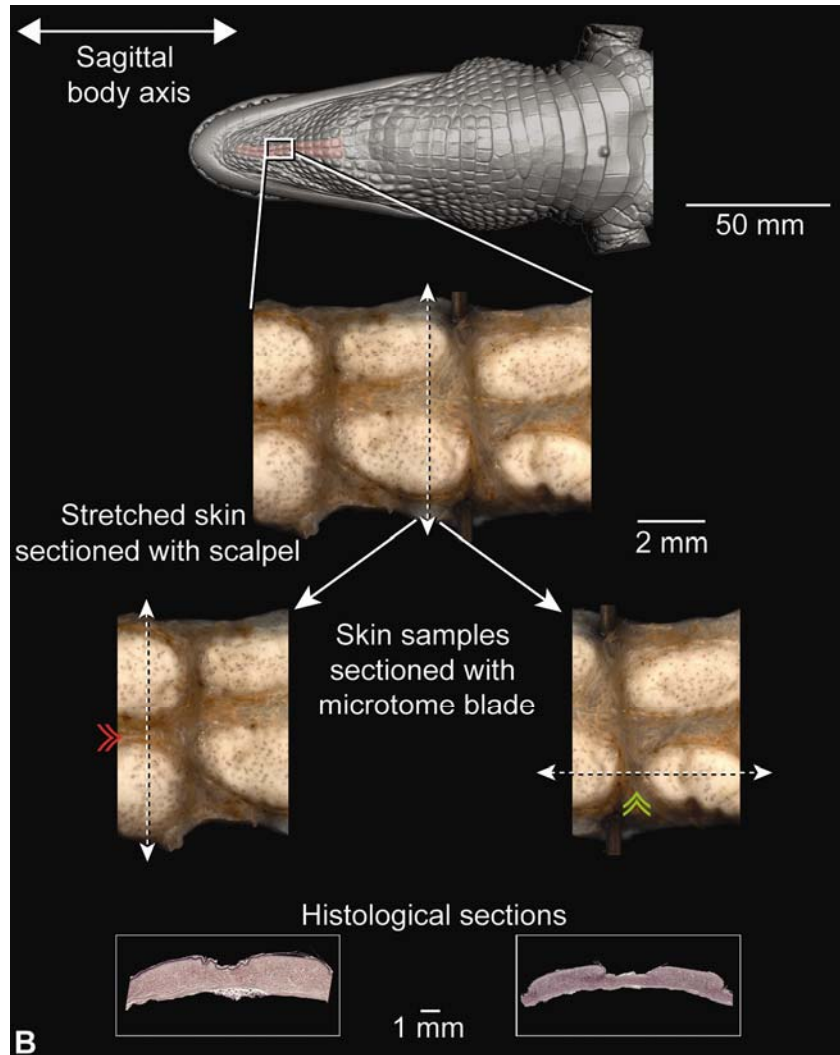
Tissue sectioning: Sections of 8-10 µm thickness were prepared with a heavy-duty, high profile disposable microtome knife (C.L. Sturkey, Inc., Lebanon, PA) mounted onto a rotary microtome (820 Spencer, American Optical, Buffalo, NY). The cutting surfaces of the Paraplast blocks were trimmed so that only a 1-2 mm margin of Paraplast® was left around the specimens. The cutting surfaces of the blocks were chilled with a cotton-tipped applicator stick soaked in ice water just before sectioning them to prevent the sections from warming, softening, and being compressed by the heat generated by cutting surface as the microtome knife cut through the wax block. The cutting surfaces were also treated with a cotton tipped-applicator stick soaked in an ice-cold polysorbate surfactant (0.05% Tween® 20, Uniqema Americas LLC, Paterson, NJ; Hicken et al. 2011) to reduce friction between the microtome knife and the block, thereby

20

ensuring smooth sections without tears. Sections were transferred to a floatation bath (150 ml deionized water in a glass slide dish) maintained at 45ºC. Because different tissues expand at different rates while floating in warm water, the temperature of the floatation bath was increased by 2-3ºC to 47-48°C for tissues that tended to resist expansion at lower temperature, such as the dense collagenous connective tissue of the dermis, and this allowed the sections to expand more evenly. In addition, 10 ml of 95% ethanol was added to the floatation bath to reduce the surface tension of the water so that the sections could spread evenly as the tissues expanded (Carson & Hladik 2009). Once the sections had sufficiently expanded and flattened, they were transferred to glass slides that had been coated with Poly-L-lysine and left to dry overnight in an incubator at 37 ºC.

Sectioning frozen tissue: Skin samples destined for lipid-staining were excised from formalin-fixed specimens and incubated overnight in 20% sucrose and 4% Paraformaldehyde cryoprotection solution. The specimens were then oriented on a metal stub, covered in O.C.T. (Optimal Cutting Temperature) compound (Sakura Finetek USA, Inc., Torrance, CA) and allowed to freeze at -32°C. Specimens were sectioned at 8-10 µm thickness with a standard low-profile disposable microtome knife (MX35 Premier+, ThermoScientific, Cheshire, WA) mounted onto a Leica CM1850 cryostat (Leica Microsystems, Ltd., Switzerland). Sections were collected onto an anti-roll plate and transferred to glass slides that had been coated with Poly-L-lysine. The slides were allowed to dry and adhere to the glass slides before staining.

Tissue Staining (see also Appendices A-C)**:** The sections on the glass slides were deparaffinized with Histochoice®, rehydrated in a series of descending ethanol concentrations, and stained. Depending on the structures of interest, different stains were applied. Harris Modified Hematoxylin and Eosin Yellowish Solution (both from Thermo Fisher Scientific, Inc., Pittsburgh, PA) were used to visualize the general morphology of the tissues and the arrangement of collagen fiber bundles. Weigert's Resorcin Fuchsin counterstained with Weigert's Iron Hematoxylin (modified from Romeis 1968) was used to visualize the arrangement of collagen and elastic fiber bundles. Oil Red O (Lucas & Stettenheim 1972) was used to stain for lipid content in the epidermis. The stained sections were mounted with Poly-Mount® (Polysciences, Inc., Warrington, PA), or VectaMount® AQ aqueous mounting medium (Vector Laboratories, Inc., Burlingame, CA) for frozen sections, and coverslipped.

21

> Measuring collagen fiber bundles in histological sections

In general, collagen fiber bundles are oriented in various directions in three-dimensional space. As a consequence, a histological section can contain transverse, longitudinal and oblique sections of collagen fiber bundles. In transverse and oblique sections of collagen fiber bundles, their entire width is visible in the plane of section. In longitudinal sections of collagen fiber bundles, however, only partial widths may be visible depending on whether the sections pass centrally or peripherally through the fiber bundles. Therefore, only measurements of the widest sections of longitudinally sectioned fibers were included, because they are likely to be close to central sections and, thus, represent the actual width of fiber bundles.

- **Imaging techniques**
  > Macroscopic Orthographic Imaging

Specimens were placed on an Illuma Hibase copy stand with adjustable side-arms that hold light fixtures (model no 132-33 M2, Bencher, Inc., Antioch, IL). Two frosted Reveal® indoor flood lamps (General Electric, Fairfield, CT) were attached to each side arm.   Digital images were taken with a vertically-mounted Spot Insight digital color camera (Meyer Instruments, Inc., Houston, TX) fitted with C-mount, manual iris, mono-focal CCTV lenses (2.2 mm, F1.4, National Electronics, Inc, Shawnee Mission, KS.; or 12.2 mm, F1.3, Goldinar M25).   The camera lens aperture was minimized to increase the depth of focus, and the working distance of the camera was set at the center of the focal length of the lens.

Orthographic imaging involves the projection of the anatomical surfaces of a specimen (i.e., dorsal, ventral, sinistral, dextral, cranial and caudal surfaces) onto planes that are at right angles to one another.   In effect, the specimen is virtually suspended in a box, and each of its surfaces is projected onto one of the sides of this box. Orienting the camera's optical axis perpendicularly to these surfaces ensures that all the perspective lines of sight are parallel to one another at any given point on the specimen and that they do not converge on a single vanishing point. This set-up eliminates distortion or foreshortening of the photographs and creates monocular images of the anatomical surfaces (Zweifel 1961; Lucas & Stettenheim 1972; Clark & Logan 1989). This imaging technique not only produces a series of 2D images that can be used to understand the 3D structure of the specimen, but also creates replicability with different stages of a dissection and, therefore, the feasibility of topographic mapping.

22

In practical terms, each surface of a specimen has to be photographed separately. In order to ensure that the images of the surfaces of a specimen are oriented at right angles to one another, the specimen needs to be rotated exactly around its midsagittal axis as each side is photographed. The alligator was placed on its side on the copy stand under the vertically-mounted digital camera so that its left lateral side could be photographed. A level was placed on the horizontal surface of the camera to ensure that the optical axis was perpendicular to the plane of the specimen surface being photographed. At the same time, the specimen's midsagittal axis was aligned with the horizontal beam of a stationary 90º laser level. A second stationary 90 º laser level with a vertical beam was placed in front of the specimen to establish the transverse axis at a 90º angle to the midsagittal axis. After having photographed the lateral side, the specimen was rotated onto its abdomen to photograph its dorsal side, while ensuring that the transverse axis remained oriented at a 90º angle to the horizontal axis. In order to photograph the ventral surface, the specimen was then rotated onto its back around its midsagittal axis, keeping both axes aligned. Keeping the specimen aligned with these two axes as the lateral, dorsal, and ventral views were photographed prevented any deviations of the specimen's position in pitch, roll or yaw and ensured that the images of the various surfaces are comparable and reproducible.

➤ Mesoscopic Imaging

The epidermal surfaces of stretched and relaxed skin pieces from each subregion (Table 2.2 and Fig. 2.1) with maximum dimensions of 50 mm x 50 mm were photographed under a MZ6 stereomicroscope (Leica Microsystems Ltd., Switzerland) with a motorized footswitch for focusing (model T-91-SE; Linemaster Switch Corp., Woodstock, CT). The stereomicroscope was placed on a Micro-g vibration isolation table [63-551 series, TMC (Technical Manufacturing Corporation), Peabody, MA] and equipped with a SPOT Insight digital color camera (Diagnostic Instruments, Inc., Houston, TX). Illumination was provided by Intralux 6000 lightboxes (Volpi USA, Auburn, NY) through two different types of fiber optic light guides. For microdissection under even illumination, a circular fiber optic ring light with an adjustable polarizing filter was fitted to the objective lens. For mesoscopic imaging with extended depth focus (EDF), a pair of flexible fiber optic light guides (10 mm active bundle diameter) were mounted on articulated stands on heavy steel bases (Volpi USA, Auburn, NY), and adjustable polarizing filters (12.2 mm diameter, Edmond Optics, Inc., Barrington, NJ) were mounted to each light guide with a rotating SM1 lens tube and cage plates (Thorlabs, Ltd., UK).

23

The digital images were captured through ImagePro software (Meyer Instruments, Inc., Houston, TX), and an extended depth of field was obtained through In-Focus Automation software (Meyer Instruments, Inc., Houston, TX). The images were processed with Adobe® Photoshop CS3 (Adobe Systems, Inc., San Jose, CA) to adjust the brightness levels of the image histogram.

➢ Microscopic Imaging

Histological sections were observed and photographed with a Nikon Eclipse 80i compound microscope mounted with a Nikon 5 megapixel CCD high-definition color camera head-DS-Fi1. NIS-Elements BR (Basic Research) software (Nikon, Inc., Melville, NY) was used to virtually stitch together magnified (100-200×) digital images of the sections in order to create high magnification large field of view images. The images were processed with Adobe® Photoshop CS3 to adjust the brightness levels of the image histogram.

➢ 3D Imaging

Virtual three-dimensional images were created from x-ray computed-tomography data of a preserved alligator specimen (DGH-AL-024; Table 2.1.) acquired with a GE 16-slice CT scanner (General Electric Company, Fairfield, CT) at the Radiology Section in Department of Veterinary Clinical Sciences at the Louisiana State University School of Veterinary Medicine. Avizo® Standard 3D analysis software (VSG, Visualization Science Group, Inc., Burlington, MA) was used to create 3D orthographic images of the integument of the head and neck of the alligator. Adobe® Photoshop CS3 (Adobe Systems, Inc., San Jose, CA) was used to color-code skin regions and subregions.

• **Regional Subdivision of the Intermandibulo-cervical Integument**

The integument of the head, neck and shoulders was classified into major skin regions by using microdissection and orthographic imaging (specimen DGH-AL-002; Table 2.1) in order to correlate the skin regions with underlying structures (e.g., the *Fascia superficialis* and the subcutaneous constrictor muscles). Upon reflection of the skin, it was found that major aspects of the skin morphology could be correlated with the topography of the three subcutaneous constrictor muscles (*Musculus intermandibularis*, *M. constrictor colli gularis*, and *M. constrictor colli cervicalis*; see 2.3.1). Along the borders of the constrictor muscles, their epimysia adhere to the overlying *Fascia superficialis* and dermis. These circumferential lines of fusion mark the

boundaries of the three main skin regions: The intermandibular, gular and cervical regions. These three skin regions could be further subdivided into skin subregions that differ in the morphology of the scales (i.e., shape and size) and interscale skin segments (i.e., width and orientation). A fourth skin region was identified, namely, the dorsal tuberculate skin region (see 2.3.5), which is not associated directly with the constrictor musculature, but whose tuberculate scales fuse to the *Fascia superficialis* and the aponeuroses of the constrictor muscles.

- **Modeling Techniques**
  - ➤ Topographic Mapping

The topographic maps of the cutaneous and subcutaneous layers were prepared from outlines of the orthographic images. The topographic maps of the individual layers were traced on translucent paper and superimposed on a lightbox in order to identify congruencies between layers. Alternatively, the individual topographic maps were scanned, digitized, and imported into Adobe® Photoshop CS3 (Adobe Systems, Inc., San Jose, CA). The individual images were placed on separate layers within a single document, and congruences between the various layers could be identified by manipulating the opacity of the different layers. The location of any adhesions between the epimysium of the constrictor musculature, *Fascia superficialis*, and the dermis were mapped onto outlines of lateral and ventral views of orthographic photographs.

  - ➤ Soft Tissue Modeling

Models of the stretching and recoil mechanisms of individual skin subregions were created using Adobe® Illustrator CS3 (Adobe Systems, Inc., San Jose, CA), and were based on histological sections. For each subregion, a model of the resting position of the scale and interscale skin was drawn by outlining the skin and subcutaneous layers from a histological section and by adding the collagen and elastic fiber bundles as inferred from histological sections specifically stained to visualize collagen and elastic fiber bundles. The same procedure was repeated for creating a model of the stretched condition of the skin. The goal was a reconstruction of the changed orientation of the collagen and elastic fiber bundles when the skin was stretched and let to recoil back into its relaxed condition. The dynamic processes of stretching and elastic recoil of the skin could be explained based on the premise that collagen lengthens to a limited degree and mainly resists stretching forces, whereas elastic fibers store energy when it is stretched, and recoils and shortens when stretching forces subside. The

25

modeling of the collagen and elastic fiber bundle orientations among the different subregions provides a functional explanation for the regional morphological differences of the skin.

2.3. Results

2.3.1. General Morphology of the Integument

The integument consists of non-imbricating, hard-cornified scales whose arrangement, shape, and size vary regionally. The scales are separated from one another by stretchable soft-cornified interscale skin segments that form interscale joints and whose width and orientation determine the direction and extent to which the skin can expand.

The intermandibulo-cervical integument (i.e., the integument cranial to the shoulder girdle) can be divided into the intermandibular, gular and cervical skin regions. These three main skin regions correspond to the topography of the three subcutaneous constrictor muscles, whose epimysia are fused to the dermis at their borders (Fig. 2.2). Each skin region can be subdivided into subregions that are characterized by distinct patterns of scales and interscale skin segments and, thus, by various directions and degrees of expansibility (Fig. 2.3).

The integument *sensu lato* comprises three main tissue layers, namely the epidermis, dermis, and *Fascia superficialis* (i.e., subcutis). The specific structure of these layers may differ between the scales and interscale skin segments, as well as among the various skin subregions.

- **Epidermis**

The epidermis is a keratinized, hard- or soft-cornified stratified epithelium. Because all stratified epithelia are keratinized (see Bragulla & Homberger 2009), the simple terms 'hard-cornified' or 'soft-cornified' will be used, but it is implied that both of these types of epithelia are also keratinized. The scale epidermis is a stratified, squamous hard-cornified epithelium (Fig. 2.4A and C). The *Stratum basale* on the basement membrane is a single layer of columnar cells with tall and narrow heterochromatic nuclei. The *Stratum spinosum* comprises 3-4 layers of polyhedral cells that are interconnected by tight cell junctions (no image). Their cell nuclei become rounder and euchromatic, and they display prominent nucleoli as the cells mature and are pushed towards the skin surface. The uppermost cells of the *Stratum spinosum* form a layer of strongly acidophilic, dying and flattened precorneus cells, of which only some have a nucleus. This precorneus layer stains intensely with eosin and Weigert's Resorcin-Fuchsin stain. The

26

non-living *Stratum corneum* is about as thick as the entire underlying living epidermis and consists of flat, compactly arranged, anucleated hard-cornified cells.

The interscale epidermis is a stratified, squamous, soft-cornified epithelium (Fig. 2.4B and D). The *Stratum basale* on the basement membrane is a single layer of square cells with round heterochromatic nuclei. The *Stratum spinosum* consists of three to four layers of flattened oval cells that are interconnected by cell junctions. The cell nuclei become wide-oval and euchromatic, and they display prominent nucleoli as the cells differentiate, i.e., keratinize, and are pushed toward the skin surface. The uppermost cells of the *Stratum spinosum* form a layer of acidophilic, dying and flattened precorneus cells of which only some have a nucleus. This precorneus layer stains less intensely than the corresponding layer of the scale epidermis when stained with eosin (Fig. 2.4A) and Weigert's Resorcin-Fuchsin. The cells in the upper layers of the *Stratum spinosum* also contain intracellular lipid droplets, which are released into the *Stratum corneum* (Fig. 2.4D). The non-living *Stratum corneum* varies in thickness, often being thicker than the underlying living epidermis. It consists of flat, anucleated soft-cornified cells that sometimes separate from one another during sectioning. The deeper layers are impregnated with lipids, whereas the upper layers are leached of lipids (Fig. 2.4D). The uppermost dead cells of the *Stratum corneum* begin to slough off from the surface of the epidermis as a *Stratum disjunctum*. In skin subregions that are in close proximity to the gular gland orifice, such as the pararamal skin subregion (see below), cell debris and lipids from its holocrine secretion are found in the creases of the interscale skin segments and may serve to condition the soft-cornified interscale epidermis, which needs to remain pliable and soft. Interscale skin segments may be studded with hard-cornified tuberosities that have the same basic epidermal structure as the scales.

- **Dermis**

The dermis can be subdivided into three layers that vary in their relative collagenous and elastic fiber composition (Fig. 2.5). The uppermost *Stratum laxum* is a loose, collagenous and elastic connective tissue; the underlying *Stratum compactum* is a dense, mostly collagenous connective tissue; and the deepest *Stratum elasticum* is a loose collagenous connective tissue with varying, but substantial amounts of elastic fiber bundles, depending on the skin subregion. Underneath the scales, the *Stratum laxum* varies in thickness (between 100-500 µm, depending

27

Figure 2.2. Orthographic images of the main skin regions of the intermandibulo-cervical integument of the American Alligator (*Alligator mississippiensis*) and their topographic relationship to the constrictor musculature. (**A**) Lateral view of the constrictor musculature of the intermandibulo-cervical envelope; the *M. intermandibularis* cannot be seen in this view; (**B**) Virtual longitudinal section through the intermandibulo-cervical envelope to show the layers and locations of adhesions; (**C**) Lateral view of the main skin regions; (**D**) Ventral view of the main skin regions. Abbreviations: *F. = Fascia*, *M. = Musculus*, *c. c. = constrictor colli*; Symbols: black arrowheads = adhesions of the constrictor epimysium to the *Fascia superficialis* and the dermis at the constrictor muscle borders.

28

Tuberculate scale of dorsal tuberculate skin region — Osteoderm

A

Mandibular ramus — *M. constrictor colli gularis* — *M. constrictor colli cervicalis*

M. intermandibularis

B

F. intermandibularis
F. c. c. gularis
F. c. c. cervicalis

F. superficialis — Dermis

Dorsal tuberculate region — Osteoderm

C

Intermandibular skin region — Gular skin region — Cervical skin region

D

50 mm
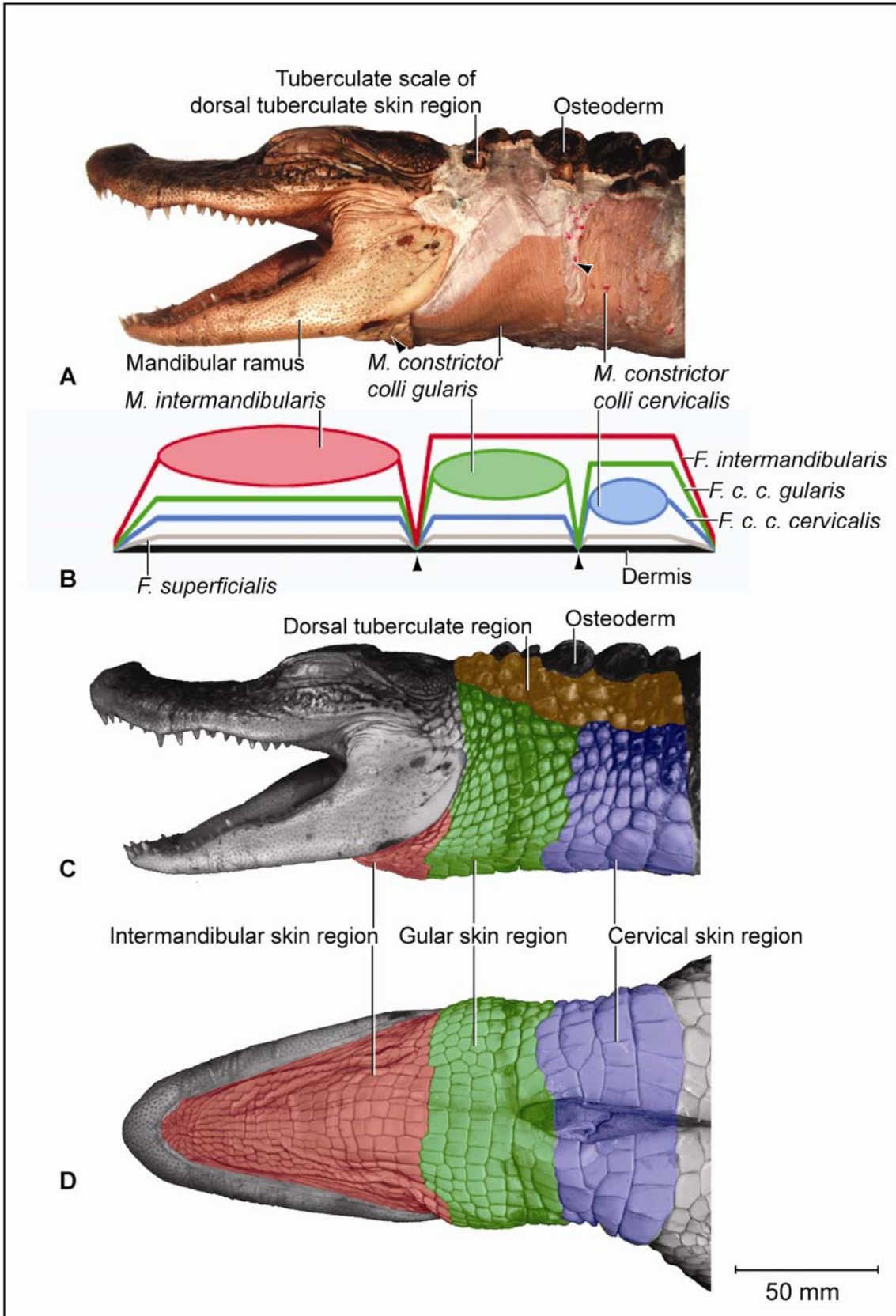
on the skin subregion), and is comprised of loose collagenous connective tissue, whose collagen fiber bundles are thin (ca. 1-8 µm) and interspersed with elastic fiber bundles of a similar diameter (ca. 1-5 µm). The elastic fiber bundles are arranged perpendicularly to the scale surface and originate from the *Stratum elasticum* and accompany the collagenous *Retinacula cutis* fiber bundles (see below).

The *Stratum compactum* underneath the scales is comprised of dense collagenous connective tissue, whose collagen fiber bundles are thick (ca. 10-50 µm) and interlaced with thin elastic fiber bundles (ca. 1-2 µm). These collagen fiber bundles are orthogonally layered with alternating fiber bundle orientations, such as obliquely from cranio-medial to caudolateral, or parallel to the transverse and sagittal body axes; and their resting configuration may be straight or wavy depending on the expansibility of the particular skin subregion (Fig. 2.5; see below for specifics about each skin subregions).

Collagen fiber bundles that originate in the deep layers of the *Stratum compactum* traverse the dermis and appear to anchor to the basement membrane underneath hard-cornified portions of the epidermis (i.e., scales and interscale tuberosities) are *Retinacula cutis* (Fig. 2.5). In general, expandable skin subregions have sparse and thin (ca. 2-5 µm) *Retinacula cutis* fibers that attach only to the basement membrane underneath hard-cornified scales. In non-expandable skin subregions, the *Retinacula cutis* fibers are numerous and thick (ca. 20-30 µm) and often traverse the parallel collagenous joint fiber bundles of the interscale skin segment (see below) to attach to interscale tuberosities, which may be almost as wide as the entire narrow interscale epidermis. In all skin subregions, the collagenous *Retinacula cutis* fiber bundles are accompanied by elastic fiber bundles that originate from the *Stratum elasticum.*

The *Stratum elasticum* under a scale is comprised of collagenous loose connective tissue, whose fiber bundles are intertwined with elastic fiber bundles that form a layered meshwork in the deepest portion of the dermis. Its structure does not differ between scales and interscale skin segments and sends elastic fiber bundles towards the surface to anchor to the basement membrane of the hard-cornified portions of the epidermis. In general, expandable skin subregions contain elastic fiber bundles that are relatively thick (ca. 5-10 µm) and form 5-20 elastic fiber layers. In less expandable skin subregions, the elastic fiber bundles are thinner (ca. 1-5 µm) and form only about three to five elastic fiber layers and might envelope dermal fat bodies.

30

Figure 2.3 Color-coded orthographic images of the skin subregions of the intermandibulo-cervical integument of the American Alligator (*Alligator mississippiensis*). (**A**) Dorsal view; (**B**) Lateral view; (**C**) Oblique lateral view; (**D**) Ventral view. Colors: Shades of red = intermandibular skin subregions, shades of green = gular skin subregions, shades of blue = cervical skin subregions, orange = dorsal tuberculate skin region.

31

Osteoderm

Dorsal tuberculate region

A

Retroarticular subregion

Lateral cervical subregion

B

Pararamal subregion

Paralingual subregion

Pterygoid subregion

Symphyseal subregion

C

Sublingual subregion

Subhyoid subregion

Posthyoid subregion

Ventral cervical subregion

D

External surface of the mandible
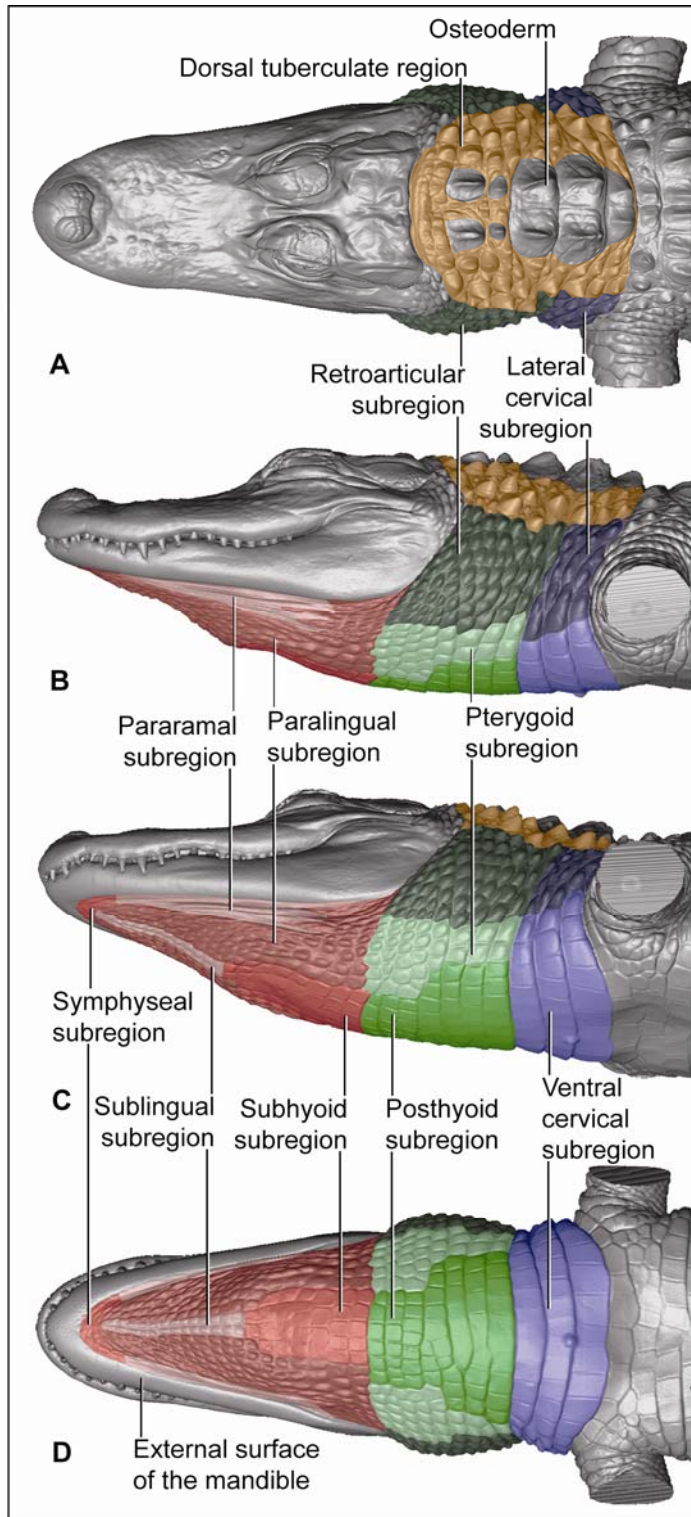
Figure 2.4 Histological images of sections through the epidermis of the intermandibulo-cervical integument of the American Alligator (*Alligator mississippiensis*). (**A-B**) Longitudinal sections from the ventral cervical skin subregion stained with H&E. (A) Section through a hard-cornified scale; the tight junctions among the cells of the *Stratum spinosum* are not visible. (B) Section through a soft-cornified interscale skin segment. (**C-D**) Transverse sections stained with Oil Red O to show intracellular lipid droplets in the cells of the *Stratum spinosum* and lipids in the deeper *Stratum corneum*. (C) Section through a hard-cornified scale (paralingual skin subregion). (D) Section through a soft-cornified interscale skin segment (pararamal skin subregion).
Abbreviation: S = *Stratum*. Symbols: Arrowheads (black = precorneous cell layer of the *Stratum spinosum*, green = melanophore).

33
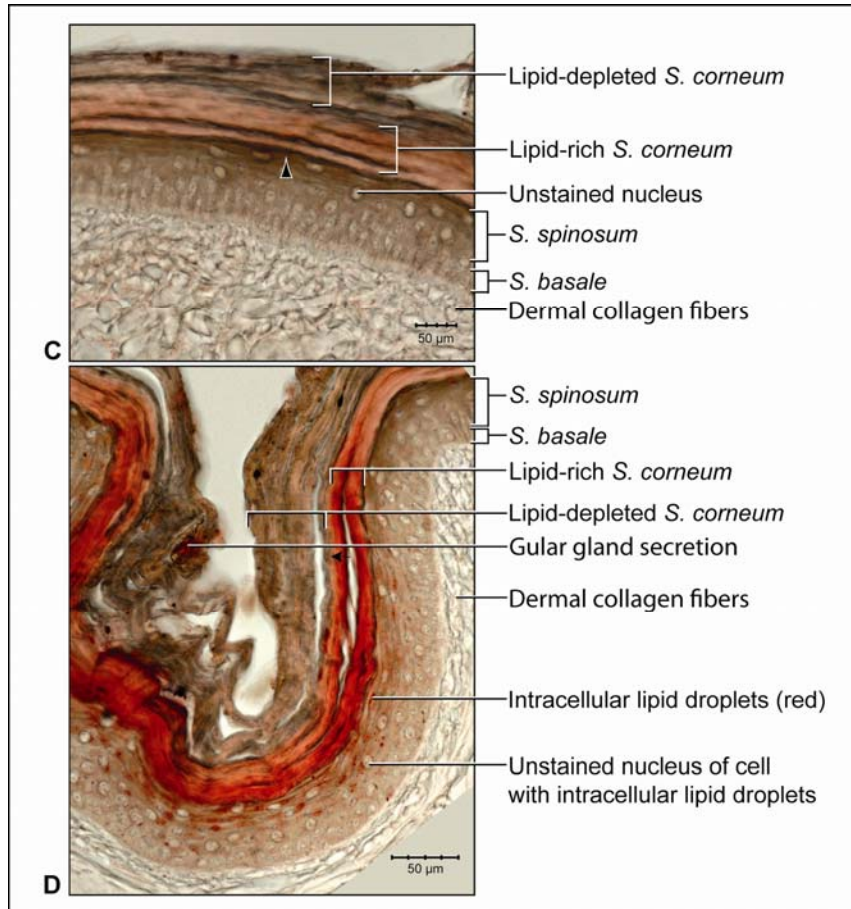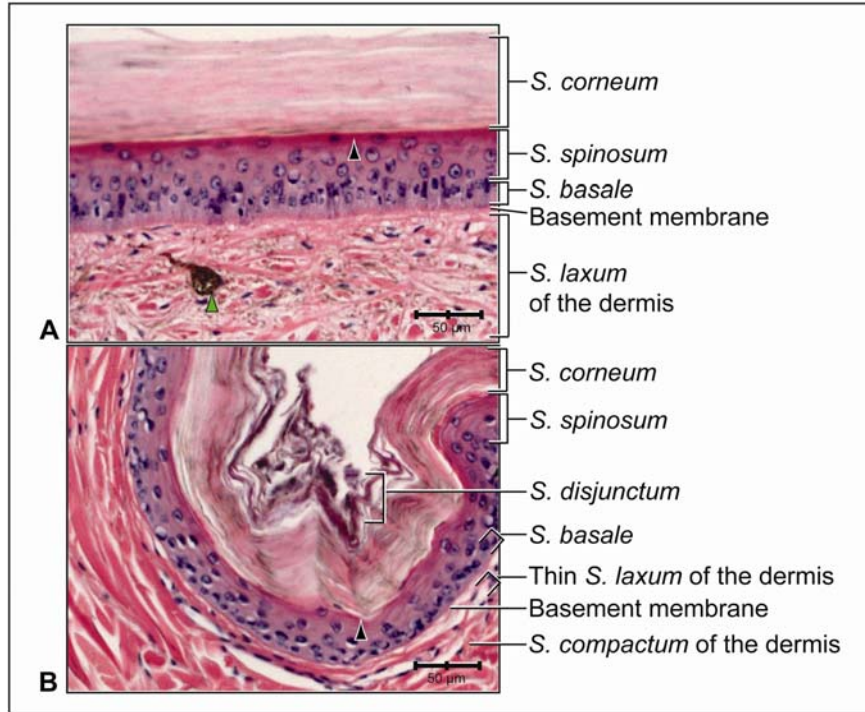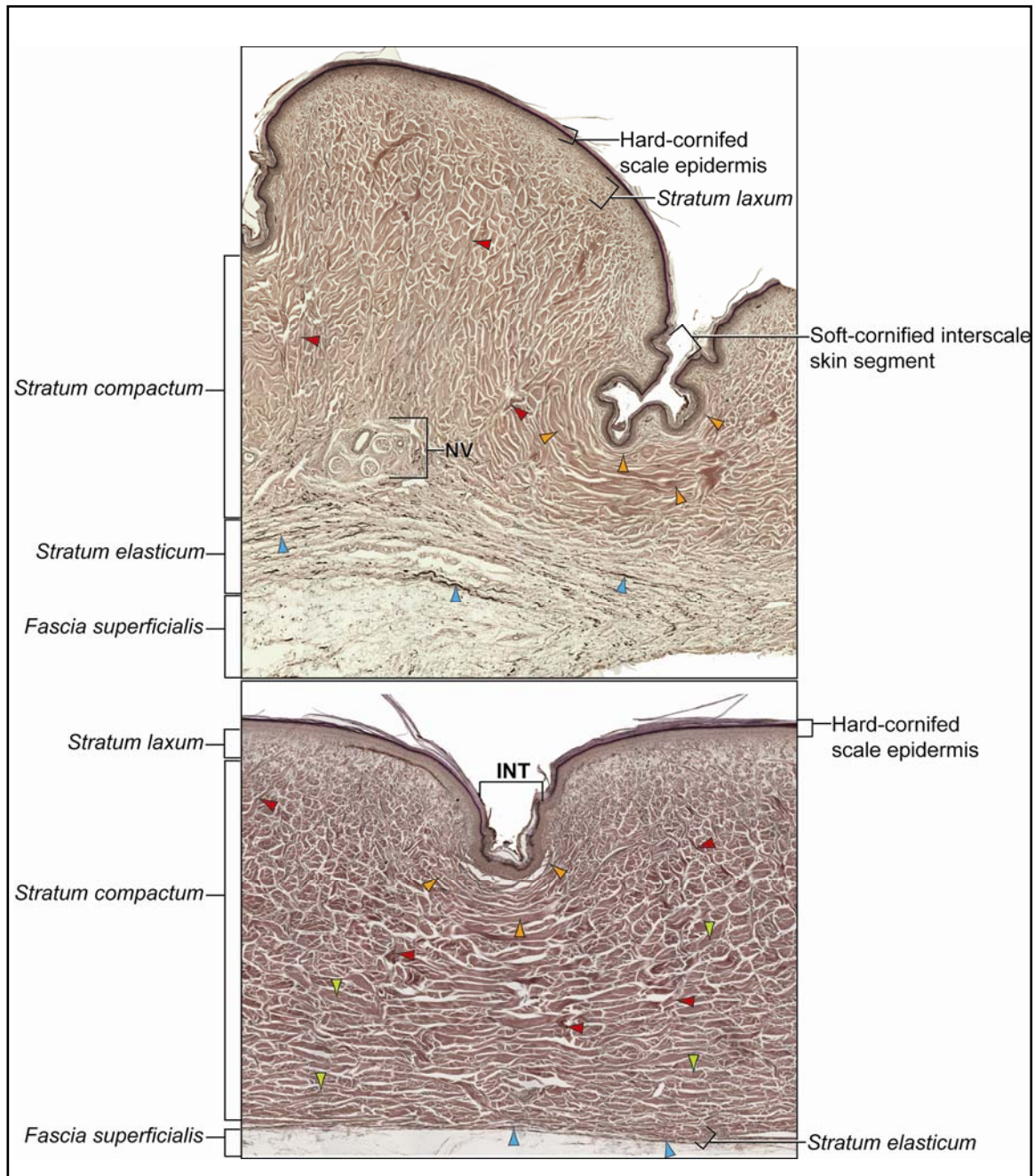
Figure 2.5. Histological images of transverse sections through the dermis of the intermandibulo-cervical integument of the American Alligator (*Alligator mississippiensis*) (Weigert's Resorcin-Fuchsin staining). (**A**) Dermis underneath a scale and an expandable interscale skin segment (e.g., paralingual skin subregion). (**B**) Dermis underneath a flexible, but non-expandable interscale skin segment (e.g., ventral cervical skin subregion). Abbreviations: DF = dermal fat body, INT = interscale skin segment, NV = neurovascular bundle, S = *Stratum*. Symbols: Arrowheads (blue = elastic fiber bundles of the *Stratum elasticum*, lime green = collagen fiber bundles of the orthogonal layers in *Stratum compactum*, orange = collagenous joint fiber bundles, red = collagenous *Retinacula cutis* fiber bundles of the *Stratum compactum*).

35

In expandable skin subregions, neurovascular bundles run along the sagittal axis of the body underneath the scale epidermis between the *Stratum elasticum* and the *Stratum compactum* and branch into smaller vessels and nerves while traversing the dermis towards the skin surface. The blood vessels terminate as capillary beds in the *Stratum laxum* under the hard-cornified scales and interscale tuberosities. Some nerve fiber bundles terminate as encapsulated lamellar mechanoreceptors, which resemble mammalian Pacinian corpuscles (von Düring & Miller 1979; Dehnhardt & Mauk 2009) or avian Herbst corpuscles (von Düring & Miller 1979; Gottschaldt 1985; Dehnhardt & Mauk 2009), at the edges of scales or underneath interscale tuberosities. In the gular and cervical skin subregions, the neurovascular bundles between the *Stratum elasticum* and the *Stratum compactum* are usually surrounded by perivascular fat. Melanophores underneath the scales and interscale segments are located in the *Stratum laxum* adjacent to the basement membrane. They are arranged in dense clusters and may be found in the *Stratum spinosum* of the epidermis in the lateral and dorsal pigmented skin, but are sparse in the lighter ventral skin.

The *Stratum laxum* underneath an interscale skin segment, thins out to be barely visible, except under the hard-cornified interscale tuberosities, whose cores are formed by the *Stratum laxum*. The *Stratum compactum* underneath the interscale skin segments are organized into layers with parallel collagen fiber bundles. The superficial, shorter fiber bundles may interconnect interscale tuberosities and connect these to the adjacent scales, whereas the deeper, longer ones span entire interscale skin segments and are anchored to the adjacent scales. These interscale collagen fiber bundles and the adjacent scales to which they attach form an interscale joint and are, therefore called collagenous joint fiber bundles.

The deeper collagenous joint fiber bundles may extend towards the center of adjacent scales and anchor to their basement membrane, thereby forming *Retinacula cutis* fiber bundles. If the deeper collagenous joint fiber bundles do not anchor to the basement membrane of scales or interscale tuberosities, they interweave with the layered collagen fiber bundles of the *Stratum compactum* underneath the scales.

In expandable skin subregions, the collagenous joint fiber bundles of the *Stratum compactum* make up the entire interscale dermis. In non-expandable skin subregions, they are found only in the most superficial portion of the interscale dermis, and the rest of the interscale dermis is made up by extensions of the orthogonal layers of collagen fiber bundles from the

36

Stratum compactum underneath the scales (Fig. 2.5). Therefore, such interscale joints are not expandable. The *Stratum elasticum* underneath the interscale skin segments does not differ from that located underneath the scales.

- *Fascia superficialis*

The structure of the *Fascia superficialis* does not differ between scales and interscale skin segments, but varies among the different skin subregions. In expandable skin subregions, the *Fascia superficialis* is an amorphous mass of loosely arranged thin (3-5 µm) collagen fiber bundles and thin (1-2 µm) elastic fiber bundles, occasionally interspersed with adipocytes. The elastic fiber bundles do not form distinct layers as in the *Stratum elasticum* of the dermis. In non-expandable skin subregions, the *Fascia superficialis* is less amorphous and may form layers with distinct collagen fiber orientations (Fig.2.5; see 3.3.2). Elastic fiber bundles may be present, but are never as numerous as in the expandable skin subregions. Under the scales of the gular and cervical skin subregions, adipose tissue is common, especially surrounding blood vessels and nerves. In some areas, especially near the ventral midline, the *Fascia superficialis* merges with the epimysium of the constrictor musculature. Blood, lymphatic vessels, and nerves are thicker in the *Fascia superficialis* than in the dermis.

2.3.2. Intermandibular Skin Region

The intermandibular skin region covers the area between the mandibular rami, and its epidermis is continuous with the epidermis that covers the external surface of the mandible (Fig. 2.2). The caudal border of the intermandibular skin region coincides with the caudal border of the underlying *M. intermandibularis* (see 2.2.3 and 3.3.3). Most of the intermandibular skin region comprises scale rows that are oriented obliquely from cranio-medial to caudo-lateral, except in the subhyoid skin subregion subtending the hyoid, where the scale rows are oriented along the transverse body axis (Fig. 2.3).

- **Symphyseal Skin Subregion**
  - ➢ Morphological Description

The small symphyseal subregion comprises three to four scale rows directly caudal to the mandibular symphysis (Fig. 2.6A and B). Its caudal border coincides with the rostral border of

37

the underlying *M. intermandibularis* and, hence, this skin subregion subtends the connective tissue that spans the gap between the mandibular symphysis and the rostral border of the *M. intermandibularis* [i.e., *Trigonum intermandibulare anterius* (Schumacher 1973)].

The symphyseal skin subregion comprises circular or triangular scales that are arranged in rows that are oriented obliquely from cranio-medial to caudo-lateral. The interscale skin segments are devoid of interscale tuberosities and are very short and shallow, projecting downwards only as deeply as the *Stratum laxum* of the dermis underlying the scales (Fig. 2.6E and F). They provide flexibility, but not expansibility, between the scales. The scales of the symphyseal skin subregion, in contrast to those of the other skin subregions, bear a small central, pigmented and soft-cornified protuberance (Fig. 2.6C and D), which resembles the protuberances that are spread over the skin that covers the external surface of the mandible. The protuberances are the epidermal parts of dermo-epidermal sensory organs that have been described as tactile sense organs or touch papillae (von Düring & Miller 1979; Denhardt & Mauk 2009), integumentary sense organs (Richardson *et al*. 2002), or dome pressure receptors (Soares 2002), and have been shown to detect hydrodynamic pressure waves at the air-water interface (Soares 2002).

The scale epidermis consists of a stratified squamous hard-cornified epithelium with a *Stratum basale* of tall columnar cells and a *Stratum spinosum* of about ten cell layers. The *Stratum corneum* is about 40-50 µm thick and consists of a compact layer of hard-cornified, flattened cells (see 2.3.1).

Underneath the scale epidermis, the dermal *Stratum laxum* consists of collagen fibers bundles that are thicker (15-30 µm) than those of the *Stratum laxum* of other skin subregions and are oriented along the transverse and longitudinal body axes, as well as perpendicularly to the skin surface. There is no sharp demarcation between the *Stratum laxum* and the *Stratum compactum* (Fig. 2.6E and F). The *Stratum compactum* comprises collagen fiber bundles that are arranged in orthogonal layers along the transverse and sagittal body axes. A *Stratum elasticum* is absent, but individual elastic fibers are interspersed among the collagen fiber bundles of the *Stratum compactum*.

In the dome pressure receptors, the epidermis consists of a stratified squamous soft-cornified epithelium (see also von Düring & Miller 1979; Denhardt & Mauk 2009) with a

Stratum basale of spherical cells and a *Stratum spinosum* of about eight cell layers with interspersed melanophores. The *Stratum corneum* is thin (about 10-15 µm) (see 2.3.1). The dermal component of the dome pressure receptor is located within the *Stratum laxum* and comprises a dermal Merkel cell column, which consists of several layers of Merkel cells encapsulated by Schwann cells and collagen fibrils and is supplied by several myelinated nerve fibers (Fig. 2.6C$_2$; see also von Düring & Miller 1979). The dermal *Stratum laxum* is thicker (ca. 500 µm) than that of a scale, but comprises thinner collagen fiber bundles (about 10-15 µm) and contains numerous blood vessels and encapsulated lamellar mechanoreceptors (see also von Düring & Miller 1979).

In both the transverse and longitudinal interscale skin segments, the epidermis consists of a stratified squamous soft-cornified epithelium with a *Stratum basale* of spherical cells and a *Stratum spinosum* of about five to six cell layers. The *Stratum corneum* is about 80 µm thick and consists of soft-cornified, flattened cells (see 2.3.1).

Underneath the epidermis of the soft-cornified interscale skin segments, the dermal *Stratum laxum* thins out and is barely visible. The *Stratum compactum* consists of parallel collagenous joint fiber bundles that are oriented along the transverse and sagittal body axes and span the interscale segments to anchor to the basement membrane of adjacent scales. The deepest collagenous joint fiber bundles are straight in their resting configuration and span both the scales and interscale skin segments. They are probably anchored in the periosteum of the mandible and possibly the dermis of the skin on the external surface of the mandible.

A *Stratum elasticum* is not clearly demarcated, but individual elastic fiber bundles are interspersed throughout the dermis and are oriented along the sagittal body axis (Fig. 2.6F$_1$).

The uniform *Fascia superficialis* is composed of thick collagen fiber bundles (ca. 200 µm) and merges with the *Stratum compactum* of the dermis and the epimysium of the underlying *M. geniohyoideus* (Fig. 2.6E$_1$).

➤ Functional Interpretation

Stretch-resisting mechanism: When the skin is stretched, the straight collagenous joint fiber bundles in the deep *Stratum compactum* tighten and resist further stretching of the skin.

Bending mechanism: Because the interscale skin segments are very short and not deeply

39
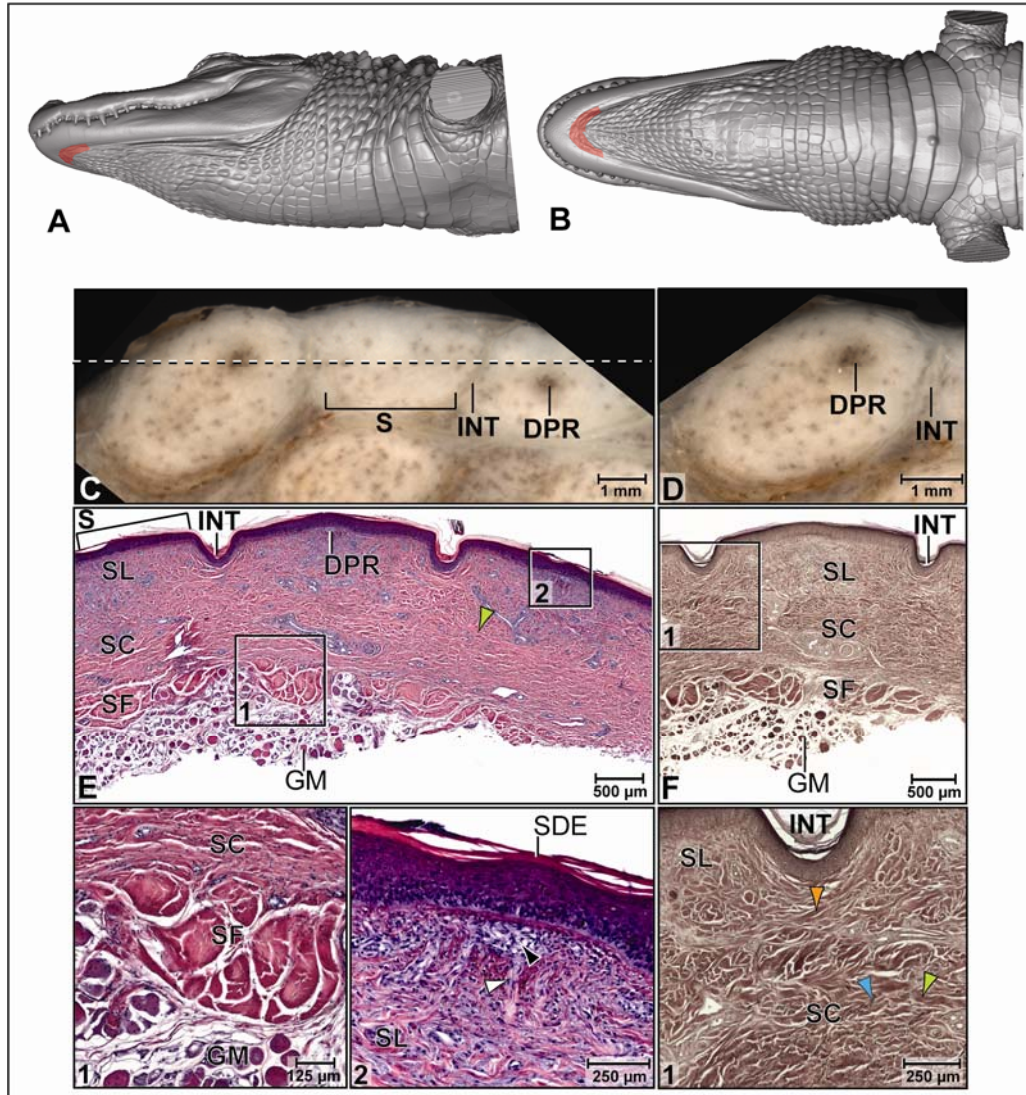
Figure 2.6. The symphyseal skin subregion of the American Alligator (*Alligator mississippiensis*). (**A-B**) Orthographic images of a 3D reconstruction (Isosurface module, Avizo®) of the skin of the head, neck, and shoulder region to indicate the location of the symphyseal skin subregion highlighted in red. (A) Ventrolateral view. (B) Ventral view. (**C-D**) Digital mesoscopic images of the skin surface. (C) Several scales and interscale skin segments. (D) Detail of a scale with a dome pressure receptor. (**E-F**) Digital micrographs of transverse histological sections. (E) Scales and interscale skin segments (H&E staining). (E$_1$) Large longitudinal collagen fiber bundles of the *Fascia superficialis*. (E$_2$) A dome pressure receptor in the *Stratum laxum* underneath a scale. (F) Scale and interscale skin segments (Weigert's Resorcin-Fuchsin staining). (F$_1$) A short, non-expandable interscale skin segment. Abbreviations: DPR = dome pressure receptor, GM = geniohyoid muscle, INT = interscale skin segment, S = scale, SC = *Stratum compactum*, SDE = soft-cornified dome epidermis, SF = *Fascia superficialis*, SL = *Stratum laxum*. Symbols: dased line = plane of section for histology; arrowheads (white = myelinated nerve fiber of DPR, black = Merkel cell dermal column of DPR, orange = collagenous joint fiber bundles of the *Stratum compactum* in the interscale skin segment, blue = elastic fiber bundles).

40

folded, they are not expandable, but nevertheless provide flexibility to the skin, so that the skin can be bent concavely or convexly. When the intermandibular skin bulges out to accommodate the movement of underlying structures, the scales rotate around the interscale joint. Some movements of the tongue during feeding pull the symphyseal skin subregion into a concave dimple, because the *Fascia superficialis* is fused to the dermis and hyoid musculature of this skin subregion (Fig. 2.7).

Functioning of a dome pressure receptor: The reduction of the loose connective tissue of the *Stratum laxum* around the dermal Merkel cell column to just a thin layer, in addition to the limited ability of this skin subregion to stretch, focuses pressure waves on just the dome pressure receptor. This interpretation is supported by the fact that the only other place, where dome pressure receptors occur, is on the external surface of the mandible, where the skin is firmly attached to the underlying bone with little, if any, loose connective tissue in between.

Figure 2.7 Photograph of a live American Alligator (*Alligator mississippiensis*) eating a turtle to show the intermandibulo-cervical skin subregions in states of expansion during feeding. Photo credit: Jessie Dickson.

- **Pararamal Skin Subregion**
  - ➢ Morphological Description

The paired pararamal skin subregions lie along the medial sides of the mandibular rami and extend from the caudal border of the symphyseal skin subregion to the paired orifices of the gular glands located at the caudal border of the intermandibular skin region (Fig. 2.8A).

In the relaxed condition, the skin is tightly pleated accordion-like into crests and grooves that parallel the mandibular rami (Fig. 2.8C and E). The crests comprise hard-cornified areas as well as soft-cornified areas. The grooves lie deeply between the crests and are completely hidden from view; they may bear some interscale tuberosities. For descriptive purposes, the crests are comparable to scales and the grooves are comparable to interscale skin segments of other skin subregions.

In the hard-cornified areas of the crests and hard-cornified tuberosities of the grooves, the epidermis consists of a stratified, squamous epithelium with a *Stratum basale* of mostly spherical cells with some rare columnar cells and a thin *Stratum spinosum* of only one to two layers of polyhedral cells. In the *Stratum corneum ,* the precorneous layer exhibits a distinct dark purple stain, if stained with Weigert's Resorcin Fuchsin, and forms a compact layer of flattened hard-cornified cells that is about as thick as the living epidermis (Fig. 2.8E$_2$).

Underneath the epidermis of the hard-cornified areas of the crests and the hard-cornified tuberosities of the grooves, the dermal *Stratum laxum* is about 125-170 µm thick. The collagen fiber bundles are loosely arranged, but the elastic fiber bundles are oriented perpendicularly to the skin surface and anchor to the basement membrane. The *Stratum compactum* is made up of parallel collagen fiber bundles that are oriented along the transverse body axis, anchor to the small hard-cornified areas of the crests, and span the deep grooves that separate the crests. Collagenous *Retinacula cutis* fiber bundles originate from the deep layers of the *Stratum compactum* and anchor to the basement membrane of the hard-cornified areas.

In the soft-cornified areas of the crests and the interscale skin segments, the epidermis consists of a stratified squamous epithelium with a *Stratum basale* and *Stratum spinosum* are not distinguishable from those in the hard-cornified areas of the crest (see 2.3.1). The *Stratum corneum* might exhibit a precorneous layer that stains lightly, if at all, with Weigert's Resorcin Fuchsin; and forms a layer of soft-cornified, flattened cells that is about as thick as the living epidermis.

Underneath the epidermis of the soft-cornified areas of the crests and the soft-cornified grooves, the dermal *Stratum laxum* is much thinner than it is under the hard-cornified areas of the crests and is barely visible. The *Stratum compactum* is formed by parallel collagenous joint fiber bundles, which are oriented along the transverse body axis, span the soft-cornified

Figure 2.8 The pararamal skin subregion of the American Alligator (*Alligator mississippiensis*). (**A-B**) Orthographic images of a 3D reconstruction (Isosurface module, Avizo®) of the skin of the head, neck, and shoulder region to indicate the location of the pararamal skin subregion highlighted in pink. (A) Ventrolateral view. (B) Ventral view. (**C-D**) Digital mesoscopic images of the skin surface. (C) Relaxed condition. (D) Stretched condition. (**E-F**) Digital micrographs of histological sections through the pararamal skin subregion cut parallel to the transverse body axis (Weigert's Resorcin-Fuchsin staining). (E) Relaxed condition. (E_1) A groove with curved collagenous joint fiber bundles of the *Stratum compactum* and elastic fiber bundles from the *Stratum elasticum*. (E_2) A crest with hard-cornified and soft-cornified areas, as well as thin collagenous *Retinacula cutis* fiber bundles accompanied by elastic fiber bundles from the *Stratum elasticum*. (F) Stretched condition. (F_1) A groove with straightened collagenous joint fiber bundles of the *Stratum compactum*. (F_2) A crest with obliquely oriented collagenous *Retinacula cutis* fiber bundles. (**G-H**) Model of the stretch and recoil mechanism of the pararamal skin subregion to show the reorientation of the collagen and elastic fiber bundles, as well as the changes in the length and thickness of the skin as it stretches and recoils. (G) Relaxed condition. (H) Stretched condition. Abbreviations: C = crest, G = groove, GGO = gular gland orifice, SC = *Stratum compactum*, SE = *Stratum elasticum*, SF = *Fascia superficialis*, SL = *Stratum laxum*. Symbols: dashed line = plane of section for histology; arrowheads (black = interscale tuberosity, blue = elastic fiber bundles of the *Stratum elasticum*, green = soft-cornified area of crest, orange = collagenous joint fiber bundles of the *Stratum compactum* of the interscale skin segment, purple = hard-cornified area of crest, red = collagenous *Retinacula cutis* fiber bundles of the *Stratum compactum* accompanied by elastic fiber bundles from the *Stratum elasticum*).
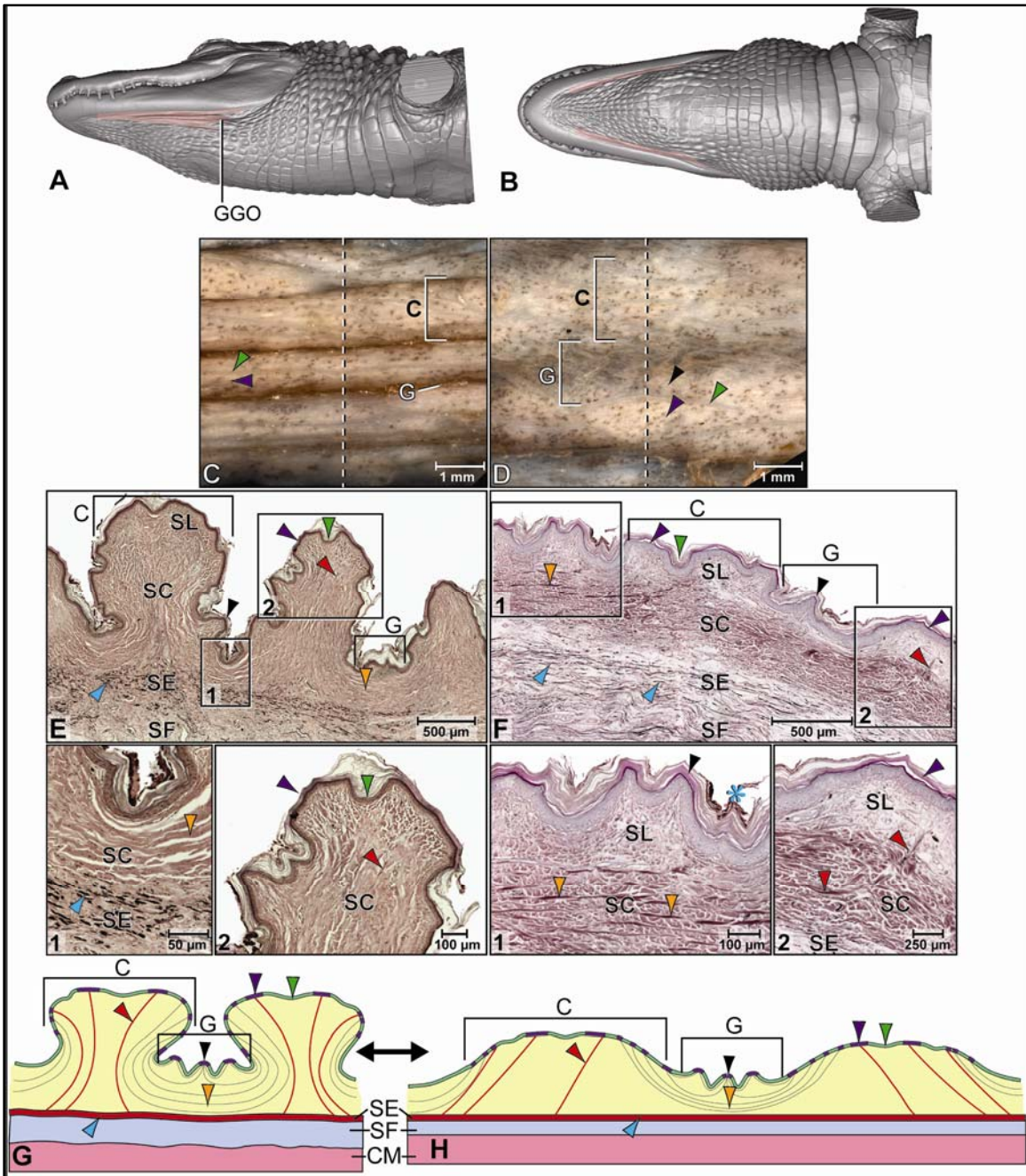
areas of the crests or soft-cornified interscale skin segments, and anchor to the basement membrane of the hard-cornified areas of the crests (Fig. 2.8E$_{1-2}$).

Underneath the *Stratum compactum,* the dermal *Stratum elasticum* is uniform and thick, consisting of about 15-20 layers of relaxed and wavy elastic fiber bundles that are oriented parallel to the transverse and sagittal body axes, as well as obliquely from craniomedial to caudolateral and from craniolateral to caudomedial (Fig. 2.8E$_1$). The elastic fiber bundles span both the crests and grooves and accompany the collagenous fiber bundles of the *Retinacula cutis* towards the skin surface to attach to the basement membrane of the hard-cornified areas of the crests and occasionally to the interscale tuberosities in the grooves (Fig. 2.8E$_2$).

The uniform *Fascia superficialis* is thick, especially near the gular gland, where it can be approximately twice as thick as the entire dermis and epidermis together. It is composed of a loose mass of collagen and elastic fiber bundles, amorphous ground substance, and large blood vessels and nerves. Near the gular gland it is interlarded with adipose tissue.

In the stretched condition, the crests are moved apart and flattened, and the skin of the grooves is stretched and exposed (Fig. 2.8D and F). The entire skin of this subregion becomes fanshaped with the apex of the fan pointing rostrally and widening caudally (Fig. 2.8A). The collagenous joint fiber bundles of the *Stratum compactum*, which span the grooves, are straightened (Fig. 2.8F$_1$). The elastic fiber bundles of the *Stratum elasticum* are also straightened and elongated. The collagenous *Retinacula cutis* fiber bundles, which originate from the deep layers of the *Stratum compactum* and are accompanied by elastic fiber bundles from the *Stratum elasticum*, are elongated and oriented obliquely to the skin surface (Fig. 2.8F$_2$). The *Fascia superficialis* is thinned, and the loosely arranged collagen and elastic fiber bundles are straightened and aligned along the direction of the stretching force.

➢ Functional Interpretation

Stretching mechanism (Fig. 2.8G → H): The skin fans out transverse-obliquely when it is stretched along the transverse body axis. As the skin stretches, the crests are pulled apart and the collagenous joint fiber bundles are tightened. As a consequence, the crests and grooves are flattened. As the elastic fiber bundles of the *Stratum elasticum* and the *Fascia superficialis* first straighten and then lengthen, they store elastic energy.

Recoil mechanism (Fig. 2.8H → G): When the stretching force subsides, the elastic fiber bundles in the *Stratum elasticum* and the *Fascia superficialis* release their elastic energy and

return to their shorter resting configuration.   The shortening of these elastic fiber bundles causes the connective tissue underneath the crests to be pushed upwards as the collagen fiber bundles of the *Stratum compactum* release their tension and return to their folded resting configuration so that the skin is folded back accordion-like. As the crests move towards each other, the grooves dip down between them.

- **Paralingual Skin Subregion**
  ➤ Morphological Description

The paired paralingual skin subregions lie along the medial sides of the paired pararamal skin subregions and extend from the caudal border of the symphyseal skin subregion to the caudal border of the intermandibular skin region (Figs. 2.2 and 2.3). The paralingual skin subregions comprise oval scales that are arranged in rows that are oriented obliquely from craniomedial to caudolateral.

In the relaxed condition, each scale touches its adjacent scale, and the long soft-cornified interscale segments are deeply folded and completely hidden from view (Fig. 2.9C and E). The epidermis of the interscale segments is studded with hard-cornified tuberosities.

The scale epidermis consists of a stratified squamous hard-cornified epithelium with a *Stratum basale* of tall columnar cells and a *Stratum spinosum* of about three to five cell layers. The *Stratum corneum* is about 25-30 µm thick and forms a compact layer of hard-cornified, flattened cells (see 2.3.1).

Underneath the scale epidermis, the dermal *Stratum laxum* is about 100 µm thick and consists of collagen and elastic fiber bundles. The collagen fiber bundles are loosely arranged, but the elastic fiber bundles are oriented perpendicularly to the skin surface and anchor to the basement membrane (Fig. 2.9E$_1$). The *Stratum compactum* comprises layers of collagen fiber bundles that are arranged in orthogonal layers and are oriented from craniomedial to caudolateral. Collagenous *Retinacula cutis* fiber bundles originate from the deep layers of the *Stratum compactum* and anchor to the basement membrane of the hard-cornified areas and are accompanied by elastic fiber bundles that originate from the *Stratum elasticum* (Fig. 2.9E$_{1-2}$). Neurovascular bundles traverse the *Stratum compactum* at the base of each scale and are oriented along the sagittal body axis (Fig. 2.9E).

46

In the interscale skin segments, the epidermis consists of a stratified, squamous soft-cornified epithelium with a *Stratum basale* of spherical cells and a *Stratum spinosum* of about 3-4 cell layers. The *Stratum corneum* is about 40 µm thick and forms a layer of soft-cornified, flattened cells (see 2.3.1).

Underneath the epidermis of soft-cornified interscale skin segments, the dermal *Stratum laxum* thins out so that it is barely visible. The *Stratum compactum* is made up of parallel collagenous joint fiber bundles that are oriented along the transverse and sagittal body axes (see 2.3.1) that span the width of the interscale skin segment and attach to the basement membrane of the hard-cornified epidermis of adjacent scales and the hard-cornified interscale tuberosities (Fig. 2.9E_3 and F_2).

In the hard-cornified interscale tuberosities, the epidermis is the same as that in the hard-cornified scale epidermis. The dermal *Stratum laxum* forms the core of the tuberosities, and the *Stratum compactum* is formed by the superficial collagen fiber bundles of the collagenous joint fibers, which attach to them.

Underneath the *Stratum compactum* of both the scales and the interscale skin segments, the uniform *Stratum elasticum* is thick, consisting of about ten to twelve layers of tightly packed, relaxed and wavy elastic fiber bundles that are oriented parallel to the transverse and sagittal body axes, as well as obliquely from craniomedial to caudolateral and from craniolateral to caudomedial. The elastic fiber bundles span both the scales and interscale skin segments and follow the collagen fiber bundles of the *Retinacula cutis* towards the surface to attach to the basement membrane of the hard-cornified scales and occasional interscale tuberosities.

The uniform *Fascia superficialis* blends with and is indistinguishable from the epimysium of the rostral one-third of the *M. intermandibularis* at the midventral line, where the three layers (epimysium, *Fascia superficialis* and dermis) are tightly adhered to one another (Fig. 2.9F). In the caudal two-thirds of the of the intermandibular region, the *Fascia superficialis* does not adhere to the epimysium of the *M. intermandibularis* and the dermis; and it is about as thick as it is under the pararamal skin subregion and is composed of loosely arranged of collagen and elastic fiber bundles, amorphous ground substance, and large blood vessels and nerves (Fig. 2.9E).

In the stretched condition, adjacent scales are moved apart and the soft-cornified interscale segments between them are unfolded, stretched, and exposed (Fig. 2.9D and F). The collagenous

47

joint fiber bundles, which span the interscale skin segments, are straightened (Fig. 2.9F$_2$). The elastic fiber bundles of the *Stratum elasticum* are also straight and longer than they were in the relaxed condition. The collagenous *Retinacula cutis* fiber bundles, which are accompanied by elastic fiber bundles from the *Stratum elasticum* and attach to the basement membrane of the hard-cornified scales, are elongated and oriented obliquely to the skin surface (Fig. 2.9F$_1$). The *Fascia superficialis* is thinned, and the loosely arranged collagen and elastic fiber bundles are straightened and aligned along the direction of the stretching force.

➢ Functional Interpretation

Stretching mechanism (Fig. 2.9G → H): Because the scales are connected by deeply in-folded segments of soft-cornified interscale skin on all sides, this subregion is expandable along both the transverse and sagittal body axes, and the stretching mechanism is the same for the interscale skin segments on all sides of the scales (rostral, caudal, medial, and lateral). As the scales are pulled apart from one another in the transverse or sagittal planes, the collagenous joint fiber bundles straighten and tighten. As a consequence, they pull down the scales, and the skin is flattened. As the elastic fiber bundles of the *Stratum elasticum* and the *Fascia superficialis* first straighten and then lengthen, they store elastic energy.

Recoil mechanism (Fig. 2.9H → G): When the stretching force subsides, the elastic fiber bundles in the *Stratum elasticum* and *Fascia superficialis* release their elastic energy and return to their shorter resting configuration. This shortening of the elastic fiber bundles causes the connective tissue underneath the scales to be pushed upwards, as the collagen fiber bundles of the *Stratum compactum* release their tension on scale edges. The hard-cornified scales move closer to one another, the collagenous joint fibers bundles of the *Stratum compactum* return to their pre-folded configuration, and the soft-cornified interscale skin segments refold.

• **Sublingual Skin Subregion**

➢ Morphological Description

The unpaired sublingual skin subregion lies along the midline of the intermandibular skin region between the paired paralingual skin subregions and extends from the caudal border of the symphyseal skin subregion to the rostral border of the subhyoid skin subregion (Fig 2.3). It comprises rectangular scales that are arranged in rows that are oriented along the transverse and

Figure 2.9 The paralingual skin subregion of the American Alligator (*Alligator mississippiensis*). (**A-B**) Orthographic images of a 3D reconstruction (Isosurface module, Avizo®) of the skin of the head, neck, and shoulder region to indicate the location of the paralingual skin subregion highlighted in dark red. (A) Ventrolateral view. (B) Ventral view. (**C-D**) Digital mesoscopic images of the skin surface. (C) Relaxed condition. (D) Stretched condition. (**E-F)** Digital micrographs of histological sections through the paralingual skin subregion cut parallel to the transverse body axis (Weigert's Resorcin-Fuchsin staining). (E) Relaxed condition. (E_1) A scale with hard-cornified epidermis and attached collagenous *Retinacula cutis* fiber bundles in the *Stratum compactum* and accompanying elastic fiber bundles from the *Stratum elasticum.* (E_2) Origin of elastic fiber bundles from the *Stratum elasticum*. (E_3) An interscale skin segment with concentrically curved collagenous joint fiber bundles of the *Stratum compactum*. (F) Stretched condition. (F_1) A scale and underlying dermis with obliquely oriented collagenous *Retinacula cutis* fiber bundles. (F_2) An interscale skin segment with the straightened collagenous joint fiber bundles of the *Stratum compactum*. (**G-H**) Model of the stretch and recoil mechanism of the paralingual skin subregion to show the reorientation of the collagen and elastic fiber bundles, as well as the changes in the length and thickness of the skin as it stretches and recoils. (G) Relaxed condition. (H) Stretched condition. Abbreviations: INT = interscale skin segment, NV = neurovascular bundle, S = scale, SC = *Stratum compactum*, SE = *Stratum elasticum*, SF = *Fascia superficialis*, SL = *Stratum laxum*. Symbols: dashed line = plane of section for histology; arrowheads (black = interscale tuberosity, blue = elastic fiber bundles of the *Stratum elasticum*, orange = collagenous joint fiber bundles of the *Stratum compactum* of the interscale skin segment, red = collagenous *Retinacula cutis* fibers of the *Stratum compactum* accompanied by elastic fiber bundles from the *Stratum elasticum*).

49
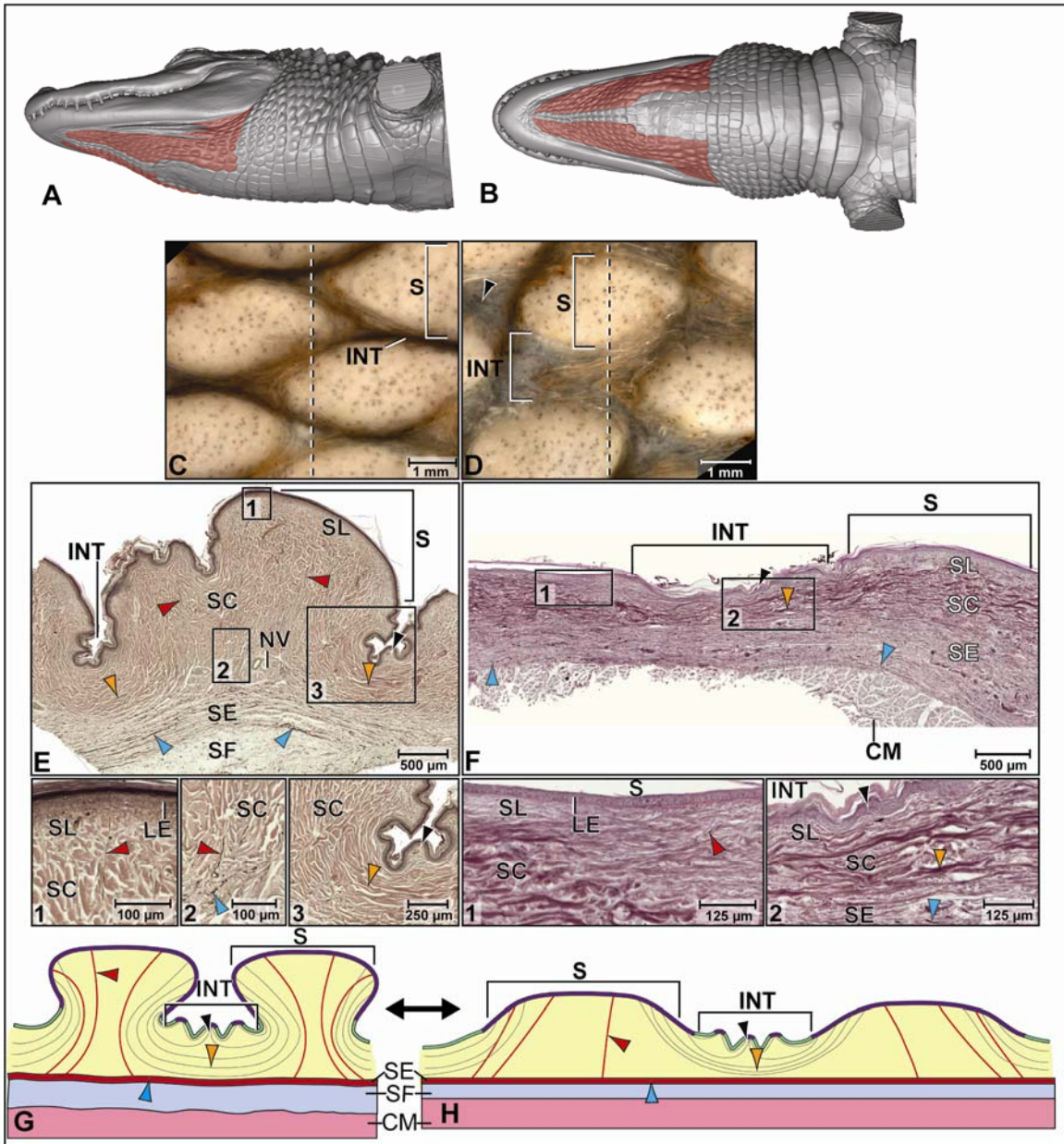
sagittal body axes.

In the relaxed condition, each scale touches its adjacent scale, while the long soft-cornified interscale segments are deeply folded and hidden from view (Fig. 2.10C and E). The epidermis of the interscale segments is studded with hard-cornified tuberosities.

The scale epidermis consists of a stratified squamous hard-cornified epithelium with a *Stratum basale* of tall columnar cells and a *Stratum spinosum* of about 3-5 cell layers. The *Stratum corneum* is about 50 µm thick and forms a compact layer of hard-cornified, flattened cells (see 2.3.1).

Underneath the scale epidermis, the dermal *Stratum laxum* is about 150-200 µm thick and consists of collagen and elastic fiber bundles. The collagen fibers are loosely arranged, but the elastic fiber bundles are oriented perpendicularly to the skin surface and anchor to the basement membrane. These elastic fiber bundles originate from the *Stratum elasticum* (Fig. 2.10E_2). The *Stratum compactum* comprises layers of wavy collagen fiber bundles that are arranged in orthogonal layers and are oriented along the transverse and sagittal body axes. Collagenous *Retinacula cutis* fiber bundles, which originate from the deep layers of the *Stratum compactum*, are accompanied by elastic fiber bundles from the *Stratum elasticum* (Fig 2.10E_2) and run perpendicular toward the skin surface, where they anchor to the basement membrane of the hard-cornified scales. Neurovascular bundles with conspicuously large lymphatic vessels (up to 500 µm diameter) run between the *Stratum compactum* and the *Stratum elasticum* underneath the scales, and are oriented along the sagittal body axis (Fig. 2.10E, E_2 and F_1).

The epidermis of the interscale skin segments consists of a stratified squamous soft-cornified epithelium with a *Stratum basale* of spherical cells and a *Stratum spinosum* of about three to five cell layers. The *Stratum corneum* is about 30 µm thick and forms a layer of soft-cornified, flattened cells (see 2.3.1).

Underneath the *Stratum compactum* of both the scales and the interscale skin segments, the uniform *Stratum elasticum* is thin, consisting only of about five to seven layers of loosely arranged, relaxed and wavy elastic fiber bundles that are oriented mainly along the transverse and sagittal body axes (Fig. 2.10E_{1-2} and F_{1-2}). The elastic fiber bundles follow the collagenous *Retinacula cutis* towards the skin surface to attach to the basement membrane of the hard-cornified scales and occasionally to the interscale tuberosities.

51

The *Fascia superficialis* is thickest under the scales (about 700-800 µm) and thins out underneath the interscale skin segments. It blends with the epimysium of the *M. intermandibularis*, where it adheres to the integument. It consists of a loose mass of collagen and elastic fiber bundles, amorphous ground substance, and large blood vessels and nerves (Fig. 2.10E).

In the stretched condition, adjacent scales are moved apart and the soft-cornified interscale skin segments between them are unfolded, stretched, and exposed (Fig. 2.10D and F). The collagenous joint fiber bundles in the *Stratum compactum* span the interscale skin segments and are straight (Fig. 2.10F$_1$). The elastic fiber bundles of the *Stratum elasticum* are also straight and longer than they are in the relaxed condition. The collagenous *Retinacula cutis* fiber bundles, which are accompanied by elastic fiber bundles from the *Stratum elasticum*, are oriented obliquely to the skin surface and straightened (Fig. 2.10F$_2$). The *Fascia superficialis* is thinned, and the loosely arranged collagen and elastic fiber bundles are straightened and aligned along the direction of the stretching force.

> Functional Interpretation

Stretching mechanism (Fig. 2.10G → H): Because the scales are separated by deeply folded segments of soft-cornified interscale skin on all sides, this skin subregion is expandable along both the transverse and sagittal body axes with the same stretching mechanism. As the scales are pulled apart from one another in the transverse or sagittal planes, the wavy collagenous joint fiber bundles are pulled taut. As a consequence, they pull down the scales to which they attach, and the skin is flattened. As the elastic fiber bundles of the *Stratum elasticum* and *Fascia superficialis* first straighten and then lengthen, they store elastic energy.

Recoil mechanism (Fig. 2.10H → G): When the stretching force subsides, the elastic fiber bundles in the *Stratum elasticum* and *Fascia superficialis* release their elastic energy and return to their shorter relaxed configuration. The shortening of the elastic fiber bundles causes the hard-cornified scales to move closer to one another, thereby pushing the connective tissue underneath the scales upwards, as the collagenous joint fiber bundles of the *Stratum compactum* release their tension on the scale edges. The hard-cornified scales move closer to one another, the collagenous joint fiber bundles of the *Stratum compactum* return to their pre-folded and wavy configuration, and the soft-cornified interscale skin segments refold.

52

- **Subhyoid Skin Subregion**

  ➢ <u>Morphological description</u>

The unpaired subhyoid subregion is a large midventral skin subregion. It lies between the paired paralingual skin subregions and extends from the caudal border of the sublingual skin subregion to the rostral border of the gular skin region (Figs. 2.2 and 2.3). Its square scales are arranged in rows that are oriented along the transverse and sagittal body axes. Among the intermandibular skin subregions, it is the only one whose expansibility along the sagittal body axis differs from the expansibility in the transverse body axis. Whereas it is bendable as well as slightly expandable along the sagittal body axis, it is only bendable along the transverse body axis. This skin subregion forms a plate that subtends and supports the hyolaryngeal apparatus (Fig. 2.7).

In the relaxed condition, along the sagittal body axis, the caudal edge of each scale is raised slightly above the rostral edge of the scale behind it (Fig. 2.11E). The interscale skin segments are short and not deeply infolded. They provide flexibility and limited expansibility between the scales. Small interscale tuberosities may be present, but are scarce. Along the sagittal body axis, the scales are on an even level (Fig. 2.11H). The interscale segments are extremely short and, therefore, only bendable, but not expandable (Fig. 2.11 H and H_1).

The scale epidermis consists of a stratified squamous hard-cornified epithelium with a *Stratum basale* of tall columnar cells and a *Stratum spinosum* of about two to three cell layers. The *Stratum corneum* is about 35-40 µm thick and forms a compact layer of hard-cornified, flattened cells (see 2.3.1).

Underneath the scale epidermis, the dermal *Stratum laxum* is about 200 µm thick and consists of collagen and elastic fiber bundles. The collagen fiber bundles are loosely arranged, but elastic fiber bundles are oriented perpendicularly to the skin surface and anchor to the basement membrane of the scale epidermis. The *Stratum compactum* comprises layers of collagen fiber bundles that are arranged in orthogonal layers and are oriented along the transverse and sagittal body axes. Collagenous *Retinacula cutis* fiber bundles, which originate from the deeper layers of the *Stratum compactum*, run perpendicularly to the skin surface and

Figure 2.10 The sublingual skin subregion of the American Alligator (*Alligator mississippiensis*). (**A-B**) Orthographic images of a 3D reconstruction (Isosurface module, Avizo®) of the skin of the head, neck, and shoulder region to indicate the location of the sublingual skin subregion highlighted in pink. (A) Ventrolateral view. (B) Ventral view. (**C-D**) Digital mesoscopic images of the skin surface. (C) Relaxed condition. (D) Stretched condition. (**E-F**) Digital micrographs of histological sections through the sublingual skin subregion cut parallel to the transverse body axis (Weigert's Resorcin-Fuchsin staining). (E) Relaxed condition. (F) Stretched condition. (E_1) An interscale skin segment with curved and wavy collagenous joint fiber bundles in the *Stratum compactum*. (E_2) Elastic fiber bundles of the *Stratum elasticum* accompanying the collagenous *Retinacula cutis* fiber bundles anchoring to the basement membrane of the scale epidermis. (F_1) An interscale skin segment with straightened collagenous joint fiber bundles of the *Stratum compactum*. (F_2) Dermis underlying an interscale skin segment with obliquely oriented collagenous *Retinacula cutis* fiber bundles. (**G-**H) Model of the stretch and recoil mechanism of the sublingual skin subregion to show the reorientation of the collagen and elastic fiber bundles, as well as the changes in the length and thickness of the skin as it stretches and recoils. (G) Relaxed condition. (H) Stretched condition. Abbreviations: CM = constrictor musculature, INT = interscale skin segment, LE = living spidermis, V = lymphatic vessel, S = Scale, SC = *Stratum compactum*, SE = *Stratum elasticum*, SF = *Fascia superficialis*, SL = *Stratum laxum*. Symbols: dashed line = plane of section for histology; arrowheads (black = hard-cornified tuberosity, blue = elastic fiber bundles of the *Stratum elasticum*, orange = collagenous joint fiber bundles of the *Stratum compactum* in an interscale skin segment, red = collagenous *Retinacula cutis* fibers of the *Stratum compactum* accompanied by elastic fiber bundles of the *Stratum elasticum*).

54
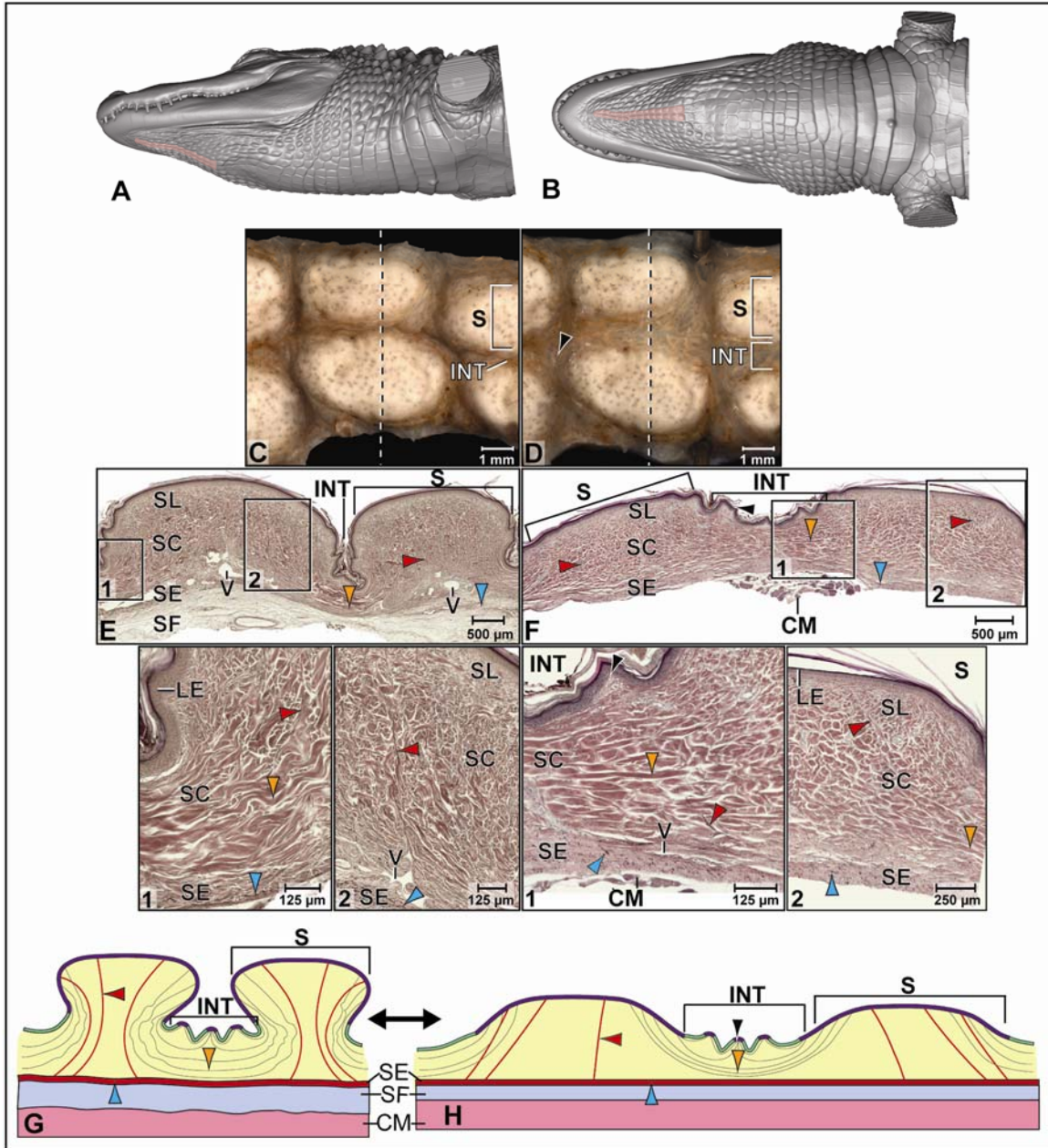
Figure 2.11 The subhyoid skin subregion of the American Alligator (*Alligator mississippiensis*) (see also Fig. 11 cont'd). (**A-B**) Orthographic images of a 3D reconstruction (Isosurface module, Avizo®) of the skin of the head, neck, and shoulder region to indicate the location of the subhyoid skin subregion highlighted in red. (A) Ventrolateral view. (B) Ventral view. (**C-D**) Digital mesoscopic images of the skin surface; the dashed line indicates the plane of section for histology. (C) Relaxed condition. (D) Convexly bent condition. (**E-F**) Digital micrographs of histological sections through the sublingual skin subregion cut parallel to the sagittal body axis (Weigert's Resorcin-Fuchsin staining). (E) Relaxed condition. (E_1) An interscale skin segment with the curved collagenous joint fiber bundles of the *Stratum compactum*. (E_2) Deep layer of the *Stratum compactum* with the origin of collagenous *Retinacula cutis* fiber bundles and sparse elastic fiber bundles from the *Stratum elasticum*. (F) Convexly bent condition. (F_1) An interscale skin segment with straightened collagenous joint fiber bundles of the *Stratum compactum*. (F_2) Deep layer of the *Stratum compactum* and collagenous *Retinacula cutis* fiber bundles. (G) Digital mesoscopic image of the skin surface; the dashed line indicates the plane of section for histology. (H) Digital micrograph of a histological section through the subhyoid skin subregion cut parallel to the transverse body axis. (H_1) Interscale skin segment that is bendable, but not expandable, with curved collagenous joint fiber bundles in the *Stratum compactum*. (H_2) Dermis underneath a scale with numerous collagenous *Retinacula cutis* fiberbundles and sparse elastic fiber bundles from the *Stratum elasticum*. (H_3) *Stratum laxum* underneath a scale with elastic fiber bundles arranged perpendicularly to the skin surface. (H_4) *Stratum elasticum* and *Fascia superficialis* with sparse elastic fiber bundles. (I-J) Model of the bending and recoil mechanism of the subhyoid skin subregion in the sagittal body axis showing the reorientation of the collagen and elastic fiber bundles and the changes in the length and thickness of the skin; the model for the subhyoid skin subregion in the transverse body axis is similar except that the interscale skin segment does not elongate. (I) Relaxed condition. (J) Convexly bent condition. Abbreviations: CM = constrictor musculature, INT = interscale skin segment, LE = living epidermis, M = encapsulated lamellar mechanoreceptor, S = scale, SC = *Stratum compactum*, SE = *Stratum elasticum*, SF = *Fascia superficialis*, SL = *Stratum laxum*. Symbols: Arrowheads (black = hard-cornified tuberosity, blue = elastic fiber bundles of the *Stratum elasticum*, orange = collagenous joint fiber bundles of the *Stratum compactum* in the interscale skin segment, lime green = straight collagen fiber bundles of the orthogonal layers of the *Stratum compactum* under a scale, red = collagenous *Retinacula cutis* fiber bundles of the *Stratum compactum* accompanied by elastic fiber bundles of the *Stratum elasticum*).

Figure 2.11 (cont'd)

58
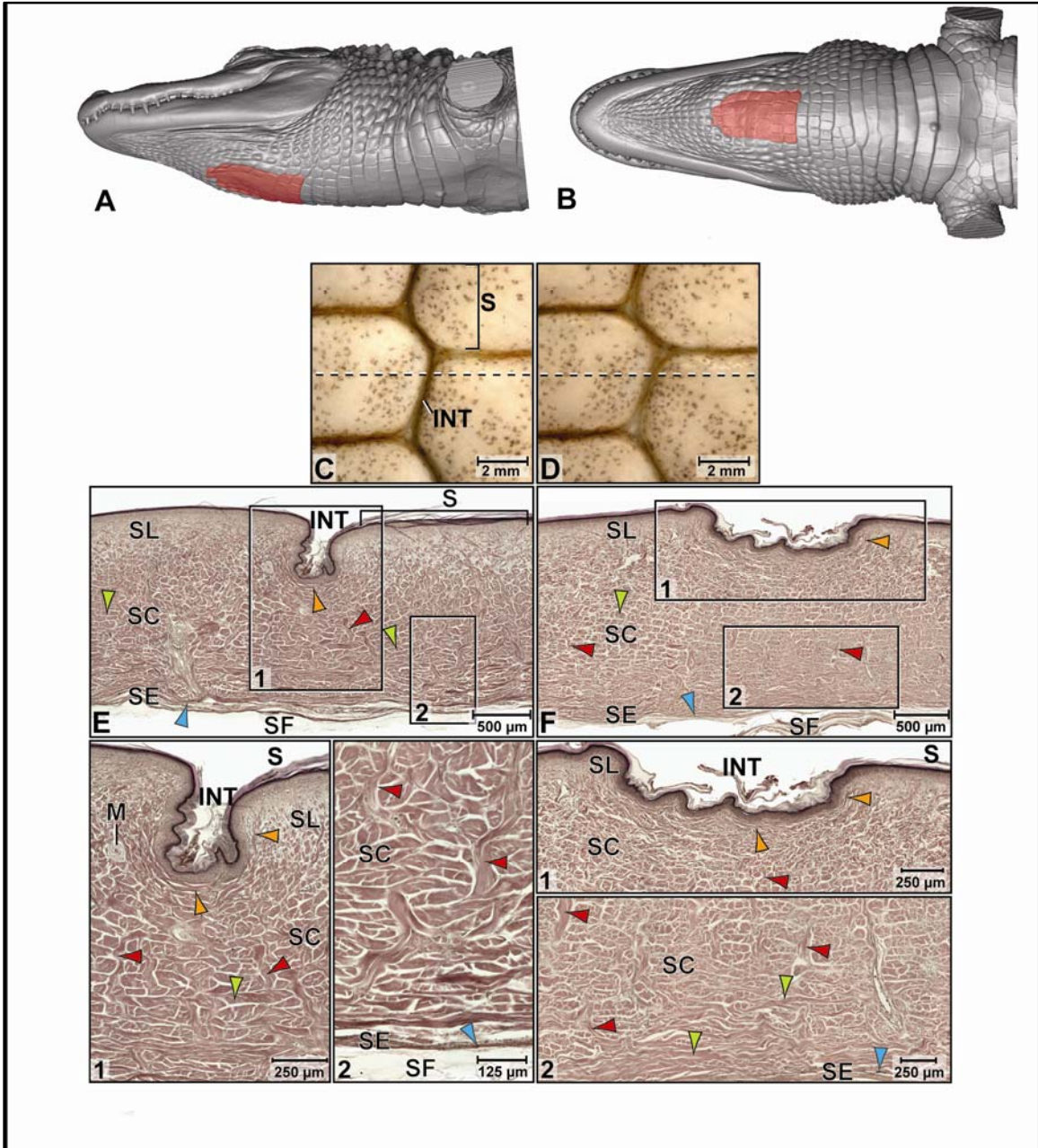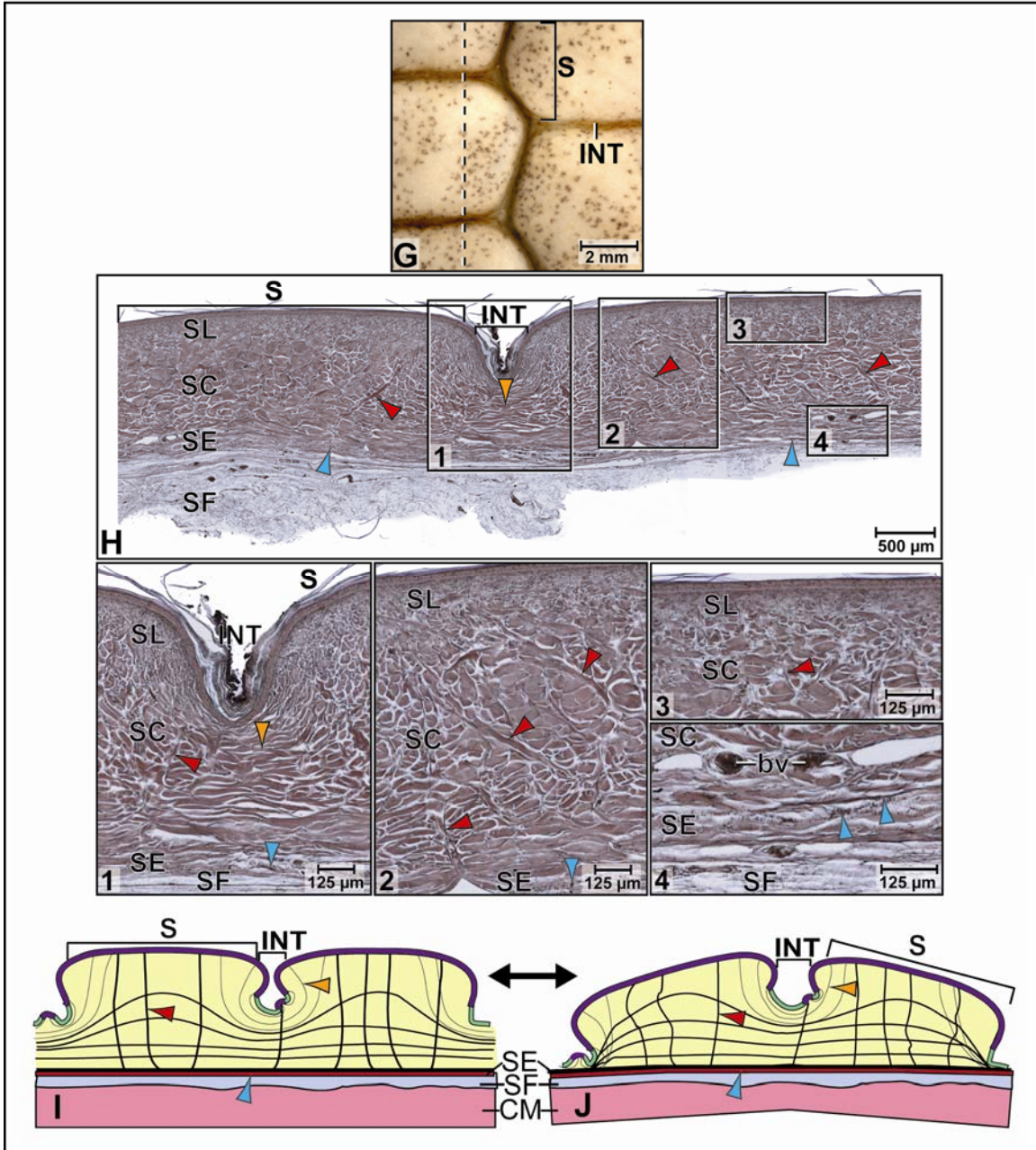
appear to anchor to the basement membrane of the scales (Figs. 2.11E$_1$,E$_2$, F$_2$, H$_1$ and H$_3$). They are accompanied by elastic fiber bundles that originate from the *Stratum elasticum* (see below).

In the interscale skin segment, the epidermis consists of a stratified squamous soft-cornified epithelium with a *Stratum basale* of spherical cells and a *Stratum spinsoum* of about 3-5 cell layers. The *Stratum corneum* is about 40 µm thick and forms a layer of soft-cornified, flattened cells (see 2.3.1).

Underneath the epidermis of the soft-cornified interscale skin segments, the dermal *Stratum laxum* thins out so that it is barely visible. Along the sagittal body axis, the most superficial layer of the *Stratum compactum* consists of parallel and short collagenous joint fiber bundles (see 2.3.1), which attach to the basement membrane of the adjacent scales (Fig. 2.11E$_1$). Along the transverse body axis, these collagenous joint fiber bundles are extremely short (Fig. 2.11H$_1$). The deeper layer of the *Stratum compactum* comprises the extension of the orthogonal collagen fiber bundles from the *Stratum compactum* underneath the scales.

Underneath the *Stratum compactum* of both the scales and interscale skin segments, the uniform *Stratum elasticum* is thin, consisting of only about three to five layers of loosely packed, relaxed elastic fiber bundles that are oriented parallel to the transverse and sagittal body axes. The elastic fiber bundles follow the collagenous *Retinacula cutis* towards the skin surface to attach to the basement membrane of the scales and of the occasional interscale tuberosities (Fig. 2.11E$_1$).

The *Fascia superficialis* is thinner (about 80 µm) than in the other intermandibular skin subregions and is composed of a loose mass of collagen and elastic fiber bundles, amorphous ground substance, and sparse blood vessels and nerves.

This subregion is flexible and bendable, but can be slightly elongated only along the sagittal body axis. In the flexed position, the caudal edge of the rostral scale is moved away from the rostral edge of the scale behind it, and the soft-cornified interscale skin segment between the two scales is flexed and stretched (Fig. 2.11D and F). The collagenous joint fiber bundles of the superficial layer of the *Stratum compactum* are straightened (Fig. 2.11F$_1$). The elastic fiber bundles of the *Stratum elasticum* are also straightened and lengthened. The collagenous *Retinacula cutis* fiber bundles are straightened near the flexed and stretched interscale skin segment, because the scale edges are slightly rotated upwards (Fig. 2.11F). The *Retinacula cutis* fiber bundles are more relaxed towards the sides of the scales that are rotated downwards in the

flexed position. The *Fascia superficialis* is thinned and the loosely arranged collagen and elastic fiber bundles are straightened and aligned along the direction of the stretching force.

➢ Functional Interpretation

Transverse bending and sagittal expansion mechanism (Fig. 2.11I → J): Because the rostral and caudal edges of the scales are separated by folded, flexible transverse interscale skin segments, this skin subregion is flexible and slightly expandable along the sagittal body axis in contrast to the lateral and medial edges of the scales. As the rostral and caudal scales are pulled apart from one another in the sagittal plane, the soft-cornified interscale skin segment between them unfolds and stretches and the collagenous joint fiber bundles straighten and become taut. As the interscale skin segment is stretched, the edges of the adjacent scales are rotated upwards, while the opposite edges of the scales edges are rotated downwards, so that the skin assumes a convex curvature. As the elastic fiber bundles of the *Stratum elasticum* and the *Fascia superficialis* first straighten and then lengthen, they store elastic energy. Along the transverse body axis, the mechanism is very similar, except that the interscale skin segments do not elongate at all.

Recoil mechanism (Fig. 2.11J → I): When the stretching force subsides, the elastic fiber bundles of the *Stratum elasticum* and *Fascia superficialis* release their elastic energy and return to their shorter resting configuration. As a consequence, the collagenous joint fiber bundles of the *Stratum compactum* release their tension on the edges of the scales edges, which rotate back to their flatter resting position and are moved closer to one another. The collagenous joint fiber bundles return to their pre-folded configuration, and the soft-cornified interscale skin segment refolds.

2.3.3. Gular Skin Region

The gular skin region is situated caudal to the angle of the jaw and covers the ventral and lateral sides of the underlying the gullet (Fig. 2.2B and C). Its rostral border coincides with the caudal border of the underlying *M. intermandibularis* and the rostral border of the *M. constrictor colli gularis*, and its caudal border coincides with the caudal border of the *M. constrictor colli gularis* and rostral border of the *M. constrictor colli cervicalis* (see 2.2.3 and 3.3.3). Ventrally, the gular skin region comprises square scales that are oriented in rows along the transverse and

60

sagittal body axes. Laterally, it comprises raised round scales that are oriented in rows along the transverse and sagittal body axes (Fig. 2.3B-D).

- **Posthyoid Skin Subregion**
  - ➢ <u>Morphological Description</u>

The large midventral posthyoid skin subregion covers the entire length of the gular skin region, extending from its rostral border to its caudal border (Figs. 2.3A and B, 2.12A and B). Laterodorsally, it is bounded by the pterygoid skin subregion (see below). Its square or rectangular scales are arranged in rows that are oriented along the transverse and sagittal body axes. The posthyoid skin subregion, like the subhyoid skin subregion, is bendable as well as expandable along the sagittal body axis, but only bendable along the transverse body axis.

In the relaxed condition, and along the sagittal body axis, the caudal edge of each scale is raised above the cranial edge of the scale behind, so that it overlaps the interscale skin segment between the two scales (Fig. 2.12E). The interscale skin segment are long and deeply folded (Fig. 2.12E$_1$) and studded with hard-cornified interscale tuberosities. They provide flexibility as well as extensibility between scales. Along the transverse body axis, the scales are on an even level (Fig. 2.12H). The interscale segments are very short and not deeply folded, reaching only as deep as the dermal *Stratum laxum* of the adjacent scales (Fig. 2.12H$_1$), and, therefore, are not extensible.

The scale epidermis consists of a stratified squamous hard-cornified epithelium with a *Stratum basale* of tall columnar cells and a *Stratum spinosum* of about three to four cell layers. The *Stratum corneum* forms a compact layer of hard-cornified, flattened cells. It is about 130-150 µm thick at the center of a scale, but thins to about 50 µm towards the overlapping caudal edge of a scale (see 2.3.1).

Underneath the scale epidermis, the dermal *Stratum laxum* is about 400-500 µm thick at the center, but thins to about 125-150 µm towards the overlapping caudal edge of the scale. The collagen fibers are loosely arranged, but the elastic fiber bundles are oriented perpendicularly to the skin surface and anchor to the basement membrane. Underneath the cranial edge of a scale, the *Stratum compactum* comprises collagen fiber bundles that are arranged in orthogonal layers and are oriented along the transverse and sagittal body axes. Collagenous *Retinacula cutis* fiber

61

bundles, which originate from the deep layers of the *Stratum compactum*, run perpendicularly to the skin surface and anchor to the basement membrane.

Underneath the caudal overlapping edge of a scale, the *Stratum compactum* comprises layers of collagen fiber bundles that are arranged in orthogonal layers and are oriented along the transverse and sagittal body axes. Because this overlapping scale edge is raised and pushed over the cranial edge of the scale behind, the collagen fiber bundles that are oriented along the sagittal body axis appear to be oriented obliquely the surface of the epidermis, and extend into the folded tip of the edge of the scale (Fig. 2.12E).

In the interscale skin segments, the epidermis consists of a stratified squamous soft-cornified epithelium with a *Stratum basale* of spherical cells and a *Stratum spinosum* of about 5-6 cell layers. The *Stratum corneum* is about 50 µm thick and forms a layer of soft-cornified, flattened cells (see 2.3.1).

Underneath the epidermis of the interscale skin segments, the dermal *Stratum laxum* thins out and is barely visible. The *Stratum compactum* is made up of parallel collagenous joint fiber bundles and elastic fiber bundles, which span the interscale skin segments and anchor to the basement membrane of adjacent scales. The elastic joint fiber bundles of the interscale skin are unique to the overlapping scales of ventral neck skin (i.e., the posthyoid and ventral cervical skin subregions).

In the hard-cornified interscale tuberosities, the epidermis is the same as that of the hard-cornified scale epidermis, and the *Stratum laxum* forms their core. Some tuberosities serve as anchoring sites for collagenous *Retinacula cutis* fiber bundles that originate from the deep layers of the *Stratum compactum* and traverse the interscale skin segment to anchor on the basement membrane.

Underneath the *Stratum compactum* of both the scales and interscale skin segments, the uniform *Stratum elasticum* is thin, consisting of about four to five layers of loosely packed, relaxed elastic fiber bundles that are oriented parallel to the sagittal body axis. Some of the elastic fiber bundles follow the collagenous *Retinacula cutis* fiber bundles towards the skin surface to attach to the basement membrane of scales and some interscale tuberosities. Underneath the cranial edges of the scales, the most superficial layers of the *Stratum elasticum* encloses dermal fat bodies that surround small arteries and nerves (Fig. 2.12F$_1$).

62

Figure 2.12 The posthyoid skin subregion of the American Alligator (*Alligator mississippiensis*) (see also Fig. 2.12 cont'd). (**A-B**) Orthographic images of a 3D reconstruction (Isosurface module, Avizo®) of the skin of the head, neck, and shoulder region to indicate the location of the posthyoid skin subregion highlighted in green. (A) Ventrolateral view. (B) Ventral view. (**C-D**) Digital mesoscopic image of the skin surface; the dashed line indicates the plane of section for histology. (C) Relaxed condition. (D) Stretched condition. (**E-F**) Digital micrographs of histological sections through the posthyoid skin subregion cut parallel to the sagittal body axis (Weigert's Resorcin-Fuchsin staining). (E) Relaxed condition. (E_1) An interscale skin segment with collagenous joint fiber bundles of the *Stratum compactum* and collagenous *Retinacula cutis* anchoring to the basement membrane of the cranial edge of the caudal scale. (F) Stretched condition. (F_1) The *Stratum compactum* underneath the caudal edge of the cranial scale with straightened collagen fiber bundles of the orthogonal dermal layers and sparse elastic fiber bundles from the *Stratum elasticum*. (F_2) An interscale skin segment with collagenous joint fiber bundles of the *Stratum compactum* and collagenous *Retinacula cutis* anchoring to the cranial edge of the caudal scale edge. (**G**) Digital mesoscopic image of the skin surface; the dashed line indicates the plane of section for histology. (**H**) Digital micrograph of a histological section through the posthyoid skin subregion cut parallel to the transverse body axis (Weigert's Resorcin-Fuchsin staining). (H_1) An interscale skin segment with collagenous joint fiber bundles of the *Stratum compactum*, collagenous *Retinacula cutis*, and extensions of straightened collagen fiber bundles of dermal orthogonal layers from underneath scales. Abbreviations: CAS = caudal scale, CRS = cranial scale, DF = dermal fat, INT = interscale skin segment, SC = *Stratum compactum*, SE = *Stratum elasticum*, SF = *Fascia superficialis*, SL = *Stratum laxum*. Symbols: Arrowheads (blue = elastic fiber bundles of the *Stratum elasticum*, lime green = straight collagen fiber bundles of orthogonal dermal layers underneath a scale, orange = collagenous joint fiber bundles of the *Stratum compactum* in the interscale skin segment, red = collagenous *Retinacula cutis* fiber bundles of the *Stratum compactum* accompanied by elastic fiber bundles from the *Stratum elasticum*).
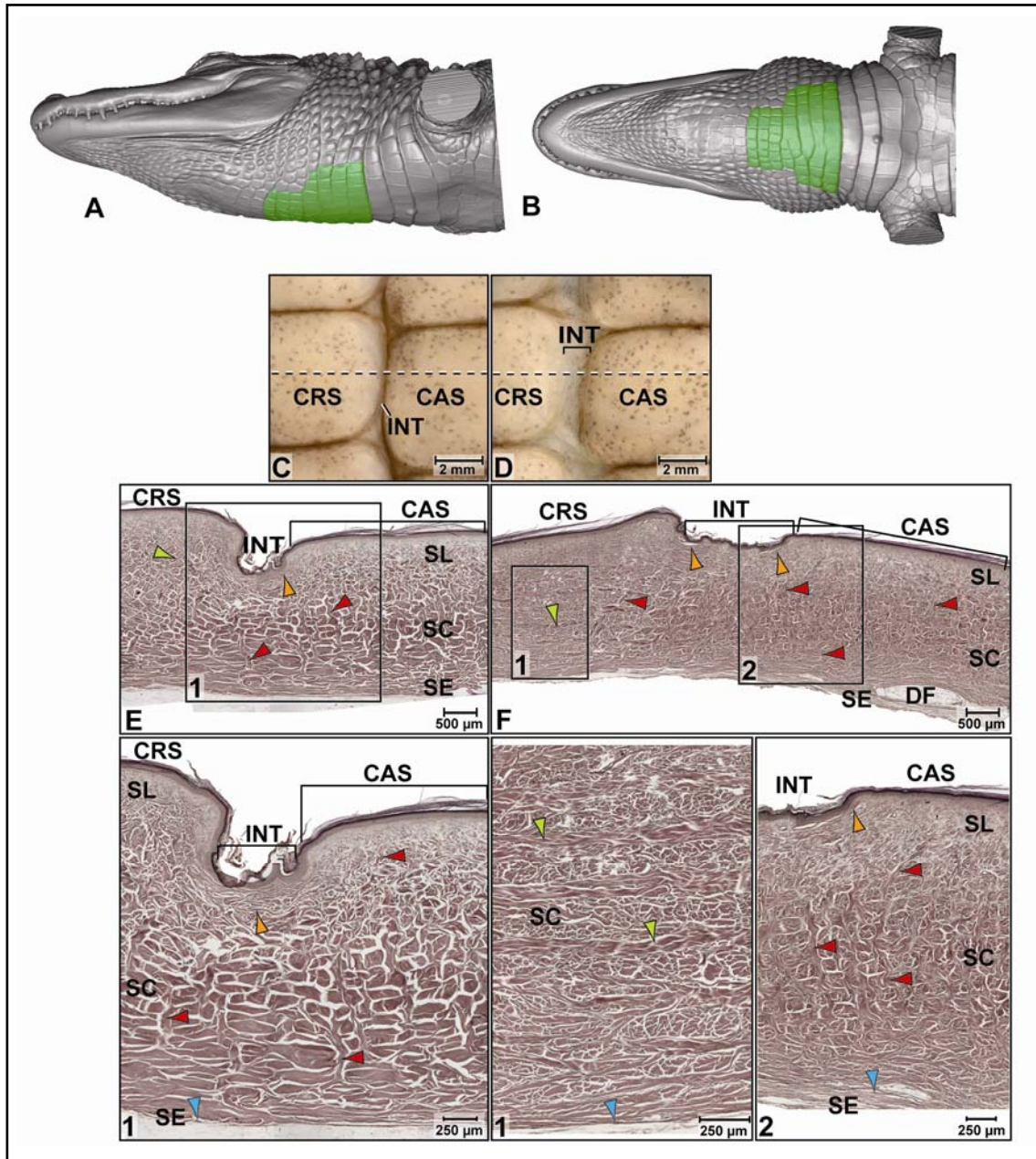
Figure 2.12 (cont'd)
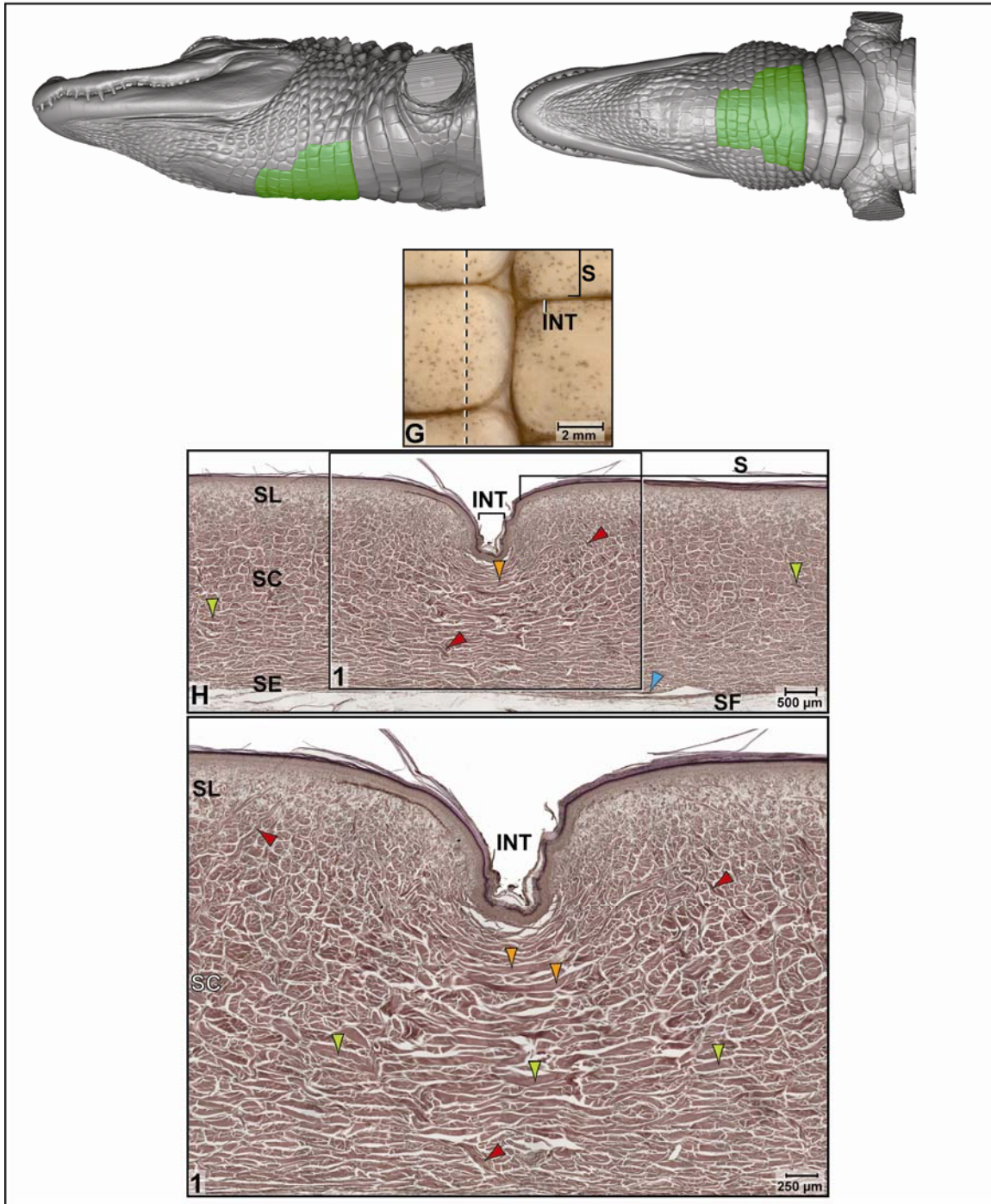
The *Fascia superficialis* is about 150 µm thick and contains loosely arranged collagen and elastic fiber bundles, amorphous ground substance and a loose network of blood vessels and nerves (Fig. 2.12H).

In the stretched condition, the caudal edge of a cranial scale is moved away from the cranial edge of the scale behind it, and both scales are brought to an even level. The interscale skin segment is stretched and exposed (Fig. 2.12D and F). The collagenous joint fiber bundles of the *Stratum compactum* are straightened, and the elastic joint fiber bundles in the *Stratum compactum* are straightened and lengthened. Likewise, the elastic fiber bundles from the *Stratum elasticum* are also straightened and lengthened, and the dermal fat bodies are compressed between them. The collagenous *Retinacula cutis* fiber bundles, which are accompanied by elastic fiber bundles from the *Stratum elasticum*, are oriented obliquely to the surface of the cranial edge of the scale to which they attach through the basement membrane. The obliquely oriented *Stratum compactum* collagen fiber bundles of the caudal scale edge that run parallel to the sagittal body axis are straightened (Fig. 2.12F and F_1). The *Fascia superficialis* is thinned, and the loosely arranged collagen and elastic fiber bundles are straightened and aligned along the direction of the stretching force.

➤ Functional Interpretation

The stretching mechanism of the transverse interscale skin segment (see model for ventral cervical skin subregion Fig. 2.15G → H): Because the cranial and caudal scale edges are separated by folded interscale skin segments, this skin subregion is expandable along the sagittal body axis. As the cranial and caudal scales are pulled apart from one another in the sagittal plane, the soft-cornified interscale skin segment between them is unfolded and expanded. The collagenous *Retinacula cutis* that anchor to the cranial edge of the caudal scale keep that edge of the scale immobilized as the caudal overlapping edge of the cranial scale is pulled away and lowered. The collagenous joint fiber bundles of the *Stratum compactum*, which anchor to the edges of the scales, straighten and the elastic joint fibers straighten and lengthen, storing elastic energy. Likewise, the elastic fiber bundles of the *Stratum elasticum* and the *Fascia superficialis* straighten, lengthen and store elastic energy. The fascial fat bodies under the cranial edge of the caudal scale are compressed.

The recoil mechanism of the transverse interscale skin segment (see model for ventral cervical skin subregion, Fig. 2.15H →G): When the stretching force subsides, the elastic joint

fiber bundles of the *Stratum compactum* of the interscale skin segment release their elastic energy and return to their shorter resting configuration. The elastic fiber bundles of the *Stratum elasticum* and *Fascia superficialis* also release their elastic energy and shorten. The shortening of the elastic fiber bundles causes the interscale skin segment to refold and the scales move closer to one another, thereby allowing the collagen fiber bundles underneath the caudal edge of the cranial scale to be pushed upwards, returning the scale edge to its overlapping resting position.

Stretch-resisting mechanism of the longitudinal interscale skin segments (Fig. 2.15K): Because the interscale skin segments of the lateral and medial edges of scales are very narrow and not deeply folded, they provide flexibility, but not circumferential expansion. As stretching forces increase, the straight collagen fiber bundles of the *Stratum compactum* oriented along the transverse body axis tighten and resist further lengthening and stretching and, thus, prevent further circumferential expansion of the skin.

- **Pterygoid Skin Subregion**
  - ➢ Morphological Description

The paired pterygoid gular skin subregions cover the bilateral ventrolateral bulges of the underlying pterygoid jaw musculature. They extend from the caudal borders of the paired paralingual skin subregions to the cranial border of the cervical skin region. Dorsolaterally, they are bounded by the retroarticular skin subregions (Fig. 2.3A and B).

The pterygoid skin subregions consist of scales that are flat and pentagonal medio-ventrally and raised and diamond-shaped latero-dorsally. The scales are arranged in rows that are generally oriented along the transverse and sagittal body axes, but the pentagonal and diamond-shaped scales require interscale skin segments that are oriented obliquely from craniomedial to caudolateral. The interscale skin segments are folded downward to a level just below that of the *Stratum laxum* of the scale dermis (Fig. 2.13E_2 and F_2) and are studded with interscale tuberosities (Fig. 2.13E_2). The infolding of the interscale skin segments and the additional, obliquely oriented interscale skin segments enable this skin subregion to expand radially as the underlying pterygoid musculature bulges when the jaws are closed (Fig. 2.7).

In the relaxed condition, each scale touches its adjacent scales, whereas the folded interscale skin segments are folded and hidden from view (Fig. 2.13A).

67

The scale epidermis consists of a stratified squamous hard-cornified epithelium with a *Stratum basale* of tall columnar cells and a *Stratum spinsosum* of about five to six cell layers. The *Stratum corneum* is about 50 µm thick and forms a compact layer of hard-cornified, flattened cells (see 2.3.1).

Underneath the scale epidermis, the dermal *Stratum laxum* is about 300 µm thick and consists of collagen fiber bundles that are thicker (about 10-20 µm) and more tightly packed than those in the *Stratum laxum* of other skin subregions. Collagen and elastic fiber bundles are oriented perpendicularly to the surface of the epidermis and anchor to its basement membrane (Fig. 2.13E$_1$); these elastic fiber bundles originate from the *Stratum elasticum* and accompany the *Retinacula cutis* fibers of the *Stratum compactum* (see below). The *Stratum compactum* comprises layers of wavy collagen fiber bundles that are arranged in orthogonal layers and are oriented along the transverse and sagittal body axes. Collagenous *Retinacula cutis* fiber bundles, which originate from the deep layers of the *Stratum compactum*, run perpendicularly to the skin surface and anchor to the basement membrane of the scales.

In the interscale skin segments, the epidermis consists of a stratified squamous soft-cornified epithelium with a *Stratum basale* of spherical cells and a *Stratum spinosum* of about six to seven cell layers. The *Stratum corneum* is about 50 µm thick and forms a layer of soft-cornified, flattened cells (see 2.3.1).

Underneath the epidermis of the interscale skin segments, the *Stratum laxum* thins out so that it is barely visible. The most superficial layer of the *Stratum compactum* is formed by parallel collagenous joint fiber bundles (see 2.3.1), which span the width of the folded interscale skin segment and attach to the basement membrane of the adjacent scales (Fig. 2.13 E$_2$, F$_2$). The deeper portion of the *Stratum compactum* is made up by an extension of the orthogonal layers of wavy collagen fiber bundles from the *Stratum compactum* underneath the scales (Fig. 2.13E and F$_{2-3}$).

In the hard-cornified interscale tuberosities, the epidermis is the same as that of the hard cornified scale epidermis, and the *Stratum laxum* forms their core. Some tuberosities serve as anchoring sites for collagenous *Retinacula cutis* fiber bundles that originate from the deep layers of the *Stratum compactum* and traverse the interscale skin segment to attach to the basement membrane (Fig. 2.13E$_2$).

Underneath the *Stratum compactum* of both the scales and the interscale skin segments, the

68

Figure 2.13 The pterygoid skin subregion of the American Alligator (*Alligator mississippiensis*). (**A-B**) Orthographic images of a 3D reconstruction (Isosurface module, Avizo®) of the skin of the head, neck, and shoulder region to indicate the location of the ventral pterygoid skin subregion highlighted in light green. (A) Ventrolateral view. (B) Ventral view. (**C-D**) Digital mesoscopic image of the skin surface; the dashed line indicates the plane of section for histology. (C) Relaxed condition (D) Stretched condition. (**E-F)** Digital micrographs of histological sections through the pterygoid skin subregion cut parallel to the transverse body axis (Weigert's Resorcin-Fuchsin staining). (E) Relaxed condition, (F) Stretched condition. (E_1) A scale with the hard-cornified epidermis and attaching collagenous *Retinacula cutis* fiber bundles accompanied by elastic fiber bundles from the *Stratum elasticum*. (E_2) An interscale skin segment with curved collagenous joint fiber bundles. (E_3) Deeper layers of the *Stratum compactum* underneath a scale with an uncompressed dermal fat pad and elastic fiber bundles of the *Stratum elasticum*. (F_1) A scale with obliquely oriented collagenous *Retinacula cutis* fiber bundles. (F_2) An interscale skin segment with straightened collagenous joint fiber bundles and straightened collagen fiber bundles of the orthogonal layers. (F_3) Deeper layers of the *Stratum compactum* underneath a scale with a compressed dermal fat pad and elastic fiber bundles from the *Stratum elasticum*. Abbreviations: A = artery, DF = dermal Fat, INT =interscale skin segment, N = nerve, S = scale, SC = *Stratum compactum*, SE = *Stratum elasticum*, SL = *Stratum laxum*. Symbols: Arrowheads (blue = elastic fiber bundles of the *Stratum elasticum*, lime green = straight collagen fiber bundles of dermal orthogonal underneath a scale, orange = collagenous joint fiber bundles of the *Stratum compactum* in the interscale skin segment, red = collagenous *Retinacula cutis* fiber bundles of the *Stratum compactum* accompanied by elastic fiber bundles from the *Stratum elasticum*).
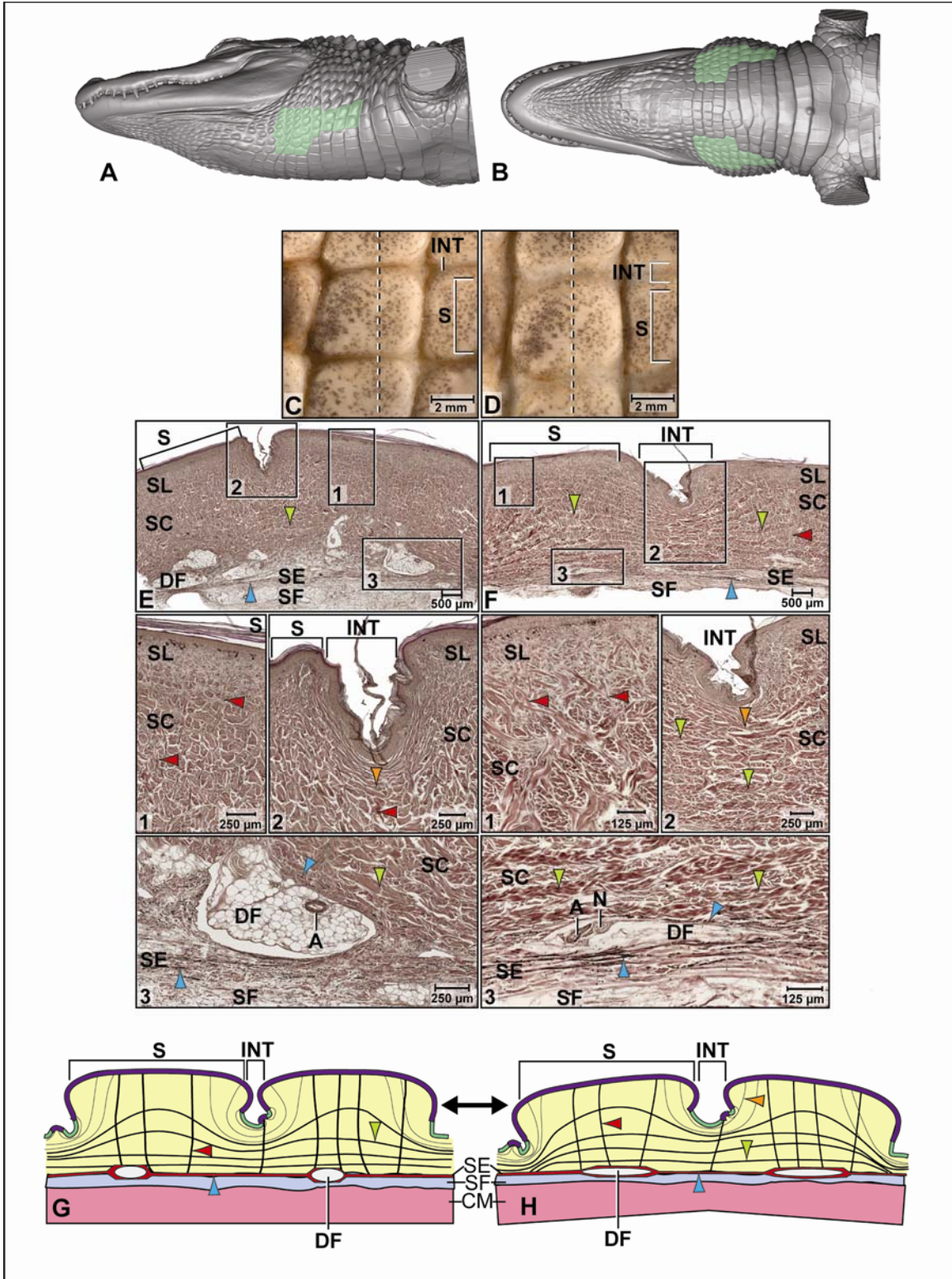
uniform *Stratum elasticum* consists of about seven to eight tightly packed, relaxed elastic fiber bundles that are oriented parallel to the transverse and sagittal body axes, as well as obliquely from craniomedial to caudolateral and from craniolateral to caudomedial (Fig. 2.13E_3 and F_3). Some elastic fiber bundles follow the collagenous *Retinacula cutis* fiber bundles towards the skin surface to attach to the basement membrane of the scales and occasionally interscale tuberosities (Fig. 2.13E_1 and F_1). Underneath the scales, dermal fat bodies, which are elongated along the sagittal body axis and encapsulate small arteries and nerves, are enclosed and separated from one another by layers of the *Stratum elasticum* (Fig. 2.13E, E_3 and F_3).

The uniform *Fascia superficialis* can be quite thick (up to 700 µm) and is composed of a loose arrangement of collagen and elastic fiber bundles, amorphous ground substance, and blood vessels and nerves that are encapsulated in fascial fat bodies.

In the stretched condition, adjacent scales are moved apart, and the interscale skin segment between them is stretched and exposed (Fig. 2.13D.). The collagenous joint fiber bundles are straightened (Fig. 2.13F, F_2). The wavy collagen fiber bundles of the deeper portions of the *Stratum compactum*, which span both the scale and interscale skin segments, are also straightened and pulled taut (Fig. 2.13F_2 and F_3). The elastic fiber bundles of the *Stratum elasticum* are straight and longer than they were in their relaxed configuration, and the dermal fat bodies are compressed between its layers. The collagenous *Retinacula cutis* fiber bundles, which are accompanied by elastic fiber bundles from the *Stratum elasticum* and attach to the basement membrane of the hard-cornified scales, are oriented obliquely to the surface of the epidermis, and the elastic fibers are elongated. The *Fascia superficialis* is thinned, the loosely arranged collagen and elastic fiber bundles are straightened and aligned along the direction of the stretching force, and the fascial fat bodies are compressed and elongated (Fig. 2.13F, F_3).

➤ Functional Interpretation

Stretching mechanism (Fig. 2.13G → H): Because of the polygonal and diamond-shaped scales, this skin subregion can expand radially (Fig. 2.7). As the scales are pulled apart from one another, the collagenous joint fiber bundles of the *Stratum compactum*, which anchor to the scales, straighten and tighten. As a consequence, they pull down on the scales, and the skin is flattened. The orthogonally oriented, wavy collagen fiber bundles of the *Stratum compactum* that span both the scale and interscale skin segments also straighten, tighten, and are compressed as the skin flattens. As the elastic fiber bundles of the *Stratum elasticum* and *Fascia superficialis*

71

straighten and lengthen, they store elastic energy. As the skin flattens, the dermal and fascia fat bodies are compressed and flattened.

Recoil mechanism (Fig. 2.13 H →G): When the stretching force subsides, the elastic fiber bundles in the *Stratum elasticum* and *Fascia superficialis* release their elastic energy and return to their shorter resting configuration. The shortening of the elastic fiber bundles pull the scales closer to one another, thereby enabling the collagen fiber bundles of the *Stratum compactum* underneath the scales to be pushed upwards, and the collagenous joint fiber bundles of the *Stratum compactum* release their tension on the scale edges. The dermal and fascial fat bodies also return to their decompressed resting configuration. As the hard-cornified scales move closer to one another, the orthogonally layered collagen fiber bundles of the deep layers of the *Stratum compactum*, which span both the scale and interscale skin segments, return to their wavy pre-folded resting configuration, and the interscale skin segments and underlying collagenous joint fiber bundles fold back to their resting position.

- **Retroarticular Skin Subregion**
  - ➢ Morphological Description

The retroarticular skin subregion is paired and extends caudally from the angle of the jaw to the cranial border of the cervical skin region in front of the shoulder (see below). Ventromedially, it is bounded by the pterygoid skin subregion and dorsomedially by the tuberculate skin subregion. They lie over the aponeurotic portion of the *M. constrictor colli gularis* and the retroarticular process of the mandible, which serves as the attachment site for the bulging pterygoid musculature (Fig. 2.3 and Fig. 2.14).

The retroarticular skin subregion consists of oval or diamond-shaped, raised and domed scales, which are arranged in rows that are oriented along the transverse and sagittal body axes, although the edges of the diamond-shaped scales create interscale skin segments that are oriented obliquely from craniomedial to caudolateral (Fig. 2.14A-D). The interscale skin segments are folded inward to a level below that of the dermal *Stratum laxum* and are studded with hard-cornified interscale tuberosities. The infolding of the interscale skin segments in three orientations enable this skin subregion to expand radially, when the underlying pterygoid musculature bulges during jaw closure (Fig. 2.7).

72

In the relaxed condition, each scale touches its adjacent scales, whereas the interscale skin segments are folded and completely hidden from view (Fig. 2.14C).

The scale epidermis consists of a stratified squamous hard-cornified epithelium with a *Stratum basale* of tall columnar cells and a *Stratum spinosum* of about four to five cell layers. The *Stratum corneum* is about 50-60 µm thick and forms a compact layer of hard-cornified, flattened cells.

Underneath the scale epidermis, the dermal *Stratum laxum* can be up to 150 µm thick and consists of collagen and elastic fiber bundles. The collagen fiber bundles are arranged in loosely packed orthogonal layers that are oriented along the transverse and sagittal body axes. The elastic fiber bundles are oriented perpendicularly to the skin surface and anchor to the basement membrane. These elastic fiber bundles originate from the *Stratum elasticum* and accompany the collagenous *Retinacula cutis* fiber bundles of the *Stratum compactum* (see below). The *Stratum compactum* comprises wavy collagen fiber bundles that are arranged in orthogonal layers and are oriented along the transverse and sagittal body axes (Fig. 2.14D$_1$). They curve slightly dorsally into the raised scales and then continue under the collagenous joint fiber bundles of the interscale skin segments (Fig. 2.14D). Collagenous *Retinacula cutis* fiber bundles, which originate from the deep layers of the *Stratum compactum*, also run perpendicularly to the skin surface and anchor to the basement membrane (Fig. 2.14D$_1$).

In the interscale skin segments, the epidermis consists of a stratified, squamous soft-cornified epithelieum with a *Stratum basale* of spherical cells and a *Stratum spinosum* of about two to three cell layers. The *Stratum corneum* is about 40-50 µm thick and forms a layer of soft-cornified, flattened cells.

Underneath the epidermis of the interscale skin segments, the dermal *Stratum laxum* thins out so that it is barely visible. The *Stratum compactum* comprises parallel collagenous joint fiber bundles (see 2.3.1), which span the width of the interscale segment and attach to the basement membrane of the adjacent scales and occupy about two-thirds of the *Stratum compactum*. The deeper portion of the *Stratum compactum* is occupied by extensions of the orthogonal layers of collagen fiber bundles from the *Stratum compactum* underneath scales (Fig. 2.14D$_1$).

In the hard-cornified interscale tuberosities, the epidermis is the same as that of the hard-cornified scale epidermis, and the dermal *Stratum laxum* forms the core. Some interscale tuberosities serve as anchoring sites for collagenous *Retinacula cutis* fiber bundles, which

73

originate from the deep layers of the *Stratum compactum* and traverse the interscale segment to attach to the basement membrane.

Underneath the *Stratum compactum* of both the scales and the interscale skin segments, the uniform *Stratum elasticum* consists of about four to five layers of tightly packed elastic fiber bundles that are oriented parallel to the transverse and sagittal body axes, as well as obliquely from caudomedial and ventral to dorsolateral and cranial. Underneath the scales, the *Stratum elasticum* divides into two layers to envelope dermal fat bodies that encapsulate small arteries and nerves. The elastic fiber bundles follow the collagenous *Retinacula cutis* fiber bundles towards the skin surface to attach to the basement membrane of scales and occasional interscale tuberosities.

The uniform *Fascia superficialis* is composed of tightly packed parallel collagen fiber bundles that are arranged in orthogonal layers that are oriented craniomedial to caudolateral, and craniolateral to caudomedial. They are thinner than those of the *Stratum compactum* and intermingle with elastic fiber bundles that are oriented along the transverse and sagittal body axes.

In the stretched condition, adjacent scales are moved apart, and the interscale segments between them are unfolded, stretched, and exposed (Fig. 2.14D and E). The collagenous joint fiber bundles are straightened and tightened. The elastic fiber bundles of the *Stratum elasticum* are also straightened and longer than in their relaxed condition. The collagenous *Retinacula cutis* fiber bundles and the accompanying elastic fiber bundles from the *Stratum elasticum* are elongated and oriented obliquely to the skin (Fig. 2.14E$_1$). The obliquely oriented collagen fiber bundles of the *Fascia superficialis* are pulled in the direction of the stretching force and become oriented along the transverse and sagittal body axis.

> Functional Interpretation

Stretching mechanism (see model for the paralingual skin subregion, Fig. 2.9G → H): Because the scales are separated by folded segments of interscale skin on all sides, this skin is expandable along both the transverse and circumferential body axes. As the scales are pulled apart from one another, the orthogonally oriented, wavy collagen fiber bundles of the *Stratum compactum* that anchor to the hard-cornified scales, straighten, tighten, and they pull down on the scales so that the skin flattens. The elastic fiber bundles of the *Stratum elasticum* and the

74

Figure 2.14 The retroarticular skin subregion of the American Alligator (*Alligator mississippiensis*). (**A-B**) Orthographic images of a 3D reconstruction (Isosurface module, Avizo®) of the skin of the head, neck, and shoulder region to indicate the location of the retroarticular skin subregion highlighted in dark green. (A) Lateral view. (B) Dorsal view. (**C-D**) Digital mesoscopic image of the skin surface; the dashed line indicates the plane of section for histology. (C) Relaxed condition. (D) Stretched condition. (**E-F**) Digital micrographs of histological sections through the retroarticular skin subregion cut parallel to the transverse body axis (Weigert's Resorcin-Fuchsin staining). (E) Relaxed condition. (F) Stretched condition. (E_1) An interscale skin segment with superficial collagenous joint fiber bundles and deep wavy collagen fiber bundles extending from the orthogonal fiber bundle layers underneath scales. (F_1) An interscale skin segment with straightened collagenous joint fiber bundles and collagen fiber bundles extending from the orthogonal fiber bundle layers underneath scales. Abbreviations: INT = interscale skin segment, S = scale, SC = *Stratum compactum*, SE = *Stratum elasticum*, SL = *Stratum laxum*. Symbols: Arrowheads (black = interscale tuberosity, blue = elastic fiber bundles from the *Stratum elasticum*, lime green = collagen fiber bundles of dermal orthogonal layers underneath a scale, orange = collagenous joint fiber bundles, red = collagenous *Retinacula cutis* fiber bundles of the *Stratum compactum* accompanied by elastic fiber bundles from the *Stratum elasticum*).

Fascia superficialis first straighten and then lengthen, storing elastic energy and compressing the dermal fat bodies.

Recoil mechanism (see model for the paralingual skin subregion, Fig. 2.9H →G): When the stretching force subsides, the elastic fiber bundles of the *Stratum elasticum* and *Fascia superficialis* release their elastic energy and return to their shorter relaxed configuration, thereby decompressing the dermal fat bodies. The shortening of the elastic fiber bundles causes the hard-cornified scales to move closer to one another, thereby pushing the connective tissue underneath the scales upwards. The collagen fiber bundles of the *Stratum compactum* release their tension on the edges of the scales. As the scales are moved closer to one another, the collagenous joint fiber bundles return to their curved configuration, and the interscale skin segments refold.

2.3.4. Cervical Skin Region

The cervical skin region lies caudal to the gular skin region and surrounds the neck just cranial to the shoulders (Figs. 2.2B and C). Its cranial border coincides with the caudal border of the underlying *M. constrictor colli gularis* and the cranial border of the *M. constrictor colli cervicalis*. Its caudal border coincides with the caudal border of the *M. constrictor colli cervicalis* (Fig. 2.3; see 2.2.3 and 3.3.3). The ventral cervical skin subregion comprises square scales, whereas the lateral cervical skin subregion comprises raised round scales. Both types of scales are arranged circumferentially and in rows along the sagittal body axis (Figs. 2.2 and 2.3B-D).

- **Ventral Cervical Skin Subregion**
  ➢ Morphological Description

The large ventral cervical skin subregion covers the entire length of the cervical skin region, extending from its rostral border to its caudal border (Fig. 2.3 and 2.15A and B). Dorsolaterally it is bounded by the lateral cervical skin subregion (see below) in front of the shoulders (Fig. 2.3).

The ventral cervical skin subregion consists of square or rectangular scales that are arranged circumferentially and in rows that are oriented along the sagittal body axis. The interscale skin segments that run parallel to the transverse body axis are long and deeply folded, and the caudal border of a cranial scale is raised above and overhangs the rostral border of the scale behind it

77

(Fig. 2.15E). These interscale skin segments allow expansion along the sagittal body axis. The interscale skin segments that run parallel to the sagittal body axis are very short and not deeply between the scales.

The scale epidermis consists of a stratified squamous hard-cornified epithelium with a *Stratum basale* of tall columnar cells and a *Stratum spinosum* of about three to four cell layers. The *Stratum corneum* forms a compact layer of hard-cornified, flattened cells and is about 130-150 µm thick at the center of the scales, but thins to about 25 µm towards the overhanging caudal edge of scales (see 2.3.1).

Underneath the epidermis of scales, the dermal *Stratum laxum* is about 400-500 µm thick, but thins to about 175 µm towards the overlapping caudal edge of scales. The collagen fibers are loosely arranged, but the elastic fiber bundles, which originate from the *Stratum elasticum*, run perpendicularly to the skin surface and anchor to the basement membrane. The *Stratum compactum* underneath the cranial edge of a scale comprises layers of collagen fiber bundles that are arranged in orthogonal layers and are oriented along the transverse and sagittal body axes. Collagenous *Retinacula cutis* fiber bundles originate from the deep layers of the *Stratum compactum*, which are accompanied by elastic fiber bundles from the *Stratum elasticum,* run perpendicularly towards the skin surface and anchor to the basement membrane (Fig. 2.15E$_2$). The *Stratum compactum* of the overhanging caudal edge of a scale comprises layers of collagen fiber bundles that are oriented along the transverse body axis, and collagen fiber bundles that traverse the dermis obliquely towards the skin surface to anchor on the basement membrane (Fig. 2.15E and G).

In the interscale skin segments, the epidermis consists of a stratified squamous soft-cornified epithelium with a *Stratum basale* of spherical cells and a *Stratum spinosum* of about five to six cell layers. The *Stratum corneum* is about 50 µm thick and forms a layer of soft-cornified, flattened cells (see 2.3.1).

Underneath the soft-cornified interscale skin segments, the dermal *Stratum laxum* thins out and is barely visible. The *Stratum compactum* consists of parallel collagen and elastic joint fiber bundles that span the interscale skin segments and anchor to the basement membrane of adjacent scales (Fig. 2.15E$_1$).

In the hard-cornified interscale tuberosities, the epidermis is the same as that in the hard-cornified scales, and the *Stratum laxum* forms the core. Some tuberosities serve as anchoring

Figure 2.15 The ventral cervical skin subregion of the American Alligator (*Alligator mississippiensis*) (see also Fig. 2.15cont'd). (**A-B**) Orthographic images of a 3D reconstruction (Isosurface module, Avizo®) of the skin of the head, neck, and shoulder region to indicate the location of the ventral cervical skin subregion highlighted in blue. (A) Ventrolateral view. (B) Ventral view. (**C-D**) Digital mesoscopic image of the skin surface; the dashed line indicates the plane of section for histology. (C) Relaxed condition. (D) Stretched condition. (**E-F**) Digital micrographs of histological sections through the ventral cervical skin subregion cut parallel to the sagittal body axis (Weigert's Resorcin-Fuchsin staining). (E) Relaxed condition. (E_1) An interscale skin segment with collagenous and elastic joint fiber bundles and collagenous *Retinacula cutis* anchoring to the cranial edge of a caudal scale. (E_2) The cranial scale edge of a caudal scale with collagenous *Retinacula cutis* fiber bundles. (F) Stretched condition. (F_1) An interscale skin segment with collagenous and elastic joint fiber bundles and collagenous *Retinacula cutis* anchoring to the cranial edge of a caudal scale. (F_2) The cranial edge of a caudal scale with collagenous *Retinacula cutis* fiber bundles. (**G-H**) Model of the stretching and recoil mechanism of the ventral cervical skin subregion along the sagittal body axis showing the reorientation of the collagen and elastic fiber bundles and the changes in the length and thickness of the skin. (G) Relaxed condition. (H) Stretched condition. (**I**) Digital mesoscopic image of the skin surface; the dashed line indicates the plane of section for histology. (**J**) Digital micrograph of a histological section through the ventral cervical skin subregion cut parallel to the transverse body to show the non-expandable longitudinal interscale skin segment (Weigert's Resorcin-Fuchsin staining). (J_1) An interscale skin segment with collagenous joint fiber bundles, *Retinacula cutis* fiber bundles, and straightened collagen fiber bundles extending from the dermal orthogonal layers underneath scales. (J_2) The *Stratum compactum* underneath a scale with straightened collagen fiber bundles of the dermal orthogonal layers. (J_3) Deep layers of the *Stratum compactum* with a dermal fat body. (**K**) Model of the bendable, but not stretchable ventral cervical skin subregion along the circumferential body axis. Abbreviations: CAS = caudal scale, CRS = cranial scale, DF = dermal fat body, INT = interscale skin segment, S = scale, SC = *Stratum compactum*, SE = *Stratum elasticum*, SF = *Fascia superficialis*, SL = *Stratum laxum*. Symbols: Arrowheads (blue = elastic fiber bundles of the *Stratum elasticum*, orange = collagenous joint fiber bundles of the *Stratum compactum*, red = collagenous *Retinacula cutis* fiber bundles of the *Stratum compactum* accompanied by elastic fiber bundles from the *Stratum elasticum*).

79
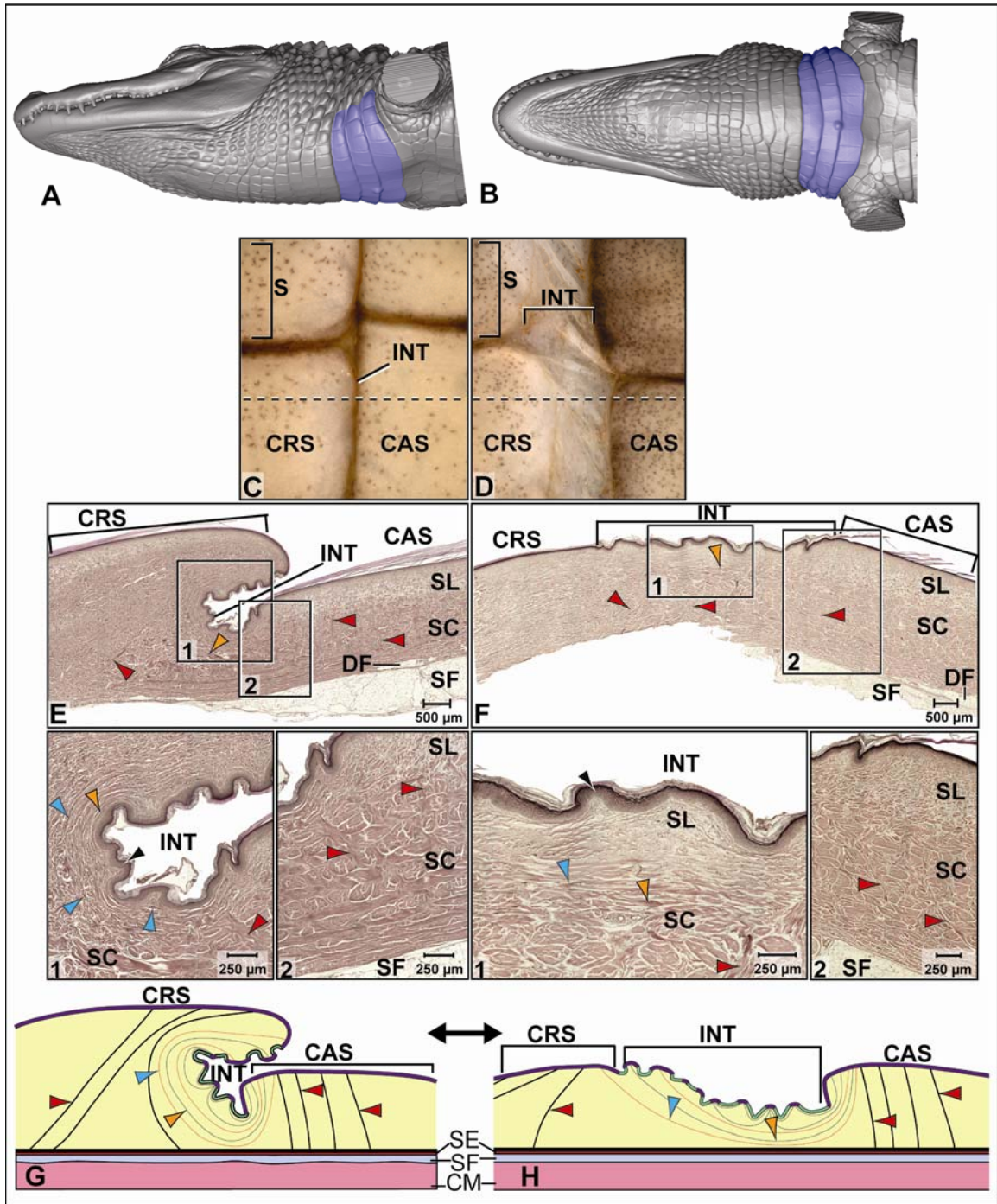
Figure 2.15 cont'd
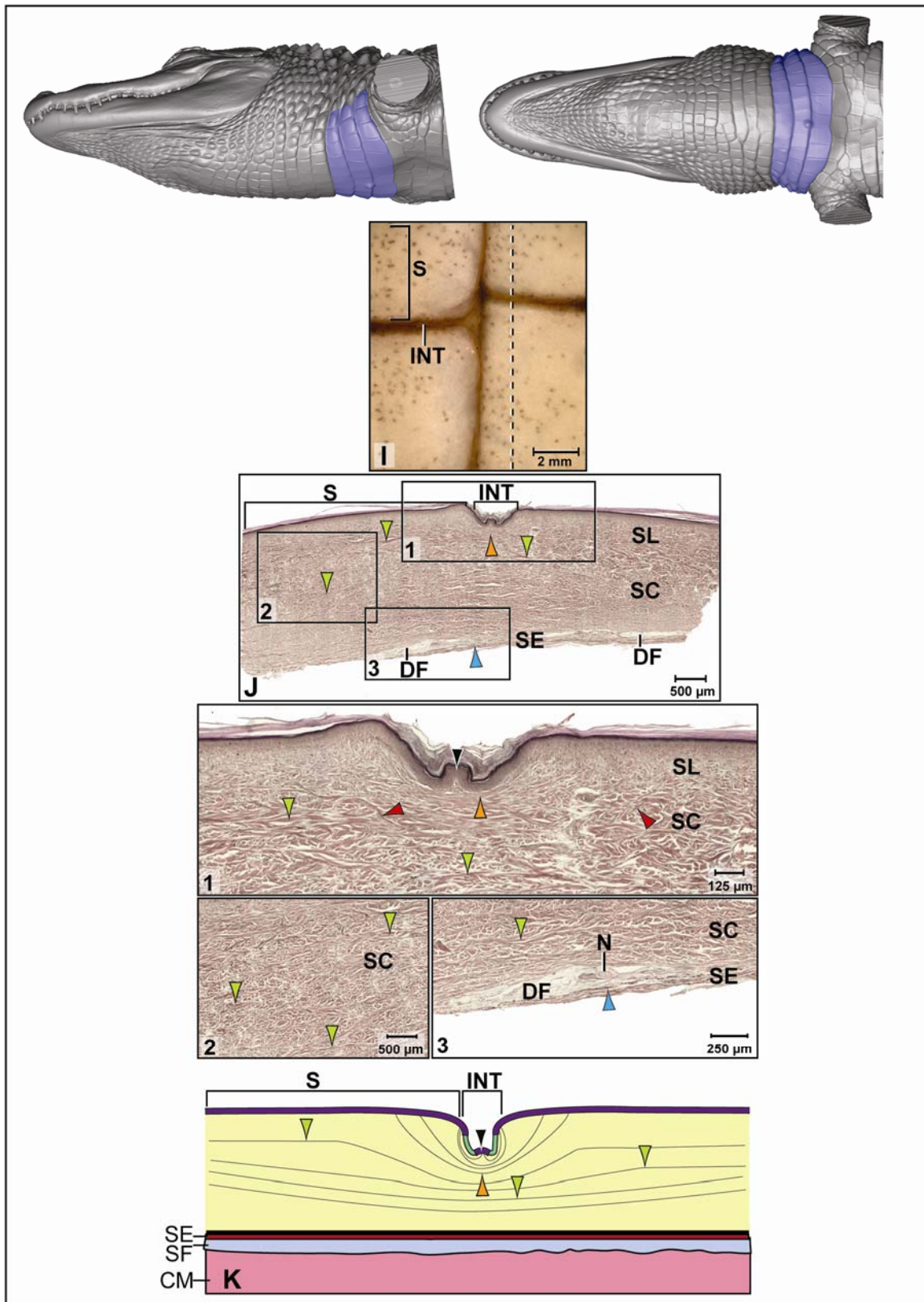
sites for collagenous *Retinacula cutis* fiber bundles that originate from the deep layers of the *Stratum compactum* and traverse the dermis to insert on the basement membrane of the epidermis.

Underneath the *Stratum compactum* of both the scales and interscale skin segments, the uniform *Stratum elasticum* is thin, consisting of about four to five layers of loosely packed, relaxed elastic fiber bundles that are oriented parallel to the sagittal body axis. The elastic fiber bundles of the *Stratum elasticum* follow the collagenous *Retinacula cutis* fiber bundles towards the skin surface to attach to the basement membrane of scales and occasionally of interscale tuberosities. Underneath the scales, and within superficial layers of the *Stratum elasticum*, dermal fat bodies encapsulate small arteries and nerves (Fig. 2.15E, J and J_3).

The uniform *Fascia superficialis* is about 50 µm thick underneath the overhanging caudal edge of a scale and is made up of a loose mass of collagen and elastic fiber bundles, amorphous ground substance and sparse blood vessels and nerves. It gets up to 1mm tick underneath the cranial edge of a scale and is heavily interlarded with fat (Fig. 2.15E).

In the stretched condition, the overhanging caudal edge of a scale is moved away from the cranial edge of the scale behind it, so that both scales are on an even level (Fig. 2.15D and F). The soft-cornified interscale skin segment is stretched and exposed (Fig. 2.15D, F and F_1). The collagenous joint fiber bundles, which span the interscale skin segments, are straightened (Fig. 2.15F_1). The elastic joint fiber bundles are lengthened and also straightened. The elastic fiber bundles of the *Stratum elasticum* are straightened and lengthened, and the dermal fat bodies are compressed. The collagenous *Retinacula cutis* fiber bundles, which are accompanied by elastic fiber bundles from the *Stratum elasticum*, run obliquely towards the cranial edge of scales to which they attach (Fig. 2.15F_2). The *Fascia superficialis* is thinned, and the loosely arranged collagen and elastic fiber bundles are straightened and aligned along the direction of the stretching force.

➢ Functional Interpretation

Stretching mechanism of the transverse interscale skin segment (Fig. 2.15G → H): Because the cranial and caudal edges of scales are separated by long, folded interscale skin segments, this skin subregion is highly expandable along the sagittal body axis. As the cranial and caudal scales are pulled apart from one another in the sagittal plane, the soft-cornified interscale skin segment between them unfolds and expands. The collagenous *Retinacula cutis* fiber bundles,

which anchor to the cranial edges of scales, anchor this scale edge to the underlying dermis as the caudal overhanging edge of the next cranial scale is pulled away and lowered. The collagenous and elastic joint fiber bundles, which anchor to the edges of the scales, straighten and the elastic joint fibers also lengthen, thereby storing elastic energy. The elastic fiber bundles of the *Stratum elasticum* and *Fascia superficialis* straighten, lengthen, and store elastic energy. The dermal fat bodies under the cranial edge of scales are compressed.

Recoil mechanism (Fig. 2.15H → G): When the stretching force subsides, the elastic joint fiber bundles of the *Stratum compactum* of the interscale skin segment release their elastic energy and return to their shorter resting configuration. The elastic fiber bundles of the *Stratum elasticum* and *Fascia superficialis* also release their elastic energy and shorten. The shortening of the elastic fiber bundles enables the interscale skin segments to refold and the scales are moved closer to one another, thereby allowing the collagen fiber bundles underneath the caudal edge of scales to be pushed upwards, returning the scale edge to its overlapping resting position.

Stretch-resisting mechanism of the longitudinal interscale skin segments (Fig. 2.15K): Because the interscale skin segments of the lateral and medial scale edges are very short, they are not expandable, but provide flexibility circumferentially. As stretching forces increase, the straight collagen fiber bundles of the *Stratum compactum* oriented along the transverse body axis become taut and resist further lengthening, stretching, and, thus, circumferential expansion of the skin.

- **Lateral Cervical Skin Subregion**
  ➢ Morphological Description

The lateral cervical skin subregion is paired and covers the area between the retroarticular skin subregion to the shoulders (Fig. 2.3). Ventromedially, it is bounded by the ventral cervical skin subregion and dorso-medially, it is bounded by the tuberculate skin region (Fig. 2.3). The lateral cervical skin subregion covers the underlying muscular portion of the *M. constrictor colli cervicalis* (see 3.3.3).

The lateral cervical skin subregion consists of raised round scales, some of which are pointed (Fig. 2.16C-D). The scales are arranged circumferentially and in rows that are oriented along the sagittal body axis (Fig. 2.16A-B). The interscale skin segments that run parallel to the sagittal body axis are short and not as deeply folded as the interscale skin segments that run

83

parallel to the transverse body axis. Hence, most of the expansibility of this skin subregion occurs along the sagittal body axis.

In the relaxed condition, the scales touch one another and the folded interscale skin segments are completely hidden from view (Fig. 2.16C). The surface of the interscale segments is studded with hard-cornified tuberosities, which are larger than in the other skin subregions.

The scale epidermis consists of a stratified squamous hard-cornified epithelium with a Stratum basale of tall columnar cells and a *Stratum spinosum* of about four to five cell layers. The *Stratum corneum* is about 175-200 µm thick, but thins to about 45 µm at the edges of the scales. It forms a compact layer of hard-cornified, flattened cells.

Underneath the epidermis of the scales, the dermal *Stratum laxum* is between 450 µm and 1.5 mm thick, depending on the height of the scales, and comprises collagen and elastic fiber bundles. The collagen fiber bundles are loosely packed in orthogonal layers that are oriented along the transverse and sagittal body axes. Elastic fiber bundles, which originate from the *Stratum elasticum*, are oriented perpendicularly to the skin and anchor to the basement membrane. The *Stratum compactum* comprises layers of wavy collagen fiber bundles that are arranged in orthogonal layers and are oriented along the transverse and sagittal body axes (Fig. 2.16E). They run perpendicularly towards the skin surface and anchor to the basement membrane. Collagenous *Retinacula cutis* fiber bundles, which originate from the deep layers of the *Stratum compactum*, also run perpendicular towards the skin surface and anchor to the basement membrane of the scales (Fig. 2.16E$_{1-2}$).

In the interscale skin segments, the epidermis consists of a stratified, squamous soft-cornified epithelieum with a *Stratum basale* of spherical cells and a *Stratum spinosum* of about 3-4 cell layers. The *Stratum corneum* is about 50-60 µm thick and forms a layer of soft-cornified, flattened cells.

Underneath the epidermis of the interscale skin segments, the dermal *Stratum laxum* thins out so that it is barely visible. The superficial layer of the *Stratum compactum* is made up by collagenous joint fiber bundles (see 2.3.1), which span the width of the interscale segment and attach to the basement membrane of adjacent scales (Fig. 2.16E$_1$). The deeper portion of the *Stratum compactum* is taken over by the extensions of the orthogonal collagen fiber bundles from the *Stratum compactum* underneath the scales.

84

Figure 2.16 The lateral cervical skin subregion of the American Alligator (*Alligator mississippiensis*). (**A-B**) Orthographic images of a 3D reconstruction (Isosurface module, Avizo®) of the skin of the head, neck, and shoulder region to indicate the location of the lateral cervical skin subregion highlighted in dark blue. (A) Lateral view. (B) Dorsal view. (**C-D**) Digital mesoscopic image of the skin surface; the dashed line indicates the plane of section for histology. (C) Relaxed condition. (D) Stretched condition. (**E-F)** Digital micrographs of histological sections through the retroarticular skin subregion cut parallel to the transverse body axis (Weigert's Resorcin-Fuchsin staining). (E) Relaxed condition. (F) Stretched condition. (E_1) An interscale skin segment with curved collagenous joint fiber bundles of the *Stratum compactum*. (E_2) Deep layers of the *Stratum compactum* with uncompressed dermal fat body surrounded by elastic fiber bundles of the *Stratum elasticum*. (F_1) An interscale skin segment with straightened collagenous joint fiber bundles and their attachment to adjacent scale. (F_2) Deep layers of the *Stratum compactum* with a compressed dermal fat body surrounded by elastic fiber bundles of the *Stratum elasticum.*. Abbreviations: A = artery, DF = dermal fat body, INT = interscale skin segment, N = nerve, S = scale, SC = *Stratum compactum*, SE = *Stratum elasticum*, SL = *Stratum laxum*. Symbols: Arrowheads (black = hard-cornified interscale tuberosity, blue = elastic fiber bundles of the *Stratum elasticum*, lime green = collagen fiber bundles of dermal orthogonal layers of the dermis underneath a scale, orange = collagenous joint fiber bundles of the *Stratum compactum* of the interscale skin segment, red = collagenous *Retinacula cutis* fiber bundles of the *Stratum compactum* accompanied by elastic fiber bundles from the *Stratum elasticum*).
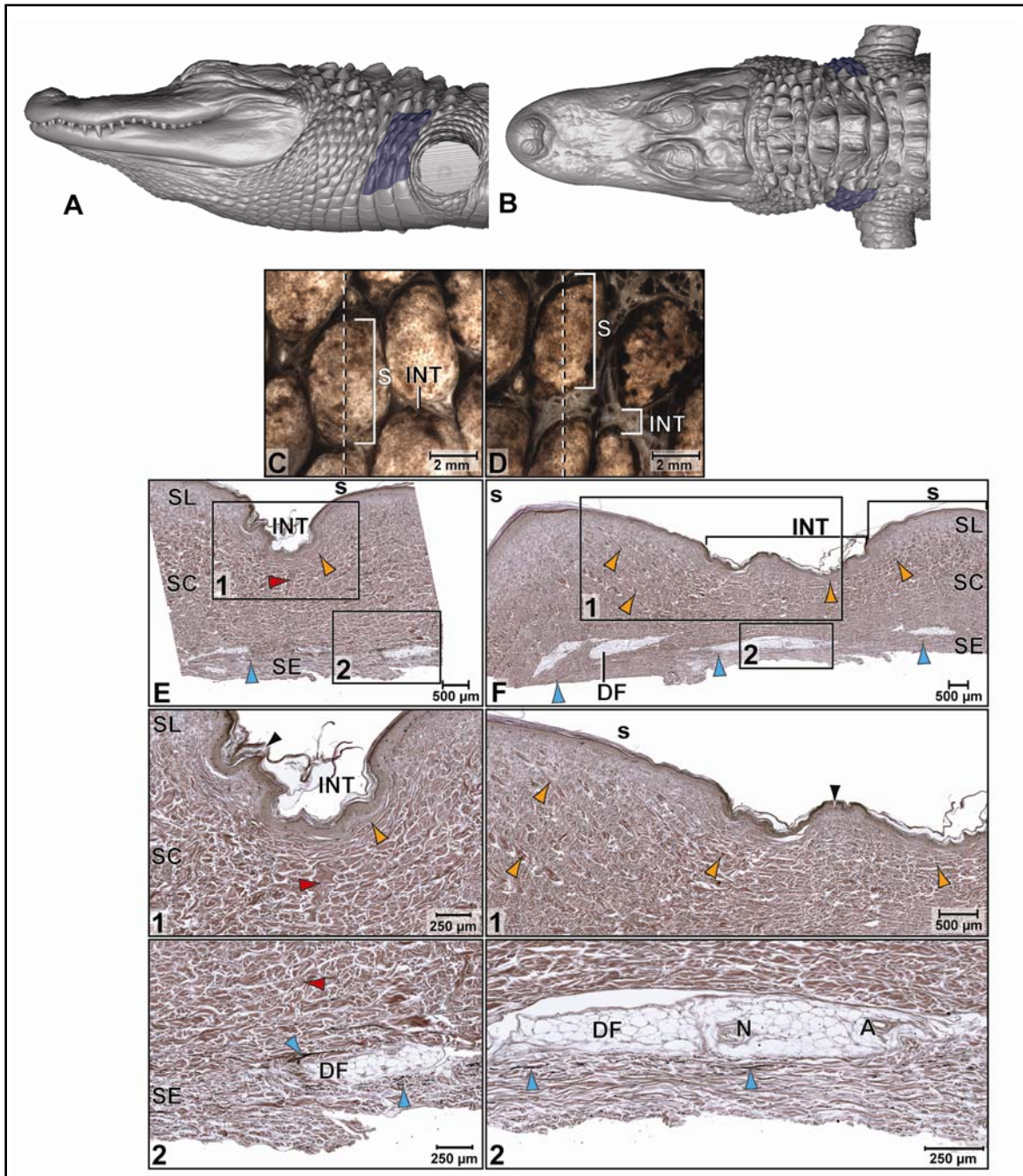
The epidermis of the hard-cornified interscale tuberosities is the same as that of the hard-cornified scale epidermis. The *Stratum laxum* forms the core of these tuberosities, some of which serve as anchoring sites for collagenous *Retinacula cutis* fiber bundles, which originate from the deep layers of the *Stratum compactum* and traverse the dermis to anchor to the basement membrane of the epidermis.

Underneath the *Stratum compactum* of both the scales and the interscale skin segments, the uniform *Stratum elasticum* consists of about six to seven layers of loosely packed elastic fiber bundles, which are oriented circumferentially and parallel to the sagittal body axes. Underneath the scales, the *Stratum elasticum* divides into two layers and envelopes dermal fat bodies that encapsulate small arteries and nerves. Some elastic fiber bundles accompany the collagenous *Retinacula cutis* fiber bundles towards the skin surface to attach to the basement membrane of scales and occasionally to hard-cornified tuberosities of the interscale skin segments.

The uniform *Fascia superficialis* is composed of tightly packed parallel collagen fiber bundles in orthogonal layers that are oriented obliquely from craniomedial to caudolateral, and from craniolateral to caudomedial. They are interspersed with elastic fiber bundles that are oriented along the transverse and sagittal body axes. The collagen fiber bundles of the *Fascia superficialis* are thinner than those of the dermal *Stratum compactum*.

In the stretched condition, adjacent scales are moved apart, and the interscale segments between them are unfolded, stretched, and exposed (Fig. 2.16D-F). The collagenous joint fiber bundles, which span the interscale skin segments, are straightened and tightened (Fig. 2.16F$_1$). The elastic fiber bundles of the *Stratum elasticum* are also straightened and longer than in their relaxed condition. The collagenous *Retinacula cutis* fiber bundles, which are accompanied by elastic fiber bundles from the *Stratum elasticum*, are oriented obliquely to the skin surface. The obliquely oriented collagen fiber bundles of the *Fascia superficialis* are pulled in the direction of the stretching force and are oriented along the transverse and sagittal body axis.

➢ Functional Interpretation

Stretching mechanism (see model for paralingual skin subregion, Fig. 2.9G → H): Because the scales are separated by folded segments of soft-cornified interscale skin on all sides, this skin is expandable circumferentially and along the sagittal body axis. As the scales are pulled apart from one another circumferentially or in the sagittal plane, the wavy collagen fiber bundles of the *Stratum compactum* that anchor to the scales, straighten, tighten, and pull down on the scales, so

that the skin is flattened, and the dermal fat bodies are compressed and elongated. The elastic fiber bundles of the *Stratum elasticum* and *Fascia superficialis* first straighten and then lengthen, storing elastic energy.

Recoil mechanism (see model for the paralingual skin subregion, Fig. 2.9H → G): When the stretching force subsides, the elastic fiber bundles in the *Stratum elasticum* and *Fascia superficialis* release their elastic energy and return to their shorter relaxed configuration. The shortening of the elastic fiber bundles move the scales closer to one another, thereby enabling the dermal fat bodies to decompress and push the connective tissue underneath the scales upwards as the collagen fiber bundles of the *Stratum compactum* release their tension on the edges of the scales. As the scales move closer to one another, the collagenous joint fiber bundles of the *Stratum compactum* return to their pre-folded and curved configuration, and the interscale skin segments refold.

2.3.5. Dorsal Tuberculate Skin Region and Subregion

The tuberculate skin region comprises only a single skin subregion of the same name. It covers the area around the cervical osteoderms and extends caudally from the occiput of the head to the last pair of cervical osteoderms cranial to the shoulder girdle (Fig.2.3 and Fig. 2.17A and B). Its medio-lateral border skirts the dorso-medial borders of the retroarticular and lateral cervical skin subregions. Its scales are tuberculate with ossification centers in the largest among them. They are arranged in rows oriented along the transverse and sagittal body axes. Interscale skin segments are very short and not folded in the relaxed condition and are studded with large hard-cornified tuberosities between the tuberculate scales (Fig. 2.17C).

The scale epidermis consists of a stratified squamous hard-cornified epithelium with a *Stratum basale* of tall columnar cells and a *Stratum spinosum* of about five to six heavily pigmented cell layers with interspersed melanophores. The *Stratum corneum* is about 45-50 µm thick at the edges of the scales.

Underneath the epidermis of the scales, the dermal *Stratum laxum* is about 300 µm thick and consist of collagen and elastic fiber bundles. The collagen fiber bundles are arranged in orthogonal layers that are oriented along the transverse and sagittal body axes (Fig. 2.17D$_1$ and E$_1$). The elastic fiber bundles run perpendicularly towards the skin surface and anchor to the basement membrane. These elastic fiber bundles originate from the *Stratum elasticum*. The

Stratum compactum comprises orthogonal layers of collagen fiber bundles that are oriented along the transverse and sagittal body axes, and some run perpendicularly towards the scales and anchor to their basement membrane (Fig. 2.17D$_{1-2}$ and E$_1$). Collagenous *Retinacula cutis* fiber bundles, which originate from the deep layers of the *Stratum compactum*, also run perpendicularly towards the skin surface and anchor to the basement membrane of the scales.

In the interscale skin segments, the epidermis consists of a stratified, squamous soft-cornified epithelieum with a *Stratum basale* of spherical cells and a *Stratum spinosum* of about five to six cell layers. The *Stratum corneum* is about 40-50 μm thick and forms a layer of soft-cornified, flattened cells.

Underneath the epidermis of the interscale skin segments, the *Stratum laxum* thins out so that it is barely visible. The *Stratum compactum* is formed by parallel collagenous joint fiber bundles (see 2.3.1), which span the width of the interscale segment and attach to the basement membrane of adjacent scales. These parallel collagenous joint fiber bundles make up about two-thirds of the *Stratum compactum*. The deeper portion of the *Stratum compactum* is made up by extensions of the orthogonal layers of collagen fiber bundles that form the *Stratum compactum* underneath the scales (Fig. 2.17D$_{1-2}$ and E$_{1-2}$).

In the hard-cornified interscale tuberosities, the epidermis is the same as that in the hard-cornified scale epidermis. The core of these tuberosities is formed by the *Stratum laxum*. These tuberosities serve as anchoring sites for collagenous *Retinacula cutis* fiber bundles that originate from the deep layers of the *Stratum compactum* and traverse the dermis.

Underneath the *Stratum compactum* of both the scales and the interscale skin segments, there is thin and individual elastic fibers are interspersed throughout the dermis and are oriented along the transverse and sagittal body axes, as well as obliquely from craniolateral to caudomedial. Elastic fiber bundles follow the collagenous *Retinacula cutis* fiber bundles towards the skin surface to attach to the basement membrane of the scales and occasionally to the interescale tuberosities.

The uniform *Fascia superficialis* is composed of tightly packed parallel collagen fiber bundles in orthogonal layers that are oriented from craniomedial to caudolateral, and from craniolateral to caudomedial. They are interspersed with elastic fiber bundles that are oriented along the transverse and sagittal body axes. The collagen fiber bundles of the *Fascia superficialis* are thinner than those of the dermal *Stratum compactum*.

89

Because the interscale skin segments are straight in their relaxed condition, as are the collagen fiber bundles of the underlying *Stratum compactum*, the skin of the tuberculate skin subregion is not expandable.

> ➢ Functional Interpretation

The stretching resisting mechanism is similar to that of the sympyseal skin subregion, only the collagen fiber bundles are thicker and the scales are tuberculate. As stretching forces increase, the straight collagen fiber bundles of the *Stratum compactum* tighten and resist further lengthening and stretching. Numerous collagenous *Retinacula cutis* fiber bundles that attach to the hard-cornified scales and interscale tuberosities also prevent the skin from being moved.

2.4. Discussion

2.4.1. Regional Variation in the Integumentary Layers

- **Epidermis**

Scale patterns in alligators are regionally variable over the entire body, but especially in the intermandibulo-cervical integument; however, microscopically, it was observed that the strata of the epidermis do not show much variation among the different skin subregions, with the pararamal skin subregion being the only exception (see below). The epidermal strata do, however, vary structurally between the non-expandable scale and the expandable interscale segments, the shapes and sizes of which, determine scale patterns.

> ➢ Keratinization of the *Stratum corneum*

The rigidness of the hard-cornified scales is attributed to the presence of beta-keratins (Mercer 1961; Landmann 1986; Alibardi & Thompson 2000; Richardson *et al.* 2002; Alibardi 2003a ,b; Alibardi *et al.* 2007). In immunohistochemistry studies, the beta-keratins in the scales of alligators show cross-reactivity with the beta-keratins of the scales of birds (Sawyer *et al.* 2000; Alibardi 2003b).

The upper layers of the *Stratum spinosum* of the scales form a pre-corneous layer, which stains intensively pink with eosin, or dark purple with Weigert's Resorcin-Fuchsin (see 2.3.1), in stark contrast to the pale staining *Stratum corneum*. Parakkal & Alexander (1972) said that this layer contains keratohyalin granules, as in the *Stratum granulosum* of the soft-cornified

Figure 2.17 The tuberculate skin region and subregion of the American Alligator (*Alligator mississippiensis*). (**A-B**) Orthographic images of a 3D reconstruction (Isosurface module, Avizo®) of the skin of the head, neck, and shoulder region to indicate the location of the tuberculate skin region highlighted in orange. (A) Lateral view. (B) Dorsal view. (**C**) Digital mesoscopic image of the skin surface; the dashed line indicates the plane of section for histology. (**D-E)** Digital micrographs of histological sections through the dorsal tuberculate skin region (Weigert's Resorcin-Fuchsin staining). (D) Transverse section. (E) Longitudinal section. (D_1) Orthogonal layers of straight collagen fiber bundles of the *Stratum compactum* in the relaxed condition. (D_2) Deep layers of the *Stratum compactum* with straight collagen fiber bundles, collagenous *Retinacula cutis* fiber bundles, and sparse elastic fiber bundles from the *Stratum elasticum* (E_1) An interscale skin segment with straightened collagenous joint fiber bundles of the *Stratum compactum* and collagenous *Retinacula cutis* fiber bundles attaching to the scale and interscale tuberosities. (E_2) Deep layers of the *Stratum compactum* with straight collagen fiber bundles, collagenous *Retinacula cutis* fiber bundles, and sparse elastic fiber bundles from the *Stratum elasticum*). Abbreviations: INT = interscale skin segment, S = scale, SC = *Stratum compactum*, SE = *Stratum elasticum*, SL = *Stratum laxum*, T = tuberculate scale. Symbols: Arrowheads (black = hard-cornified interscale tuberosity, blue = elastic fiber bundles of the *Stratum elasticum*, lime green = collagen fiber bundles of dermal orthogonal layers underneath a scale, orange = collagenous joint fiber bundles of the *Stratum compactum* of the interscale skin segment, red = collagenous *Retinacula cutis* fiber bundles of the *Stratum compactum* accompanied by elastic fiber bundles from the *Stratum elasticum*).
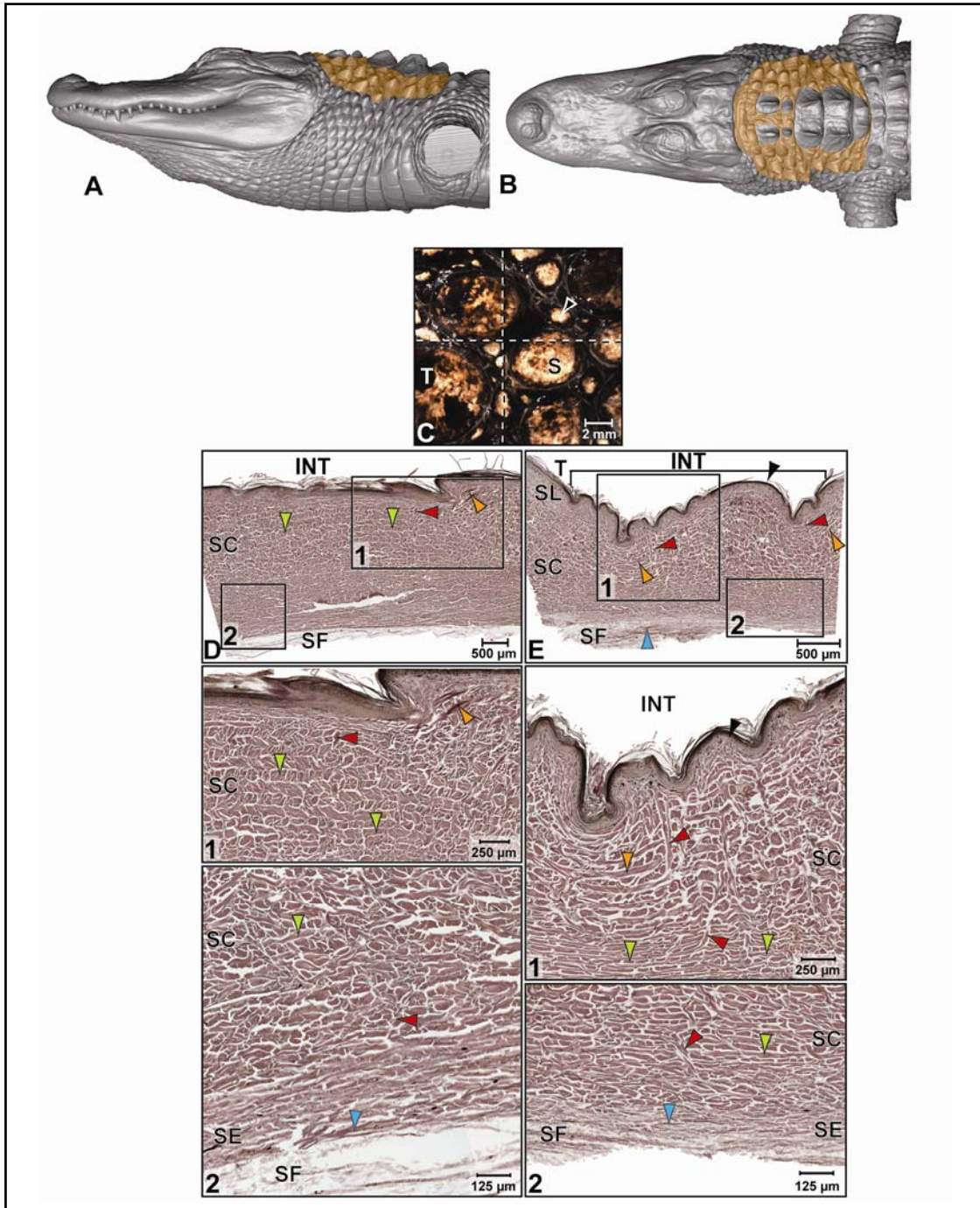
epidermis of mammals (see Bragulla & Homberger 2009). Landmann (1986) also described a granular layer under the *Stratum corneum* of the scale epidermis in camains, though he dismissed the idea that these were keratohyalin granules because they were not basophilic. Indeed, this layer is strongly eosinophilic in the scale epidermis of alligators. More recently, Alibardi and Toni (2007), who observed this layer with toluidine blue stain, determined that this layer is a transitional layer of the scale epidermis, in which beta-keratins begins to replace the alpha-keratins produced by the cells in the basal and lower layers of the *Stratum spinosum*.

The flexibility of the soft-cornified interscale epidermis is attributed to the presence of alpha-keratins (Mercer 1961; Landmann 1986; Alibardi & Thompson 2000, 2001; Richardson *et al.* 2002; Alibardi *et al.* 2007), which are phylogenetically old keratins and are conserved in all vertebrates (Sawyer *et al.* 2000; Alibardi 2003a; Bragulla & Homberger 2009). In the upper layers of the *Stratum spinosum*, an eosinophilic pre-corneous layer; however it stained much less intensely with eosin, and was lightly stained or unstained with Weigert's Resorcin-Fuchsin. The interscale epidermis does not contain beta-keratins (Alibardi & Thompson 2001), and the presence of this precorneous cell layer in the interscale epidermis raises some questions regarding the beta-keratin content of this layer described by Alibardi & Toni (2007), or the assumption that the interscale epidermis does not contain beta-keratin (Alibardi & Thompson 2001).

> Lipogenesis in the *Stratum spinosum* and Conditioning of the *Stratum corneum*

When stained with the lipophilic stain Oil Red O, the *Stratum corneum* of the interscale epidermis stains intense red, indicating that this layer is saturated with lipids, much like the pliable alpha-keratinized *Stratum corneum* of birds (Lucas & Stettenheim 1972; Matoltsy & Huszar 1972; Menon & Menon 2000; Stettenheim 2000) and mammals (Spearman 1966, Wertz *et al.* 1986, Khnykin *et al.* 2011). The lipids are probably necessary to keep the pliable interscale skin conditioned, but might also act as a type of "glue" to keep the flattened cells of this layer somewhat held together during distension and folding of the epidermis in expandable skin regions. This explanation seems likely, given that the rigid hard-cornified scale *Stratum corneum* stains very lightly, if at all, with Oil Red O.

The middle and upper layers of the *Stratum spinosum* of the interscale epidermis showed intracellular lipid droplets, which are most likely source of the lipid content of the *Stratum corneum* that keeps the flexible soft-cornified interscale skin segments conditioned and pliable.

93

Alibardi and Thompson (2001) describe lipid droplets associated with the *Stratum spinosum* of the hard-cornified scale epidermis, but this could not be confirmed this with the histological methods used in this study.

> Cell Morphology of the *Stratum basale*

In the scale epidermis, the *Stratum basale* comprises tall columnar cells. Cylindrical cells have been described by previous authors (Lange 1931; Matoltsy & Huszar 1972; Alibardi & Thompson 2000, 2001; Alibardi 2003b), but these authors did not specifically associate this cell type with the hard-cornified scale epidermis, except for Alibardi & Thompson (2001), who described it for the outer scale surfaces. This study, confirmed that most hard-cornified regions of the epidermis had a basal layer of tall columnar cells. An exception, however, were the hard-cornified areas of the crests of the pararamal skin subregion, which had spherical basal cells that we found to be typical for the soft-cornified interscale skin segments.

In the interscale epidermis, the *Stratum basale* comprises spherical cells. Like the tall columnar cells of the scale epidermis, this cell type has been described as a feature of the crocodilian epidermis, but not in reference to the scale or interscale skin segments, except Alibardi and Thompson (2001), who describe the basal cells of the hinge region as low cuboidal.

The epidermis of the pararamal skin subregion might represent a transitional morphological type between hard-cornified scale epidermis and the soft-cornified interscale epidermis. The hard-cornified areas of the crests of the pararamal skin subregion show the precorneous layer of the *Stratum spinosum* described by Alibardi and Toni (2007), and it stains dark purple with Weigert's Resorcin-Fuchsin and intensely pink with H&E, as observed in true hard-cornified scales in this study; however the basal cells are distinctly like those of the spherical soft-cornified interscale skin segments.

- **Dermis**

Many authors have noted that scale patterns vary between different body regions, and that these patterns are so static within a species that they can be used for taxonomic purposes (Lange 1931; Maderson, 1964; Soulé & Kerfoot 1972; Spearman 1973; Landmann 1986; Brazaitis 1987; Jayne 1988; Arnold *et al*. 2002; Richardson *et al*. 2002; Kim 2010). Although some authors have stated that different mechanical demands on different parts of the body are correlated with regional variants of scale patterns (Maderson 1984; Alibardi & Thompson 2000; Maderson &

94

Alibardi 2000; Homberger & de Silva 2003), there have been no studies that correlate the underlying structure of the dermis with the direction and extent of expansibility and movement in the different skin subregions of reptiles. This study is unique in that it shows the biomechanical importance of the arrangement and orientation of dermal collagen and elastic fiber bundles for the dynamic process of skin expansion in different skin subregions.

➤ Orientation of Collagen Fiber Bundles in the *Stratum compactum*

Szirmai (1970) discusses the biomechanical properties of collagen fibers and how they react to stretching forces during mechanical testing, but admits that understanding how regional variation in the biomechanical properties of the skin correlate with the collagen and elastic fiber architecture of the dermis is speculative at best. Citing Szirmai, Moss (1972) briefly discusses the theoretical importance of the three-dimensional architecture of collagen and elastic fiber networks in the dermis for the biomechanical properties of certain skin regions of vertebrates. Some authors have pinpointed regional variations in mechanical properties of snake skin (Jayne 1988, Rivera *et al.* 2005) and shark skin (Naresh *et al.* 1997). Jayne (1988) explains the potential significance of the collagen and elastic fiber orientation for the mechanical properties of snake skin, but falls short of showing how the orientation of the fibers affect mechanical properties of the skin regions. Naresh *et al.* (1997) does correlate specific details (e.g., collagen fiber orientation and elastic fiber distribution) of the resting dermal architecture with mechanical properties, but he only speculates about the dynamic process of how the architecture changes during normal body movements.

It is known that, unlike in mammals and birds, the collagen fiber bundles of the reptilian dermis, especially those of crocodilians and turtles, are highly organized and arranged in orthogonal layers (Krause 1922; Lange 1931; Maderson 1964; Matoltsy & Huszar 1972; Moss 1972; Dhouailly & Maderson 1984; Landmann 1986; Craig *et al.* 1987; Jayne 1988; Alibardi and Thompson 2000; Maderson & Alibardi 2000; Richardson *et al.* 2002; Vickaryous & Hall 2008). Except for Craig *et al.* (1987), these authors imply that the entire dermis of these animals is homogenously organized over the entire body. However, the resting orientation and length of the collagen fiber bundles relative to the body axes differed among skin subregions. Alibardi and Thompson (2000) discuss the dermis's influence in regional differences of scale patterning in the growing alligator embryo, but do not mention the dynamic change in orientation of the collagen and elastic fiber bundles in the dermis during normal movements in an adult animal.

> *Retinacula cutis*

Retinacula cutis (i.e., skin ligaments) are collagen fiber bundles that anchor the skin to subcutaneous layers (e.g., the deep fascia or bone), thereby increasing the skin's resistance to stretching forces while allowing it to maintain its flexibility (Nash *et al.* 2004; Moore 2010). These structures have been described in humans because of their clinical significance for wound healing and cosmetic surgery (Nash *et al.* 2004; Moore *et al.* 2010), but they are described here in the alligator for the first time. In the alligator, the skin ligaments are most numerous in the non-expandable, but flexible, skin subregions, and originate from the deep layers of the *Stratum compactum* and anchor to the basement membrane of the scales or hard-cornified tuberosities of the interscale skin segments, thereby restricting movement of the scales relative to one another. Nash *et al*. (2004) describe the morphological variation (i.e. thickness and number) of skin ligaments in different regions of the body. This study revealed that the morphology and distribution of the *Retinacula cutis* varied in expandable and non-expandable skin subregions in the alligator, being shorter, thicker and more numerous in places where the scales must remain stable (e.g., the cranial edges of the scales of the ventral cervical skin subregion) and being longer, thinner and less numerous in places where the scales are moved great distances relative to one another in expandable skin subregions (e.g., the sublingual skin subregion). The *Retinacula cutis* and their accompanying elastic fiber bundles, and the hard-cornified scales and tuberosities form a passive fibro-elastic skeletal system. The tendon-like *Retinacula cutis* fibers anchor to the rigid scales and tuberosities, which transmit forces as the scales are moved passively, allowing them to resist stretching forces and dictating how the interscale skin is folded in its resting condition. The resilience of the elastic fiber bundles allows passive recoil and repositioning of the skin to its resting configuration when stretching forces are released, and the *Retinacula cutis* help to guide the skin back into its resting configuration.

> *Stratum elasticum*

An elastic membrane between the dermis and *Fascia superficialis* is known for birds (Lange 1931, Homberger & de Silva 2000, Orellana *et al.* 2012; Homberger & Orellana in prep.), lizards (Lange 1931, personal observations) and snakes (Lange 1931, Close & Cundall 2012). However, this layer has never been described in alligators. In alligators, this study shows that the elastic portion of the integument comprises the deepest layer of the dermis itself, namely the *Stratum elasticum*, and is not a separate structure separating the dermis from the underlying

www.manaraa.com

Fascia superficialis. In birds, the elastic membrane, together with the fatty *Fascia superfialis* forms a subcutaneous layer responsible for passive repositioning of feathers after active erection with smooth dermal feather muscles (Homberger & de Silva 2000). As the feathers are moved actively by the smooth dermal muscles, the non-compressible fat bodies in the *Fascia superficialis* bulge into the elastic membrane, causing its fibers to lengthen and store elastic energy (Homberger & de Silva 2000). When the erector feather muscles relax, the elastic fiber bundles of the elastic membrane release their elastic energy, helping to return the feathers and skin to their resting condition passively (Homberger & de Silva 2000). The *Stratum elasticum* in the alligator works in a similar way. Instead of active movement of the skin with dermal musculature, the passive expansion of the interscale skin segments due to external forces causes the dermal collagen fiber bundles fibers to change their orientation and tension on the attachments to the scales, and the skin flattens and lengthens. Lengthening of the skin causes the elastic fiber bundles of the *Stratum elasticum* to be stretched and store elastic energy, which is released once stretching forces subside and the dermal collagen fiber bundles return to their resting configuration.

  ➢ Reconstructing the Evolutionary History of the Alligator Integument

Crocodilians and birds are the last surviving Archosaurs, and a functional-morphological comparison of their integument can yield insights into the evolution history of the structures of their fundamentally different integuments. The integument of the common Archosaurian ancestor probably resembled the integument of extant squamates in having imbricating scales and smooth dermal musculature (Homberger & de Silva 2000; Homberger 2002; Orellana *et al.* 2012; Homberger & Orellana in prep.). This study on the expansion and recoil mechanism of the skin of alligators shows that mechanism of scale movement in extant archosaurian reptiles (i.e., crocodilians) differs fundamentally from the active movement of feathers by smooth dermal musculature in birds. As archosaurian scales became larger and more plate-like in crocodilians and dinosaurs, the dermal musculature was no longer needed and was lost; hence, crocodilian and dinosaurian plate-like, non-imbricating scales are a derived condition; and the avian integument, while evolving specialized and derived appendages, retained the dermal musculature so that they can actively move their feathers. Both crocodilian and bird skins share many ancestral features such as dermal fat (though elaborate in birds, alligators retain some isolated

97

dermal fat bodies that surround small blood vessels and nerves), and an elastic layer responsible for passive recoil of the skin after being actively (birds) or passively (alligators) stretched.

2.4.2. The Expansibility of the Skin Regions and its Implications for the Alligator Feeding Mechanism

- **Characteristics of Expandable Skin**

Expandable skin subregions are characterized by wide and deep interscale skin segments that are often deeply folded in the relaxed condition. These expandable interscale skin segments have an underlying *Stratum compactum* whose entire thickness is occupied by the collagenous joint fiber bundles that anchor to the hard-cornified basement membrane of adjacent scales. The *Stratum compactum* under the scales is comprised of orthogonal layers of straight collagen fibers that are oriented obliquely caudolateral or craniomedial to the sagittal body axis; thus they have the ability to change their angles relative to the body axis so that the skin can lengthen. Alternatively, the collagen fiber bundles of the *Stratum compactum* under the scales can be wavy in the resting configuration and oriented along the sagittal or transverse body axis (e.g., the sublingual skin subregion). In this way they can straighten to allow lengthening of the skin. The *Stratum elasticum* of expandable skin subregions comprises many layers of tightly packed elastic fiber bundles that are oriented at various angles along the body axes. Sparse and thin *Retinacula cutis* fibers anchor the scales and hard-cornified tuberosities to the deep layers of the dermis.

- **Characteristics of Non-expandable Skin**

Non-expandable skin subregions are characterized by narrow interscale segments whose *Stratum compactum* have a thin superficial layer of short collagenous joint fiber bundles that anchor to the hard-cornified basement membrane of adjacent scales. The *Stratum compactum* under the scales is comprised of orthogonal layers of straight collagen fiber bundles that are oriented parallel to the sagittal or transverse body axes; hence, they are already aligned in the direction of the stretching force and will resist further lengthening of the skin by becoming taut. The *Stratum elasticum* of the non-expandable skin subregions comprise few layers of loosely packed elastic fiber bundles that are oriented at various angles to the body axes. These elastic fiber bundles are probably not so important for elastic recoil of these non-expandable skin subregions, but are a result of the continuity of the *Stratum elasticum* within the entire

98

intermandibulo-cervical integument. Thick and numerous *Retinacula cutis* fibers anchor the scales and hard-cornified tuberosities tightly to the deep layers of the *Stratum compactum*.

Some skin subregions are expandable along the sagittal body axis, but not expandable along the transverse body axis (e.g., the ventral cervical skin subregion). In these cases, the non-expandable properties of the dermis can be seen in the transverse sections through the non-expandable interscale skin segment; and the expandable properties of the dermis are seen in the longitudinal sections through the expandable interscale skin segment.

- **Intermandibular Skin Region**
  - ➢ Expandable Skin Subregions

The intermandibular region comprises skin subregions that are expandable oblique to and parallel to the transverse and sagittal body axes, with the exception of the subhyoid and symphyseal skin subregions. Crocodilians have the ability to acquire very large prey items. The expansibility of the intermandibular skin region allows the manipulation and positioning of these large prey items within the oral cavity prior to swallowing.

The pararamal skin subregion is the most expandable subregion—most of the transverse and ventral expansion of the intermandibular skin region occurs here along the mandibular rami as the longitudinal skin folds of the paramal subregion are flattened and the dermis is elongated transversely. The fanned shape of this skin subregion allows the skin to stretch below the rigid frame of the angle of the jaws. In the alligator, large prey items pass through the oral cavity to the pharynx by enlarging the space below the mandible. Expansion of the intermandibular skin region transversely and ventrally requires the depression of the stiff, cartilaginous hyoid apparatus. The hyoid apparatus is supported by the non-expandable plate-like subhyoid skin subregion as it is depressed against the skin.

Expandable skin regions require conditioning in order to remain pliable. It is unlikely that the lipogenic layers of the *Stratum spinosum* of the epidermis of the pararamal skin subregion can produce enough lipid content to maintain the pliability of this skin subregion (see Khnykin *et al* 2011). The grooves of this skin subregion are continuous with the orifice of the lipid-producing gular gland at the caudal angle of the jaws. The anatomical data presented supports the hypothesis that the secretions from these glands provide the extra lipid content needed to keep this skin subregion adequately conditioned. Expansion and compression of the skin in this

subregion would help to massage the oily secretion along the grooves. The lower level of the *Stratum corneum* in this skin subregion is rich in lipid content, but stains lightly in the upper layers; however, the *Stratum disjunctum* can often be observed with cell-like debris that stains positively with Oil Red O for lipids, suggesting that that a superficial layer of lipid-rich material is being deposited on the surface of the interscale *Stratum corneum*, supplementing the lipid content being produced from the underlying *Stratum spinosum*. Stettenheim (2000) suggested an analogous function for the uropygial gland as an accessory conditioning gland in birds, and Elias *et al*. (1987) alluded to this function for the sebaceous glands of mammals.

> Non-expandable Skin Subregions

The intermandibular skin region has to be expandable because it must accommodate large prey items before swallowing. However, there are two skin subregions in the intermandibular skin region that are non-expandable: the symphyseal skin subregion behind the mandibular symphysis, and the subhyoid skin subregion that subtends the hyoid apparatus.

The symphyseal skin subregion is the only skin subregion that contains dome pressure receptors (see Soares 2002). These mechanoreceptors, located under the hard-cornified scales, are covered by flexible soft-cornified epidermis, which is more easily deformed by hydrodynamic pressure waves. The *Stratum laxum* under these scales is limited to just the area surrounding the Merkel cell dermal column. The loose connective tissue of the *Stratum laxum* is deformable. Because this skin subregion does not expand at its interscale skin segments, the dermal fibers do not change their configuration, and hence, the skin does not flatten or lengthen, or perform any other movement that would unnecessarily disturb the mechanoreceptor. The isolation of the dome pressure receptor within the *Straum laxum* ensures that only pressure waves stimulate the sense organs. This interpretation is supported by the fact that the only other area where DPRs are found in alligators are over the non-moveable skin that covers the external surface of the mandible. It is not known why the dome pressure receptors are retained on the symphyseal skin subregion in alligators, or why they are retained over the whole body in crocodiles and caimans, or if the dome pressure receptors of the mandibular skin has a different function that the dome pressure receptors found on the body scales.

The other non-expandable skin subregion is the subhyoid skin subregion. This skin subregion lies directly over the hyoid apparatus, which is depressed during feeding (Cleuren & De Vree 1992, 2000). The depression of the rigid cartilaginous hyoid body against the skin,

100

especially under the weight of a heavy food items, necessitates the skin to form a firm, but flexible plate. It does this with square shaped scales that have very narrow and non-expandable interscale skin segments between them. Somewhat more flexibility is possible along the sagittal body axis because the caudal edge of the cranial scale is slightly raised above the cranial edge of the scale behind it, increasing the length of the transverse interscale skin segment ever so slightly. This skin subregion is the most cranial skin subregion that shows a small degree of scale overlap. This overlap increases caudally (see below).

- **Gular Skin Region**

The gular skin region surrounds the most mobile elements of the feeding apparatus. The hyoid apparatus is not only depressed, but also retracted (Cleuren & De Vree 1992, 2000), so it moves against the subhyoid skin subregion and also against the cranial part of the posthyoid skin subregion; the bony retroarticular process moves dorso-ventrally under the retroarticular skin subregion as the jaws are opened; and pterygoid muscles bulge against the pterygoid and retroarticular skin subregions when the jaws are closed. The skin subregions of the gular skin region expand in different amounts and directions, depending on which structures move beneath it.

The posthyoid skin subregion is a continuation of the stiff plate formed by the subhyoid skin subregion, but caudally the circumferential interscale skin segments become wider, and the scales become more and more overlapped to facilitate expansion of the skin along the sagittal body axis and, hence, dorso-ventral movements of the head and neck, especially during cranio-inertial feeding (see Gans 1969; Busbey 1989; Cleuren & De Vree 1992, 2000).

The pterygoid and retroarticular skin subregions expand radially to accommodate the bulging pterygoid musculature. The scales, though oriented in transverse rows, have oblique edges, much like the patches on a soccer ball. The obliquely oriented expandable interscale segments allow the skin to expand radially as the bulging pterygoid muscles contract around the retroarticular processes to close the jaws.

As the pterygoid and retroarticular skin subregions expand radially, tension builds circumferentially in the posthyoid skin subregion, whose longitudinal interscale skin segments are non-expandable. This causes the posthyoid skin to stiffen and to be lifted dorsally, so that closing the jaws effectively narrows the entrance to the throat. This is supported by Busbey's

101

(1989) and Cleuren & De Vree's (1992, 2000) kinematic study showing that the alligator opens its jaws as large food items pass into the pharynx. Opening the jaws would allow the pterygoid muscles and the skin of the pterygoid and retroarticular subregions to relax, releasing the circumferential tension on the posthyoid skin subregion and allowing the circumferential interscale skin segments to unfold as the skin of the throat expands along the sagittal body axis and the hyoid apparatus is depressed and retracted. The circumferential interscale skin segments expand and lengthen even more as the head is lifted dorsally to help shift the food item backwards into the throat.

The deep layers of the *Stratum compactum* of the dermis of these skin subregions contain numerous dermal fat bodies under the scales, which surround nerves and blood vessels. This perivascular dermal fat serves as a hydraulic cushion to distribute pressure around the nerves and blood vessels so that they are not crushed as the muscles bulge under the skin and push them against the hard surface of the overlying scales.

- **Cervical Skin Region**

The scales of the ventral cervical skin subregion are in the most extreme overlapping configuration, which allows the head and neck to be flexed and extended dorso-ventrally and laterally. The lateral cervical skin subregion can expand along the transverse body axis as the ventral cervical skin subregion lengthens sagittally. This combination of transverse expansion and sagittal lengthening of the skin allows the neck skin to expand ventrally, but will result in narrowing of the diameter of the throat. Because the longitudinal interscale skin segments of the ventral cervical skin subregion, like the posthyoid skin subregion, cannot expand, the diameter of the neck and throat cannot be increased. This interpretation is supported by the fact that the skin overlies the *M. constrictor colli cervicalis*, which has extensive non-expandable dorsal and ventral aponeuroses, whose fibers encircle the circumference of the neck and limit circumferential expansibility (see Chapter 3).

- **Dorsal tuberculate skin region**

The dorsal tuberculate skin subregion is not expandable due to the orthogonally arranged collagen fiber bundles being oriented along the transverse and sagittal body axes being straight and taut in their resting configuration. The tall pointy tuberculate scales serve as attachment sites

102

for adhesions between the aponeuroses of the constrictor musculature, the superficial fascia, and the dermis, and so the tuberculate scales, along with the bony osteoderms of the neck (i.e. the nuchal rosette, Richardson *et al.* 2002), can be categorized as an exoskeleton (see also Chapter 3). If the skin could stretch in this region, these tuberculate scales and osteoderms would be less effective as attachment sites.

It is also possible that these conical scales, along with the ridged surface of the osteoderms function to reduce drag during swimming. The ribbed placoid scales of sharks (Reif 1985, Lang *et al.* 2008) and the texturized feathers of birds (Nachtigall 1998, Homberger & de Silva 2000; Homberger 2002) have been shown to have this turbulence-reducing effect during swimming and flying, respectively. Scales serving this function would need to be stabilized in a non-expandable skin region.

2.5. Conclusions

The functional-anatomical data presented here has shown that, while the intermandibular skin region is expandable, alligators cannot and do not swallow large prey items relative to their head size, because the cervical integument that surrounds the neck and throat is not circumferentially expandable. Instead, the alligator has evolved structural characteristics of the head (e.g., a strong akinetic skull, long jaws and an expandable intermandibular region) to subdue large prey items, but these must be broken down before passing through the throat.

2.6. References

Alibardi, L. & Thompson, M.B. 2000. Scale morphogenesis and ulstrastructure of the dermis during embryonic development in the alligator (*Alligator mississippiensis*, Crocodilia, Reptilia). Acta Zoological (Stockholm) 81: 325-338.

Alibardi, L. & Thompson, M.B. 2001. Fine structure of the developing epidermis in the embryo of the American alligator (*Alligator mississippiensis*, Crocodilia, Reptilia). Journal of Anatomy 198: 265-282.

Alibardi, L. 2003a. Adaptation to the land: The skin of reptiles in comparison to that of amphibians and endotherm amniotes. Journal of Experimental Zoology (Mol Dev Evol) 298B: 12-41.

Alibardi, L. 2003b. Immunocytochemistry and keratinization in the epidermis of crocodilians. Zoological Studies 42(2): 346-356.

Alibardi, L. & Toni, M. 2007. Characterization of keratins and associated proteins involved in the corneification of crocodilian epidermis. Tissue & Cell 39: 311-323.

Alibardi, L. Toni, M. & Dalla Valle, L. 2007. Hard cornification in reptilian epidermis in comparison to cornification in mammalian epidermis. Experimental Dermatology 16: 961-976.

Arnold, E.N., Azar, D., Ineich, I. & Nel, A. 2002. The oldest reptile in amber: A 120 million year old lizard from Lebanon. Journal of Zoology, London 258: 7-10.

Banerjee, T.K. & Mittal, A.K. 1980. Histochemistry of snake epidermis. Pp. 23-34 *in* The Skin of Vertebrates (R.I.C. Spearman & P.A. Riley, eds.). Academic Press, London.

Bonner, J. 2010. Tooth to tail oddities in an ancient croc. Nature 1038: 389.

Bragulla, H.H. & Homberger, D.G. 2009. Structure and functions of keratin proteins in simple, stratified, keratinized and cornified epithelia. Journal of Anatomy 214: 516-559.

Brazaitis, P. 1987. The identification of crocodilian skins and products. Pp. 373-386 *in* Wildlife Management: Crocodiles and Alligators (Webb, G.J., Manolis, S.C., Whitehead, P.J., eds). Surrey Beatty & Sons Pty Limited in association with the Conservation Commission of the Northern Territory, Chipping Norton.

Busbey, A.B. III. 1989. Form and function of the feeding apparatus of *Alligator mississippiensis*. Journal of Morphology 202(1): 99-127.

Carson, F.L. & Hladik, C. 2009. Histotechnology: A self-instructional text, 3rd Edition American Society for Clinical Pathology Press, Chicago.

Clark, C. & Logan, L.E. 1987. Copy Photography. Pp. 488-495 *in* The Guild Handbook of Scientific Illustration (Hodges, E.R.S., ed.). Van Nostrand Reinhold, New York.

Cleuren, J. & De Vree, F. 1992. Kinematics of the jaw and hyolingual apparatus during feeding in *Caiman crocodilus*. Journal of Morphology 212: 141-154.

Cleuren, J. & De Vree, F. 2000. Feeding in crocodilians. Pp. 337-358 *in* Feeding: Form, Function and Evolution in Tetrapod Vertebrates (Schwenk, K., ed.). Academic Press, San Diego.

Close, M. and Cundall, D. Extensible tissues and their contribution to macrostomy in snakes. Integrative and Comparative Biology, abstract 89.1.

Craig, A.S., Eikenberry, E.F. & Parry, D.A.D. 1987. Ultrastructural organization of the skin: Classification on the basis of mechanical role. Connective Tissue Research 16: 213-223.

Cummins, C.L. 1986. The morphology of the hyoid apparatus and gular region of the Snowy Egret, *Egretta thula* (Molina), (Aves: Ardeidae). M.S. Thesis, Louisiana State University A&M College, Baton Rouge.

104

Cummins, C.L. & Homberger, D.G. 1986. The morphology of the gular region of the Snowy Egret, *Egretta thula* (Molina). American Zoologist 26: 66A.

Cundall, D. & Greene. 2000. Feeding in Snakes. Pp. 175-291 *in* Feeding: Form, Function and Evolution in Tetrapod Vertebrates (K. Schwenk, ed.). Academic Press, San Diego.

Dehnhardt, G. & Mauk, B. 2009. The Physics and Physiology of Mechanoreception. Pp. 287-299 *in* Sensory Evolution on the Threshold: Adaptations in Secondarily Aquatic Vertebrates (Thewissen, J.G.M. & Nummela, S., eds.). University of California Press, Berkley.

De Vree, F. & Gans, C. 1994. Feeding in Tetrapods. Pp. 93-117 *in* Advances in Comparative and Environmental Physiology, Volume 18 (Bels, V., Chardon M. & Vandewalle, P, eds.). Springer-Verlag, Berlin.

Diefenbach, C. 1975. Gastric function in *Caiman crocodilus* (Crocodylia: Reptilia)—I. Rate of gastric digestion and gastric motility as a function of temperature. Comparative Biochemistry and Physiology 51A: 259-265.

Douhailly, D. & Maderson, P.F.A. 1984. Ultrastructural observations on the embryonic development of the integument of *Lacerta muralis* (Lacertilia, Reptilia). Journal of Morphology 179: 203-228.

Elias, J.A., McBrayer, L.D., Reilly, S.M. 2000. Prey transport kinematics in *Tupinambis teguixin* and *Varanus exanthematicus*: Conservation of feeding behavior in 'chemosensory-tongued' lizards. The Journal of Experimental Biology 203: 791-801.

Elias, P.M., Menon, G.K., Grayson, S., Brown, B.E. & Rehfeld, S.J. 1987. Avian sebokeratocytes and marine mammal lipokeratinocytes: Structural, lipid biochemical, and functional considerations. The American Journal of Anatomy 180: 161-177.

Frolich, L.M. 1997. The role of the skin in the origin of amniotes: Permeability barrier, protective covering and mechanical support. Pp. 327-352 *in*: Amniote Origins: Completing the Transition to Land (S.S. Sumida & K.L.M. Martin, eds.). Academic Press, San Diego.

Gans, C. 1969. Comments on inertial feeding. Copeia 1969(4): 855-857.

Gans, C. 1974. Biomechanics: An Approach to Vertebrate Biology. The University of Michigan Press, Ann Arbor. Pp. 22-71

Grigg, G. & Gans, C. 1993. Morphology and physiology of the Crocodylia. Ch. 40 *in* The Fauna of Australia, Vol. 2A, Australian Government Publishing Service, Canberra.

Hicken, C.E., Linbo, T.L., Baldwin, D.H., Willis, M.L., Myers, M.S., Holland, L., Larsen, M., Stekoll, M.S., Rice, S.D., Collier, T.K., Scholz, N.L. & Incardona, J.P. 2011. Proceedings of the National Academy of Science 108(17): 7086-7090.

Homberger, D.G. 1986. The lingual apparatus of the African Grey Parrot, *Psittacus erithacus* Linné (Aves: Psittacidae): Description and theoretical mechanical analysis. Ornithological Monographs No. 39. The American Ornithologists' Union, Washington, D.C.

Homberger, D.G. 1999. The avian tongue and larynx: Multiple functions in nutrition and vocalization. Pp. 94-113 *in* Proceddings of the 22nd International Ornithological Congress, Bird Life: South Africa.

Homberger, D.G. & de Silva, K. 2000. Functional microanatomy of the feather-bearing integument: Implications for the evolution of birds and avian flight. American Zoologist 40: 553-574.

Homberger. D.G. 2002. The aerodynamically streamlined body shape of birds: Implications for the evolution of birds, feathers, and avian flight. Pp. 227-252 *in* Proceedings of the 5th symposium of the Society of Avian Paleontology and Evolution, Beijing, 1-4 June 2000 (Zhou, Z. & Zhang, F., eds.). Science Press, Beijing, China.

Homberger, D.G. & de Silva, K.N. 2003. The role of mechanical forces on the patterning of the avian feather-bearing skin: A biomechanical analysis of the integumentary musculature in birds. Journal of Experimental Zoology (Mol Dev Evol) 298B: 123-139.

Jayne, B.C. 1988. Mechanical behavior of snake skin. Journal of Zoology, London 214: 125-140.

Khnykin, D., Miner, J.H. & Jahnsen, F. 2011. Role of fatty acid transportiers in the epidermis: Implications for health and disease. Dermato-Endocrinology 3(2): 53-61.

Kim, J.Y, Kim, k.S., Lockley, M.G. & Seo, S.J. 2010. Dinosaur skin impressions from the Cretaceous of Korea: New insights into modes of preservation. Palaeoecology 293: 167-174.

Krause, R. 1921. Mikroskopische Anatomie der Wirbeltiere in Einzeldarstellungen. II. Vögel und Reptilien. Walter de Gruyter & Co., Berlin & Leipzig, Pp. 319-323.

Landmann, L. 1986. Chapter 9: Epidermis and Dermis. Pp. 150-187 *in* Biology of the Integument, Vol. 2J (Bereiter-Hahn, A.G. Matoltsy & K.S. Richards eds.). Springer Verlag, Berlin.

Lang, A.W., Motta, P., Hidalgo, P. & Westcott, M. 2008. Bristled shark skin: A microgeometry for boundary layer control? Bioinspiration & Biomimetics 3: 1-9.

Lange, B. 1931. Integument der Sauropsiden. Pp. 375-448 *in* Handbuch der vergleichenden Anatomie der Wirbeltiere, Band 1 (L. Bolk, E. Göppert, E. Kallius & W. Lubosch eds.). Urban & Schwarzenberg, Berlin.

Lillywhite, H.B. & Maderson, P.F.A. 1982. Skin structure and permeability. Pp. 397-442 *in* Biology of the Reptilia, Vol. 12, Physiology C, Physiological Ecology (C. Gans & F.H. Pough eds.). Academic Press, London.

Lucas, A.M. & Stettenheim, P.R. 1972. Avian anatomy: Integument. Part II. Pp. 660-665 *in* Agricultural Handbook 362. United States Department of Agriculture, Washington, D.C.

Maderson, P.F.A. 1964. The skin of lizards and snakes. British Journal of Herpetology 3(6): 151-154.

Maderson, P.F.A. 1984. The squamate epidermis: A new light has been shed. Pp. 111-124 *in* The structure, Development, and Evolution of Reptiles (M.W. Ferguson ed.). Academic Press, London.

Maderson, P.F.A. & Alibardi, L. 2000. The development of the Sauropsid integument: A contribution to the problem of the origin and evolution of feathers. American Zoologist 40: 513-529.

Matoltsy, A.G. & Huszar, T. 1972. Keratinization of the reptilian epidermis: An ultrastructural study of the turtle skin. Ultrastructure Research 38: 87-101.

Menon, G.K. & Menon J. 2000. Avian epidermal lipids: Functional considerations and relationship to feathering. American Zoologist 40: 540-552.

Mercer, E.H. 1961. Keratin and Keratinization. Pergamon Press, New York.

Metzger, K.A. & Herrel, A. 2004. 3-D analysis of inertial transport in tegus: Modulation of jaw and craniocervical kinematics. Integrative and Comparative Biology 44(6): 604.

Metzger, K.A. & Herrel, A. 2004. 3-D analysis of inertial transport in tegus: Modulation of jaw and craniocervical kinematics. Integrative and Comparative Biology 44(6): 604.

Montuelle, S.J., Herrel, A., Schaerlaeken, V., Metzger, K.A., Mutuyeyezu, A. & Bels, V.L. 2009. Inertial feeding in the teiid lizard *Tupinambis merianae*: The effect of prey size on the movements of the hyolingual apparatus and the cranio-cervical system. The Journal of Experimental Biology 212: 2501-2510.
.
Moore, K.L., Dalley, A.F. & Agur, A.M.R. 2010. Clinically Oriented Anatomy, 6th ed. Lippencott Williams & Wilkins, Baltimore, MD.

Moss, M.L. 1972. The vertebrate dermis and the integumental skeleton. American Zoologist 12: 27-34.

Nachtigall, W. 1998. Starlings and starling models in wind tunnels. Journal of Avian Biology 29: 478-484.

Naresh, M.D., Arumugam, V. & Sanjeevi, R. 1997. Mechanical behavior of shark skin. Journal of Bioscience 22(4): 431-437.

Nash, L.G., Phillips, M.N., Nicholson, H., Barnett, R. & Zhang, M. 2004. Skin ligaments: Regional distribution and variation in morphology. Clinical Anatomy 17(4): 287-293.

Neill, W.T. 1975. The Last of the Ruling Reptiles: Alligators, Crocodiles, and their Kin. Columbia University Press, New York.

Parakkal, P.F. & Alexander, N.J. 1972. Keratinization: A Survey of Vertebrate Epithelia. Academic Press, New York. Pp. 14-25.

Pianka, E.R. 1995. Evolution of body size: Varanid lizards as a model system. The American Naturalist 146(3): 398-414.

Reilly, S.M., McBrayer, L.D. & White, T.D. 2001. Prey processing in amniotes: Biomechanical and behavioral patterns of food reduction. Comparative Biochemistry and Physiology Part A 128: 397-415.

Reif, W.-E. 1985. Morphology and hydrodynamic effects of the scales of fast swimming sharks. Fortschritte der Zoologie 30: 483-485.

Richardson, K.C., Webb, G.J.W., & Manolis, S.C. 2002. Crocodiles: Inside Out. A Guide to the Crocodilians and their Functional Morphology. Surrey Beatty & Sons, Chipping Norton.

Rivera, G., Savitzky, A.H. & Hinkley, J.A. 2005. Mechanical properties of the integument of the common gartersnake, *Thamnophis sirtalis* (Serpentes: Colubridae). The Journal of Experimental Biology 208: 2913-2922.

Romeis, B. 1968. Mikroskopische Technik. R. Oldenbourg Verlag, München.

Savitzky, A.H., Townsend, V.R., jr., Hutchinson, D.A. & Mori, A. 2004. Dermal characteristics, scale row organization & the origin of macrostomy in snakes. Journal of Morphology 260:325.

Sawyer, R.H., Glenn, T., French, J.O., Mays, B., Shames, R.B., Barnes, G.L., Jr., Rhodes, W. & Ishikawa, Y. 2000. The expression of beta (β) keratins in the epidermal appendages of reptiles and birds. American Zoologist 40:530-539.

Schumacher, G.-H. 1973. The head muscles and hyolaryngeal skeleton of turtles and crocodilians. Pp. 101-199 *in* Biology of the Reptilia (Gans, C. & Parsons, T.S., eds.), Academic Press, London.

Schwenk, K. 2000. Feeding in lepidosaurs. Pp. 175-291 *in* Feeding: Form, Function and Evolution in Tetrapod Vertebrates (Schwenk, K., ed.). Academic Press, San Diego.

Smith, K.K. 1985. Strain gauge measurement of mesokinetic movement in the lizard *Varanus exanthematicus.* Journal of Experimental Biology 114: 53-70.

Smith, K.K. 1986. Morphology and function of the tongue and hyoid apparatus in *Varanus* (Varanidae, Lacertilia). Journal of Morphology 187: 261-287.

Soares, D. 2002. An ancient sensory organ in crocodilians. Nature 417: 241-242.

Soulé, M. & Kerfoot, W.C. 1972. On the climatic determination of scale size in a lizard. Systematic Zoology 21(1): 97-105.

Spearman, R.I.C. 1966. The keratinization of epidermal scales, feathers, and hairs. Biological Review 41: 59-96.

Spearman, R.I.C. 1973. The skin of reptiles. Pp. 83-90 *in* The Integument: A Textbook of Skin Biology. Cambridge University Press, London.

Stettenheim, P.R. 2000. The integumentary morphology of modern birds—An overview. American Zoologist 40: 461-477.

Szirmai, J.A. 1970. The organization of the dermis. Pp. 1-17 *in* Advances in Biology of the Skin, Vol. 10 (Montagna, W., Bentley, J.P. & Dobson, R.L., eds.). Appleton-Century-Crofts, New York.

Vickaryous, M.K. & Hall, B.K. 2008. Development of the dermal skeleton in *Alligator mississippiensis* (Archosauria, Crocodylia) with comments on the homology of osteoderms. Journal of Morphology 269: 398-422.

von Düring, M. & Miller, M.R. 1979. Sensory nerve endings of the skin and deeper structures of reptiles. Pp. 407-441 *in* Biology of the Reptilia, Vol. 9, Neurobiology A. (Gans, C., ed.). Academic Press, London.

Wertz, P.W., Stover, P.M., Abraham, W. & Downing, D.T. 1986. Lipids of chicken epidermis. Journal of Lipid Research 27: 427-435.

Westneat, M.W. 2007. Twice bitten. Nature 449: 33.

Zweers, G.A. 1982. Pecking of the pigeon (*Columba livia* L.). Behavior 81(2/4): 173-230.

Zweifel, F.W. 1961. The handbook of biological illustration, 2nd Edition. The University of Chicago Press, Chicago, pp. 28-37.

Chapter 3

**The Intermandibulo-cervical *Fascia superficialis* and Constrictor Musculature
of the American Alligator (*Alligator mississippiensis*)**

3.1. Introduction

Underneath the skin (i.e., the *Cutis* consisting of the *Epidermis* and *Dermis*), two additional tissue layers contribute to the outer wall of the floor of the mouth, gullet, and throat, namely the subcutaneous *Fascia superficialis* and the constrictor musculature.

During feeding, the expandable skin of the intermandibular region can expand parallel to, perpendicular to, or obliquely to the sagittal and transverse body axes because of the oblique orientation of the interscale skin segments, which are determined by oval shaped, scales that are oriented transversely or obliquely to the body axes. The only exception is the subhyoid subregion, which can only expand slightly along the sagittal body axis because the square scales are oriented in transverse rows, and only the transverse interscale segments are expandable. In the gular skin region the skin is subdivided into subregions with square scales that are oriented in transverse rows, and whose interscale skin expands mainly along the sagittal body axis. Transverse rows with diagonal edges, which cause the interscale skin segments to be oriented obliquely, hence, expansion occurs radially to accommodate the bulging pterygoid musculature underneath. In the cervical regions, expansion of the skin occurs mainly along the sagittal body axis, because the square scales are oriented in circumferential and longitudinal rows, and only the circumferential interscale skin segments are expandable (see Chapter 2).

The *Fascia superficialis* of tubular animals and structures must be arranged helically around the neck. This type of organization of the non-expandable collagen fiber bundles allows bending movements without kinking, and, because the collagen fiber bundles can change their angle relative to the body axes, elongation of the fascia can occur without the need to lengthen the collagen fiber bundles (Wainwright 1978; Homberger & Walker 2004; Frolich 1997). This type of arrangement of the *Fascia superficialis* has been documented for swimming animals, such as sharks (Wainwright 1978; Homberger & Walker 2004), and reptiles such caimans and vipers (Craig *et al*. 1987) in which the helically arranged *Fascia superficialis* acts as an exotendon that functions in aspects of the animal's locomotory apparatus (Wainwright 1978; Craig *et al.* 1987; Homberger & Walker 2004), in the case of sharks. Based on these biomechanical principles and examples in sharks, we hypothesized that the inextensible collagen fiber bundles of the *Fascia superficialis* of the neck of the alligator must also be arranged helically around the neck at oblique angles, as the neck must bend from side to side and dorsoventrally during cranio-inertial

111

feeding and prey dismemberment; and transversely, circumferentially or longitudinally oriented collagen fiber bundles could not elongate to allow these movements.

The constrictor muscles have transverse or circumferentially oriented muscle fiber bundles in order to effectively constrict the neck. As their fibers shorten, the radius of the circular space that they enclose (i.e., the neck) decreases (Brasseur, J.G. 2007). In feeding activities, this helps to push the food bolus backwards towards the stomach (Brasseur, J.G. 2007). Hence, the *Fascia superficialis* and the constrictor muscles must expand passively along the same body axes *in tandem* with the skin, even though their constituent tissue types are organized differently along the sagittal and transverse body axes due to biomechanical constraints and must, therefore be expanded through different mechanisms. It is hypothesized that the integument, the *Fascia superficialis*, and the constrictor musculature together create an intermandibulo-cervical envelope that is quite obviously performing properly, despite differences in their fundamental tissues types and biomechanical properties. This functional-morphological study intends to gain a better understanding of the interplay between the skin and subcutaneous layers of the head and neck during feeding and, thereby, contribute to a better understanding of the structure and functioning of complex systems comprising components with different properties.

3.2. Materials and Methods

3.2.1. Materials

Two alligator specimen (DGH-AL-001 and 002) were part of the Comparative Anatomy Teaching Collection at the Department of Biological Sciences, Louisiana State University, Baton Rouge.   They had been obtained from Rockefeller Wildlife Refuge in 1999 by a former student, euthanized at the School of Veterinary Medicine, Louisiana State University, Baton Rouge, and perfused with 4% buffered formaldehyde solution through the left carotid artery.

3.2.2. Methods

- **Anatomical Techniques**
  - ➢ Microdissection

Specimens were dissected under stereomicroscopes (Wild Heerbrugg M3, Leica Microsystems Ltd., Switzerland), one of which was fitted with a dual ocular discussion tube (Wild Bridge Type 355110).   Illumination was provided through a fiber-optic ring-light fitted

112

with a polarizing filter and connected to a lightbox (Intralux 6000 or HCL 150, Volpi USA, Auburn, NY). Dissection tools included two pairs of fine stainless steel forceps (Dumoxel non-magnetic #5, Fine Science Tools, Inc., Foster City, CA; and SS Pakistan, Carolina Biological Supply Company, Burlington, NC), and a pair of stainless steel iridectomy microdissecting scissors (SS Pakistan, Carolina Biological Supply Company, Burlington, NC). The forceps were honed by hand under high magnification (160×) using a natural black Arkansas novaculite stone (Fine Science Tools, Foster City, CA).

The cutaneous and subcutaneous layers were dissected layer by layer under high magnification (64× and 160×). Adhesions between two tissue layers were marked by first separating them around the adhesion and then sewing a colored thread into the lower tissue layer around the base of the adhesion. The two tissue layers were then separated from each other by bisecting the adhesion above the threaded marker. In this way, the adhesions between two tissue layers could later be correlated with structures above and below the two tissue layers (see below).

- **Imaging techniques**
  - ➢ Macroscopic Orthographic Imaging

Specimens were placed on an Illuma Hibase copy stand with adjustable side-arms that hold light fixtures (model no 132-33 M2, Bencher, Inc., Antioch, IL). Two frosted Reveal® indoor flood lamps (General Electric, Fairfield, CT) were attached to each side arm. Digital images were taken with a vertically-mounted Spot Insight digital color camera (Meyer Instruments, Inc., Houston, TX) fitted with C-mount, manual iris, mono-focal CCTV lenses (2.2 mm, F1.4, National Electronics, Inc, Shawnee Mission, KS.; or 12.2 mm, F1.3, Goldinar M25). The camera lens aperture was minimized to increase the depth of focus, and the working distance of the camera was set at the center of the focal length of the lens.

Orthographic imaging involves the projection of the anatomical surfaces of a specimen (i.e., dorsal, ventral, sinistral, dextral, cranial and caudal surfaces) onto planes that are at right angles to one another. In effect, the specimen is virtually suspended in a box, and each of its surfaces is projected onto one of the sides of this box. Orienting the camera's optical axis perpendicularly to these surfaces ensures that all the perspective lines of sight are parallel to one another at any given point on the specimen and that they do not converge on a single vanishing point. This set-

113

up eliminates distortion or foreshortening of the photographs and creates monocular images of the anatomical surfaces (Zweifel 1961; Lucas & Stettenheim 1972; Clark & Logan 1989). This imaging technique not only produces a series of 2D images that can be used to understand the 3D structure of the specimen, but also creates replicability with different stages of a dissection and, therefore, the feasibility of topographic mapping.

In practical terms, each surface of a specimen has to be photographed separately. In order to ensure that the images of the surfaces of a specimen are oriented at right angles to one another, the specimen needs to be rotated exactly around its midsagittal axis as each side is photographed. The alligator was placed on its side on the copy stand under the vertically-mounted digital camera so that its left lateral side could be photographed. A level was placed on the horizontal surface of the camera to ensure that the optical axis was perpendicular to the plane of the specimen surface being photographed. At the same time, the specimen's midsagittal axis was aligned with the horizontal beam of a stationary 90º laser level. A second stationary 90 º laser level with a vertical beam was placed in front of the specimen to establish the transverse axis at a 90º angle to the midsagittal axis. After having photographed the lateral side, the specimen was rotated onto its abdomen to photograph its dorsal side, while ensuring that the transverse axis remained oriented at a 90º angle to the horizontal axis. In order to photograph the ventral surface, the specimen was then rotated onto its back around its midsagittal axis, keeping both axes aligned. Keeping the specimen aligned with these two axes as the lateral, dorsal, and ventral views were photographed prevented any deviations of the specimen's position in pitch, roll or yaw and ensured that the images of the various surfaces are comparable and reproducible.

➢ Mesoscopic Imaging

The *Fascia superficialis* was photographed from the internal surface under a MZ6 stereomicroscope (Leica Microsystems Ltd., Switzerland) with a motorized footswitch for focusing (model T-91-SE; Linemaster Switch Corp., Woodstock, CT). The stereomicroscope was placed on a Micro-g vibration isolation table [63-551 series, TMC (Technical Manufacturing Corporation), Peabody, MA] and equipped with a SPOT Insight digital color camera (Diagnostic Instruments, Inc., Houston, TX). Illumination was provided by Intralux 6000 lightboxes (Volpi USA, Auburn, NY) through two different types of fiber optic light guides. For microdissection under even illumination, a circular fiber optic ring light with an adjustable polarizing filter was fitted to the objective lens. For mesoscopic imaging with extended depth focus (EDF), a pair of

114

flexible fiber optic light guides (10 mm active bundle diameter) were mounted on articulated stands on heavy steel bases (Volpi USA, Auburn, NY), and adjustable polarizing filters (12.2 mm diameter, Edmond Optics, Inc., Barrington, NJ) were mounted to each light guide with a rotating SM1 lens tube and cage plates (Thorlabs, Ltd., UK).

The digital images were captured through ImagePro software (Meyer Instruments, Inc., Houston, TX), and an extended depth of field was obtained through In-Focus Automation software (Meyer Instruments, Inc., Houston, TX). The images were processed with Adobe® Photoshop CS3 (Adobe Systems, Inc., San Jose, CA) to adjust the brightness levels of the image histogram.

3.3. Results

3.3.1. Integument

The detailed functional morphology of the intermandibulo-cervical integument was described in Chapter 2. The skin of the intermandibular region is highly expandable along the transverse and sagittal body axes, allowing for the acquisition, positioning and manipulation of large prey items within the oral cavity. In contrast, the gular and cervical skin regions expand mostly along the sagittal body axis to allow dorsoventral and lateral flexions and extensions of the neck, whereas circumferential expansions are severely limited, which constrains the size of the food items that may pass from the mouth cavity to the stomach.

The three main skin regions (except for the tuberculate skin region) were delimited by adhesions of the constrictor muscle epimysia with the *Fascia superficialis* and the dermis. The locations of these adhesions corresponded to a change in scale and interscale morphology (see 2.2.3). This part of the study explores the functional-morphological relationships of the subcutaneous layers to the skin in the head, neck, and shoulders.

3.3.2. *Fascia superficialis*

The histology of the *Fascia superficialis* of each skin subregion was described in Chapter 2. In this section, the microanatomy of the *Fascia superficialis* will be described to understand the layered organization of its collagen fiber bundles, which is not visible in histological sections.

115

The *Fascia superficialis* is anchored to skeletal elements, such as the mandibular rami in the intermandibular region, the osteoderms on the dorsal side of the neck (i.e., the nuchal rosette, Richardson *et al.* 2002), and the spinous processes of the cervical vertebrae just caudal to the skull. Along the midventral line, the fiber bundles meet at an angle. The *Fascia superficialis* can be divided into three laminae (superficial, middle, and deep) based on their distinct collagen fiber orientations (Fig. 3.1). These laminae are interconnected by loose connective tissue, which allows them some translational movement relative to one another.
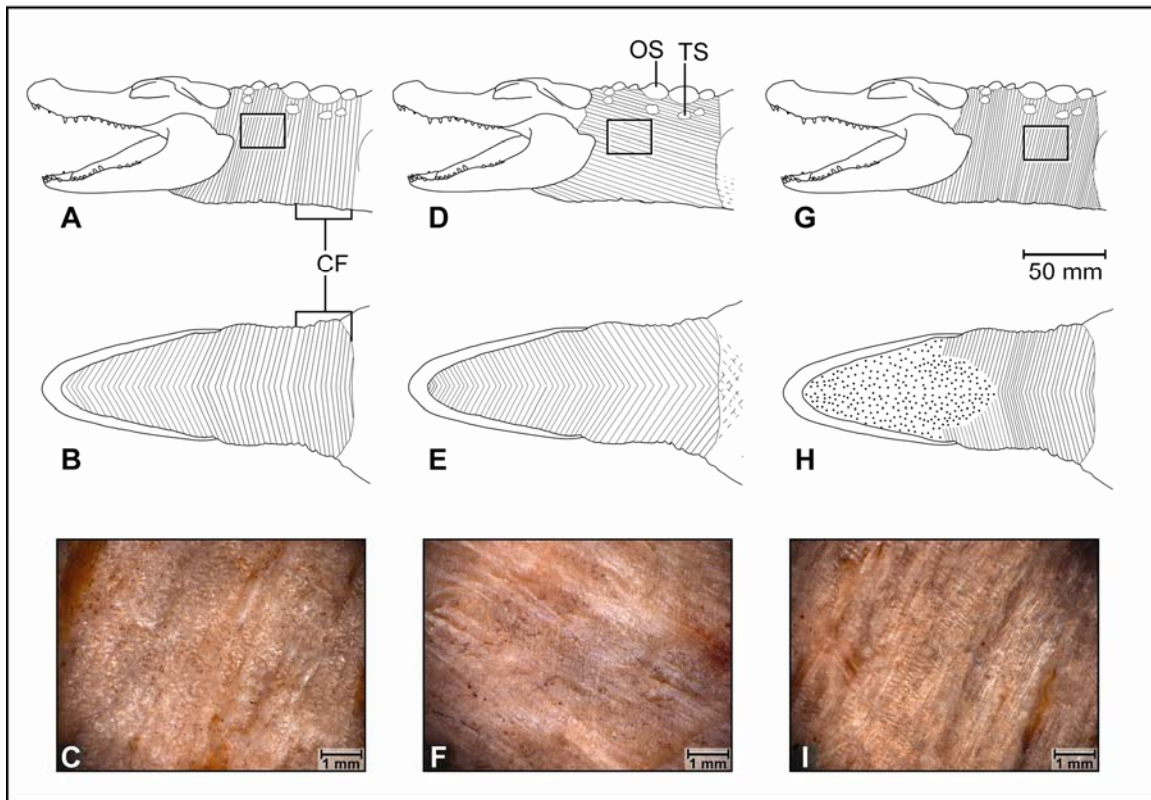
Figure 3.1 Diagrams of the collagen fiber orientations of the three laminae of the *Fascia superficialis* of the American Alligator (*Alligator mississippiensis*), drawn on outlines of an orthographic digital image of the head, neck, and shoulders. (**A-B**) Superficial lamina. (A) Lateral view. (B) Ventral view. (**C-D**) Middle lamina. (C) Lateral view. (D) Ventral view. (**E-F**) Deep lamina. (E) Lateral view. (D) Ventral view. Symbols: Parallel lines = collagen fiber bundles, dotted = diffuse fat tissue of the gliding surface of the deep lamina, dashed = attachment to muscle and skin of the pectoral region.

- **The Superficial Lamina of the *Fascia superficialis***

  ➢ Morphological Description

  The superficial lamina (Fig. 3.1A-C) lies directly underneath the dermal *Stratum elasticum*. It originates from the spinous processes of cranial cervical vertebrae and osteoderms. Along the midventral line, its collagen fiber bundles form wide angles that point rostrally in the resting condition, but are arranged more circumferentially in the caudal parts of the neck.

  In the intermandibular region, the collagen fiber bundles on the internal surface of the superficial lamina span the space between the mandibular rami, cross each other along the midventral line, and continue on the external side to anchor on the opposite mandibular rami. In the gular and cervical regions, the collagen fiber bundles on the internal surface of the superficial lamina run rostrally from their dorsal origins towards the midventral line as they wrap around one side of the neck. After crossing the midventral line, they continue their course on the opposite and external side of the superficial lamina to anchor dorsally. In this manner, the superficial lamina of the *Fascia superficialis* is actually a helically cross-wise sheet of collagen fiber bundles.

  ➢ Functional Interpretation

  Where the collagen fiber bundles of the superficial lamina forms wide oblique angles along the midventral line in the intermandibular and gular regions, the long collagen fiber bundles can adjust to radially out-pushing forces by realigning themselves more circumferentially and, thus, being able to wrap themselves around a larger circumference without lengthening. In these regions, the superficial lamina can also expand longitudinally without lengthening its fibers by changing the angle between their helically crossing fiber bundles. Lengthening of the superficial lamina of the *Fascia superficialis* in this manner is limited, though, because it is correlated with a concomitant narrowing and tightening of the fascia around the neck.

  In the caudal part of the cervical region, however, the collagen fiber bundles of the superficial lamina are already arranged nearly circumferentially and cannot realign themselves to adjust to an increased radius. Therefore, these collagen fiber bundles constrain an expansion of this part of the neck, such as during the deglutition of large prey items, because they will straighten, tighten, and resist further lengthening.

- **The Middle Lamina of the *Fascia superficialis***
  - ➤ Morphological Description

The middle lamina (Fig. 3.1D-F) lies directly underneath the superficial lamina. It originates from the mandibular rami, the occipital region of the skull, the spinous processes of cranial cervical vertebrae and osteoderms. Its collagen fiber bundles run caudally towards the shoulder girdle at a flatter angle than and in the opposite direction from those of the superficial lamina. Therefore, the collagen fiber bundles form more acute angles that point caudally or even run parallel along the midline. The middle lamina differs from the superficial and deep laminae by its less densely arranged, thinner, and somewhat wavy collagen fiber bundles

  - ➤ Functional Description

The more longitudinally aligned collagen fiber bundles of the middle lamina cannot realign themselves to any significant degree along the direction of a stretching force arising, for example, from bending the neck, but can adjust to an increased circumference of the neck by spreading apart its collagen fiber bundles. The role of the middle lamina appears to be a strengthening of the *Fascia superficialis* as a whole by providing a layer of collagen fiber bundles that are arranged cross-wise to the superficial and deep laminae.

- **The Deep Lamina of the *Fascia superficialis***
  - ➤ Morphological Description

The deep lamina (Fig. 3.1G-I) lies underneath the middle lamina of the *Fascia superficialis,* and directly external to the epimysium of the constrictor musculature (see below). Its collagen fiber bundles are oriented in the same direction as the superficial lamina (see above) and they also form the same type of helically wound sheet of cross-wise arranged collagen fiber bundles, which anchor on the mandibular rami, spinous processes of cranial vertebrae and osteoderms.

However, in the intermandibular region, the deep lamina is less rigidly organized as the collagen fiber bundles become thinner and intermingle with an amorphous ground substance that is interlarded with diffuse fat (Fig. 3.1H). This fat was absent in alligators that had been fasting (unpublished personal observation).

  - ➤ Functional Interpretation

In the intermandibular region, the plumped-up deep lamina may cushion the superficial layers of the integument and distribute pressures created by hard prey items and the hyoid

118

apparatus when prey items are manipulated and crushed inside the oral cavity during feeding. The less dense connective tissue of the deep lamina may also help the *Fascia superficialis* glide over the underlying constrictor muscles.

In the gular and cervical regions, the collagen fiber bundles of the deep lamina function like those of the superficial lamina, except that the caudalmost collagenous fiber bundles in the cervical region are not nearly as circumferential as those of the superficial lamina, but are nevertheless limited in their expansibility by the circumferential fibers of the superficial lamina.

3.3.3. Constrictor Musculature

The constrictor musculature is the most superficial striated musculature of the head and neck and can be subdivided into three identifiable muscles (Fig. 3.2 and Table 3.1). The proportion of their muscular and aponeurotic portions determines their overall expansibility.

- *Musculus intermandibularis*
  - ➢ Morphological Description

The *M. intermandibularis* is a sheetlike muscle whose fiber bundles span the space between the mandibular rami (Fig. 3.2B and D) and attaches fleshily along a bony ridge that runs obliquely from cranioventral to caudodorsal on the splenial bone, which covers the internal surface of the mandibular ramus. Its rostral border is located slightly caudal to the mandibular symphysis, thereby leaving a triangular area that is not covered by muscle [i.e., the *Trigonum intermandibulare anterius* (Schumacher 1973); Fig. 3.2D]. Its caudal border is formed by the caudalmost muscle fiber bundles, which originate from the mandibular ramus rostral to another triangular area that is not covered by muscle [i.e., the *Trigonum intermandibulare posterius* (Schumacher 1973); Fig. 3.2D]. In the midline, the caudal muscle fiber bundles of the *M. intermandibularis* interweave with the rostral muscles fiber bundles of the *M. constrictor colli gularis* (see below).

  - ➢ Functional Interpretation

The *M. intermandibularis* is stretched by prey items being manipulated in the oral cavity; it returns the floor of the mouth (i.e., skin, tongue, and hyoid apparatus) back to their resting condition when it contracts and shortens. The long, obliquely oriented muscle fiber bundles in the caudal two-thirds of the muscle allow a large expansion of the floor of the mouth and

119
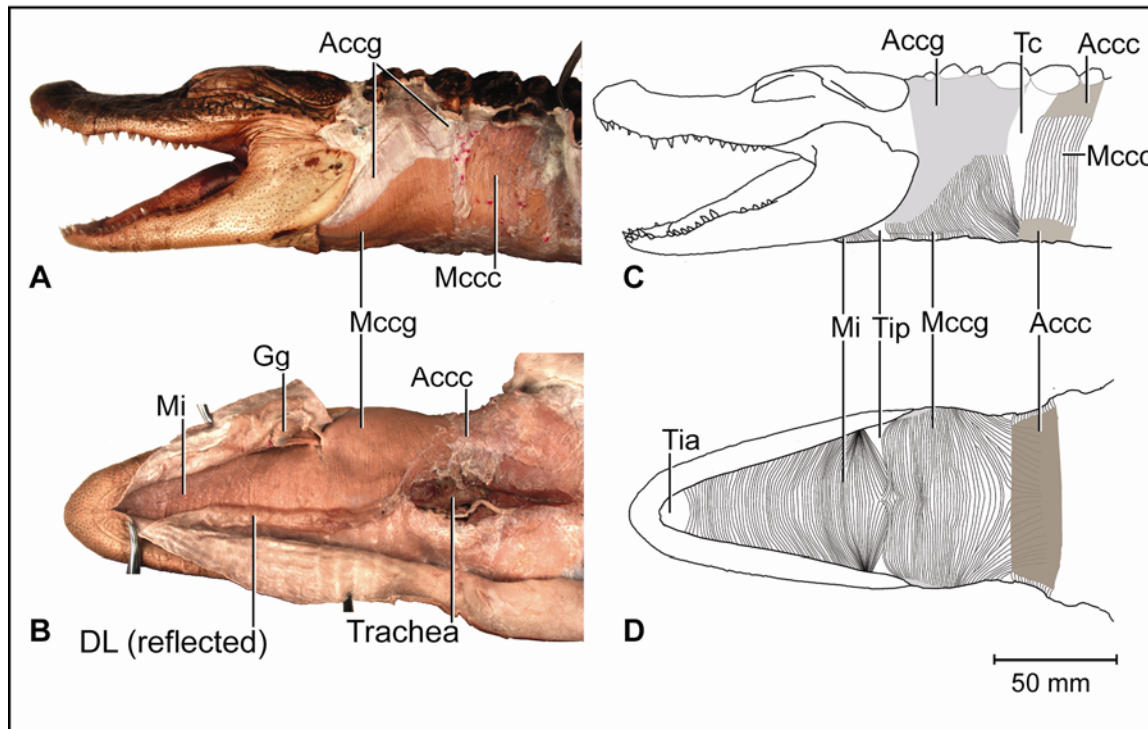
Figure 3.2 Orthographic images of the three constrictor muscles of the American Alligator (*Alligator mississippiensis*). (**A-B**) Macroscopic orthographic digital images; (A) Lateral view, (B) ventral view. (**C-D**) Orthographic schematic drawings; (C) Lateral view, (D) ventral view. Symbols: Accc = Aponeurosis of the *M. constrictor colli cervicalis*, Accg = Aponeurosis of the *M. constrictor colli gularis*, DL = Deep Lamina of the *Fascia superficialis*, Gg = Gular gland, Mccc = *Musculus constrictor colli cervicalis*, Mccg = *M. constrictor colli gularis*, Mi = *Musculus intermandibularis*, Tc = *Trigonum cervicalis*, Tia = *Trigonum intermandibulare anterius*, Tip = *Trigonum intermandibulare posterius*.

Table 3.1 Synonyms for the Constrictor Musculature of the American Alligator (*Alligator mississippiensis*)

Author	Species	Constrictor Muscles		
Dubansky & Homberger (this study)	*Alligator mississippiensis*	*Musculus intermandibularis*	*Musculus constrictor colli gularis*	*Musculus constrictor colli cervicalis*
Richardson *et al.*, 2002	*Alligator mississippiensis*	Intermandibular Muscle	Sphincter colli Muscle	Not specified
Schumacher 1973	*Alligator mississippiensis*	*M. intermandibularis*	*M. constrictor colli, Pars anterior, Pars posterior, Pars profundus*	Not specified
Chiasson 1962	*Alligator mississippiensis*	Intermandibular muscle	Not specified	Not specified
Sondhi 1958	*Gavialis gangeticus*	*M. mylohyoideus anterior principalis*	*M. mylohyoideus posterior*	*M. constrictor colli*
Poglayen-Neuwall 1953	*Alligator mississippiensis*	*M. intermandibularis/ M. constrictor I ventralis, Pars oralis & Pars caudalis*	*M. sphincter colli*	Not specified
Reese 1915	*Alligator mississippiensis*	*Intermaxillaris* or Mylohyoid muscle	Sphincter colli muscle	Not specified
Rathke 1866	*Crocodylus* spp.	*M. mylohyoideus*	*M. mylohyoideus posterior*	Not specified

121

intermandibular region, as they can first align themselves in the direction of the stretching force and then passively lengthen.

- *Musculus constrictor colli gularis*
  - ➢ Morphological Description

The *M. constrictor colli gularis* is a muscle sheet with aponeuroses, which envelops the gular region of the neck caudal to the angle of the jaws and the occipital region of the skull (Fig. 3.2A-D). The cranial portion of the muscle covers the underlying pterygoid muscles and attaches aponeurotically to the angular and articular bones of the retroarticular process of a mandibular ramus (Fig. 3.2A and C). Its cranial border is formed by muscle fiber bundles that are transversely oriented and slightly curve cranially towards the midline, they interweave with the muscle fiber bundles of the caudal border of the *M.intermandibularis* (Fig. 3.2B and D). Laterally, the muscle fiber bundles of the two muscles are separated by a triangular area that is not covered by muscle [i.e., the *Trigonum intermandibulare posterius* (Schumacher 1973); Fig. 3.2D), where the epimysia of the *M. intermandibularis* and *M. constrictor colli gularis* are fused to the *Fascia superficialis* and dermis (see Fig. 2.2B), and which marks the boundary between the intermandibular and gular skin regions.

The caudal portion of the *M. constrictor colli gularis* envelops the neck caudal to the retroarticular process of the mandible. Its dorsal aponeurosis fuses with the deep lamina of the *Fascia superficialis* and anchors to the spinous processes of the rostralmost cervical vertebrae and the osteoderms.

  - ➢ Functional Interpretation

The *M. constrictor colli gularis* constricts the gular region and assists the *M. intermandibularis* in raising the hyoid apparatus into its resting position after having been depressed during deglutition. It has also been implicated in the emetic reflex in *Crocodylus*, which was described as "backwards inertial feeding" (Andrews 2000). The relatively short muscle fiber bundles in combination with a relatively long aponeurosis cannot and do not allow as much expansion as the long, obliquely oriented muscle fiber bundles of the *M. intermandibularis*, because they are already aligned in the direction of the stretching forces. Therefore, any expansion of the muscle is solely the result of passive lengthening of the muscle

122

fiber bundles and not of a reorientation relative to the body axes. The long collagenous aponeuroses significantly limit the expansion of the muscle as a whole.

- *Musculus constrictor colli cervicalis*
  - ➤ Morphological Description

The *M. constrictor colli cervicalis* is a muscle sheet with its associated aponeurosis and envelops the neck just cranial to the shoulder girdle (Fig. 3.2A-D). Dorsolaterally, its cranial border is separated from the caudal border of the *M. constrictor colli gularis* by a transversely elongated triangular area that is not covered by muscle [the *Trigonum cervicalis* (Dubansky & Homberger subm.; Fig. 3.2C), where the epimysia of the *M. constrictor colli gularis* and *M. constrictor colli cervicalis* are fused to the *Fascia superficialis* and dermis (Fig. 2.2B), and which marks the boundary between the gular and cervical skin regions.

Dorso-medially, the dorsal aponeurosis of the *M. constrictor colli cervicalis* fuses with the deep lamina of the *Fascia superficialis* and anchors to the osteoderms located cranially to the shoulder girdle (Fig. 3.2C). The ventral aponeurosis anchors to the midventral line of the neck (Fig. 3.2D). Hence, the *M. constrictor colli cervicalis* has only a relatively short muscular portion compared to two significant non-expandable collagenous aponeuroses.

  - ➤ Functional Interpretation

The *M. constrictor colli cervicalis* constricts the cervical region just in front of the shoulder girdle. The circumferentially oriented muscle fiber bundles cannot expand as much as the obliquely oriented muscle fibers of the *M. intermandibularis*, because they are already aligned in the direction of the stretching forces and are also much shorter. Therefore, any expansion of the muscle is solely the result of passive lengthening of the muscle fiber bundles, and not their reorientation relative to the body axes. The dorsal and ventral aponeuroses, which are comprised of non-extensible collagen fiber bundles, encircle the neck like a collar, thereby limiting circumferential expansion of the muscle.

3.4. Discussion

This study shows structural correlates between the skin expansibility of the skin and that of the *Fascia superficialis* and constrictor musculature. Hence, the hypothesis that these three

123

tissue layers form a mechanically coherent system that allows and restricts expansion of the different neck regions *in tandem* was confirmed.

3.4.1. The Intermandibular Region

Like the intermandibular skin region (see Chapter 2), the *Fascia superficialis* of the intermandibular region and the *M. intermandibularis* are both built to allow maximum expansion along the sagittal and transverse body axes. In addition to be being built for expansion, the deep lamina of the *Fascia superficialis* is specialized into a gliding surface to allow smooth movements between the layers during expansion of this region. A similar fascial layer has been described in the intermandibular region of rorqual baleen whales, which expand enormously to take in large volumes of water during feeding (Pivorunas 1979). Hence, all three layers of the intermandibular region of the intermandibulo-cervical envelope are expandable.

3.4.2. The Gular Region

The gular skin region (see Chapter 2) varies in the amount and direction of expansibility depending on the movement of underlying structures. The skin covering the pterygoid musculature is specialized to expand radially to accommodate the bulging pterygoid musculature. Therefore, it only needs to expand as the jaws are closed and the gular region is compressed. The collagen fiber bundles of the *Fascia superficialis*, which covers the pterygoid musculature and retroarticular process are oriented at cross-wise angles to one another. Therefore, they reorient themselves to accommodate the bulging musculature. The rest of the gular skin subregions are non-expandable circumferentially, but can lengthen sagittally. Likewise, the *Fascia superficialis* can lengthen sagittally by reorienting its collagen fiber bundles, but its circumferential expansibility is limited by the overlying skin. The muscular portion of the *M. constrictor colli gularis* covers the pterygoid musculature and can, therefore, expand to adjust to it when it contracts and bulges. However, this is not a circumferentially expandable muscle, because its dorsal half is formed by an extensive non-expandable collagenous aponeurosis. Hence, the expandable regions of the gular skin region correlate with the expandable regions of the *Fascia superficialis* and constrictor musculature, whereas the overall circumferential expansibility of the gular region is limited.

124

3.4.3. The Cervical Region

The cervical skin region (see Chapter 2) is expandable along the sagittal body axis. The collagen fiber bundles of the *Fascia superficialis* can change their angles relative to the transverse and sagittal body axes, but only in a way that allows expansion along the sagittal body axis. Because the collagen fiber bundles of the superficial lamina of the *Fascia superficialis* are oriented circumferentially around the neck, expansion in this direction will be met with resistance from this layer. Likewise, the *M. constrictor colli cervicalis* is aponeurotic ventrally and dorsally, and these collagen fiber bundles are also oriented circumferentially around the neck, limiting circumferential expansion. Hence, the sagittally expandable cervical skin correlates with the ability of the *Fascia superficialis* and *M. constrictor colli cervicalis* to expand sagittally; however, circumferential expansion is limited in all three layers.

3.5. Conclusion

The intermandibulo-cervical skin, *Fascia superficialis*, and constrictor musculature form a layered, structurally cohesive system of various tissues that surround and envelope the head and neck. All tissue layers are constructed in the intermandibular region to allow for maximum expansibility to manipulate large food items, while circumferential expansibility decreases in the gular region, and is extremely limited in the cervical region. These data support our findings that the intermandibulo-cervical integument limits circumferential expansibility of the neck and, therefore, constrains the size of the food bolus that can be swallowed.

3.6. References

Andrews, P.L.R., Axelsson, M., Franklin, C. & Holmgren, S. 2000. The emetic reflex in a reptile (*Crocodylus porosus*). The Journal of Experimental Biology 203: 1625-1632.

Brasseur, J.G., Nicosia, M.A. & Miller, L.S. 2007. Function of longitudinal vs. circular muscle fibers in esophageal peristalsis, deduced with mathematical modeling. World Journal of Gastroenterology 13(9): 1335-1346.

Chiasson, R.B. 1962. Laboratory Anatomy of the Alligator. WM. C. Brown Company Publishers, Dubuque.

Craig, A.S., Eikenberry, E.F. & Parry, D.A.D. 1987. Ultrastructural organization of the skin: Classification on the basis of mechanical role. Connective Tissue Research 16: 213-223.

125

Clark, C. & Logan, L.E. 1987. Copy Photography. Pp. 488-495 *in* The Guild Handbook of Scientific Illustration (Hodges, E.R.S., ed.). Van Nostrand Reinhold, New York.

Frolich, L.M. 1997. The role of the skin in the origin of amniotes: Permeability barrier, protective covering and mechanical support. Pp. 327-352 *in* Amniote Origins: Completing the Transition to Land (Sumida, S.S. & Martin, K.L.M., eds.). Academic Press, San Diego.

Homberger, D.G. & Walker, W.F. 2004. Vertebrate Dissection, 9th ed. Brooks Cole.

Lucas, A.M. & Stettenheim, P.R. 1972. Avian anatomy: Integument. Part II. Pp. 660-665 *in* Agricultural Handbook 362. United States Department of Agriculture, Washington, D.C.

Pivorunas, A. 1979. The feeding mechanisms of baleen whales. American Scientist 67: 432-440.

Poglayen-Neuwall, I. 1953. Undersuchungen der Kiefermuskulatur und deren Innervation an Krokodilen. Anatomischer Anzeiger 99(16/17): 257-276.

Rathke, H. 1866. Untersuchungen über die Entwickelung und den Körperbau der Krokodile. von Wittich, Wilhelm, eds

Reese, A.M. 1915. The Alligators and its Allies. G.P. Putnam's Sons, New York.

Richardson, K.C., Webb, G.J.W., & Manolis, S.C. 2002. Crocodiles: Inside Out. A Guide to the Crocodilians and their Functional Morphology. Surrey Beatty & Sons, Chipping Norton.

Schumacher, G.-H. 1973. The head muscles and hyolaryngeal skeleton of turtles and crocodilians. Pp. 101-199 *in* Biology of the Reptilia (Gans, C. & Parsons, T.S. eds.), Academic Press, London.

Sondhi, K.C. 1958. The hyoid and associated structures in some Indian reptiles. Annals of Zoology 2(11): 157-239.

Wainwright, S.A., Vosburgh, F., Hebrank, J.H. 1978. Shark skin: function in locomotion. Science 202:747-749.

Zweifel, F.W. 1961. The handbook of biological illustration, 2nd ed. The University of Chicago Press, Chicago. Pp. 28-37.

Chapter 4
Conclusions

4.1. Requirements for Swallowing Large Prey Items

Comparisons with ardeid birds (e.g., herons and egrets) and varanid reptiles (e.g., Komodo Dragons), both of whom are known to swallow prey items that are large relative to their head and neck size (Smith 1986; Pianka 1995; Homberger 1999; Schwenk 2000; Montuelle *et al.* 2009), illustrate three requirements for swallowing large food items, of which the alligator only meets one.

- **Gape (*Isthmus cranium*)**

Ardeid birds, varanid lizards, and crocodilians all have enlarged gapes, which allows them to acquire and orally manipulate large food items. Cranial kinesis in both ardeid birds (Bout & Zweers 2001; Metzger 2002) and varanid lizards (Metzger 2002; Moreno 2008) has been thought to increase gape for swallowing large prey items. This strategy works well for birds, which cannot crush or chew their food because of a lack of teeth (Homberger 1999), and varanids, which have a weak bite force (Moreno 2008). Hence, birds and varanid lizards widen the *Isthmus cranium* so that they can swallow their food whole. But a kinetic skull is not an option for crocodilians, which rely on a rigid akinetic skull to generate strong bite forces to capture large prey, to dismember them using the "death roll" (Fish 2007), to and crush bones and shells. Crocodilians have increased their gape by elongating their jaws. Combined with a highly expandable intermandibular skin region, crocodilians can accommodate relatively large prey items within their oral cavity.

- **Hyoid Suspensory Apparatus (*Isthmus faucium*)**

The width of the *Isthmus faucium*, which forms the entrance into the pharynx from the oral cavity, is formed by the underlying hyoid horns and their attachment to more distal structures in the head and neck (Homberger 1999; Homberger & Walker 2004). In mammals, the hyoid apparatus is suspended directly from the skull by a chain of bony ossicles or ligaments (Homberger 1999, Homberger & Walker 2004). Hence, the entrance to the pharynx is constrained by a rigid frame of bone or non-expandable ligaments. In ardeid birds (Cummins 1986; Homberger & Cummins 1986; Homberger 1999) and the Savannah Monitor (*Varanus exanthematicus*) (Smith 1986) the hyoid horns are built into the neck musculature, below the

128

level of the mandible. Hence, the hyoid apparatus can be moved passively as the throat musculature expands to widen the entrance to the pharynx when large food items are swallowed. Homberger (1999) has called this type of hyoid suspensory apparatus a "loose hyoid suspension", which differs from a "tight hyoid suspension" found in birds that swallow small food items (Homberger 1986; Homberger & Meyers 1989; Homberger 1999). Structural details of the hyoid suspensory apparatus are best known for the snowy egret (*Egretta thula*) (Cummins 1986; Cummins & Homberger 1986), the African Grey Parrot (*Psittacus erithacus*) (Homberger 1986), and domesticated chicken (Homberger & Meyers 1989). Smith (1986) describes how the tip of the cartilaginous ceratohyal in the Savannah Monitor (*Varanus exanthematicus*) lies in the cervical muscles caudal to the *M. depressor mandibulae*, but no further anatomical details are provided. Virtually nothing is known of the hyoid suspensory apparatus of crocodilians, but it can be assumed that, due to its specialized function for sealing the pharynx (Busbey 1989), the hyoid apparatus is probably not built into the throat musculature and, therefore, cannot be moved passively as it expands during feeding. It is, therefore, hypothesized here that the specialized hyoid apparatus in alligators acts as a constraint for food size and limits the expansion of the *Isthmus faucium*.

- **Thoracic Inlet (*Isthmus thoracis*)**

Photographs of skeletal material show that, when compared to head size, the thoracic inlet (i.e., the *Isthmus thoracis*), which is formed by the scapulocoracoid, coracoid and sternum, is proportionately wider in both ardeid birds and Komodo dragons than in crocodilians. In the alligator, the large head is much wider than the narrow *Isthmus thoracis*, indicating that although large food items can be acquired and manipulated within the oral cavity, they are unlikely to pass through the narrow thoracic inlet. Alligators are known to crush and dismember prey items before swallowing them (Fish 2007), and there is anecdotal evidence that crocodilians can regurgitate food items that are too big to swallow, while Andrews *et al.* (2000) has shown that crocodilians are able to vomit indigestible food residues.

4.2. Implications for Feeding in the Alligator

In order to allow large prey items to pass through the throat during deglutition, the intermandibulo-cervical integument must be circumferentially expandable. In the alligator, as

129

the anatomical data show, that the scale and interscale patterns vary regionally, and that this regionalization of scale and interscale skin morphology is functionally related to the amount and direction of expansibility in the different skin subregions. In addition, the underlying *Fascia superficialis* and constrictor musculature are constructed in a way to match the extent and direction of expansibility of each skin region so that the layers of the intermandibulo-cervical envelope can expand *in tandem*. The intermandibular region expands to allow the acquisition and manipulation of large prey items within the oral cavity but, unlike birds and other reptiles that can swallow large prey items relative to the size of their head and neck, the lack of circumferential expansibility of the cervical region necessitates that the large food items be broken down to a smaller size before swallowing. The functional significance is, that the cervical region of the intermandibulo-cervical envelope, with its non-circumferentially expandable skin, fascial laminae, and constrictor musculature acts as a safeguard to prevent the swallowing of food items that are too large to pass through the narrow thoracic inlet.

4.3. References

Andrews, P.L.R., Axelsson, M., Franklin, C. & Holmgren, S. 2000. The emetic reflex in a reptile (*Crocodylus porosus*). The Journal of Experimental Biology 203: 1625-1632.

Bout, R.G. & Zweers, G.A. 2001. The role of cranial kinesis in birds. Comparative Biochemistry and Physiology Part A 131: 197-205.

Busbey, A.B. III. 1989. Form and function of the feeding apparatus of *Alligator mississippiensis*. Journal of Morphology 202(1): 99-127.

Cummins, C.L. 1986. The morphology of the hyoid apparatus and gular region of the Snowy Egret, *Egretta thula* (Molina), (Aves: Ardeidae). M.S. Thesis, Louisiana State University A&M College, Baton Rouge.

Cummins, C.L. & Homberger, D.G. 1986. The morphology of the gular region of the Snowy Egret, *Egretta thula* (Molina). American Zoologist 26: 66A.

Fish, F.E. 2007. Death roll of the alligator: mechanics of twist feeding in water. The Journal of Experimental Biology 210: 2811-2818.

Homberger, D.G. 1986. The lingual apparatus of the African Grey Parrot, *Psittacus erithacus* Linné (Aves: Psittacidae): Description and theoretical mechanical analysis. Ornithological Monographs No. 39. The American Ornithologists' Union, Washing, D.C.

130

Homberger, D.G. & Meyers, R.A. 1989. Morphology of the lingual apparatus of the domestic chicken, *Gallus gallus*, with special attention to the structure of the fasciae. American Journal of Anatomy 186: 217-257.

Homberger, D.G. 1999. The avian tongue and larynx: Multiple functions in nutrition and vocalization. Pp. 94-113 *In*: Adams, N.J. & Slotow, R.H. (eds.), Proceedings of the 22nd International Ornithological Congress. University of Natal, Durban, South Africa. BirdLife, Johannesburg, South Africa.

Homberger, D.G. & Walker, W.F. 2004. Vertebrate Dissection, 9th ed. Brooks Cole, Belmont.

Metzger, K. 2002. Cranial kinesis in Lepidosaurs: Skulls in motion. Pp. 15-46 *In*: Aerts, P., D'Août, Herrel, A. & Van Damme, R. (Eds.). Topics in Functional and Ecological Vertebrate Morphology. Shaker Publishing, Maastricht.

Montuelle, S.J., Herrel, A., Schaerlaeken, V., Metzger, K.A., Mutuyeyezu, A. & Bels, V.L. 2009. Inertial feeding in the teiid lizard *Tupinambis merianae*: The effect of prey size on the movements of hyolingual apparatus and the cranio-cervical system. The Journal of Experimental Biology 212: 2501-2510.

Moreno, K., Wroe, S., Clausen, P., McHenry, C., D'Amore, D.C., Rayfield, E.J. & Cunningham, E. 2008. Cranial performance in the Komodo dragon (*Varanus komodensis*) as revealed by high-resolution 3-D finite element analysis. Journal of Anatomy 212: 736-746.

Pianka, E.R. 1995. Evolution of body size: Varanid lizards as a model system. The American Naturalist 146(3): 398-414.

Schwenk, K. 2000. Feeding in Lepidosaurs. Pp. 175-291 *in* Feeding (Schwenk, K., ed.). Academic Press, San Diego.

Smith, K.K. 1986. Morphology and function of the tongue and hyoid apparatus in *Varanus* (Varanidae, Lacertilia). Journal of Morphology 187: 261-287.

131

Appendix A
Weigert's Elastic Stain

Recipe, procedure and results modified from Romeis 1968. Van Gieson's counter stain was omitted in order to better show the contrast between the collagen fiber bundles and the elastic fiber bundles. Van Gieson's counter stain was only used to test for the presence of smooth dermal musculature.

Table A.1. Results

Tissue	Color
Elastic fibers	Black or dark purple
Collagen fibers	Red with Van Gieson's stain; Light-bluish purple without Van Gieson's stain
Nuclei	Gray or black
Other (i.e., muscle, living epidermis, etc.)	Yellow with Van Gieson's stain Light bluish-purple without Van Gieson's stain

Weigert's Resorcin-Fuchsin stain (Romeis 1968)

-Re-use after use; add 95% ethanol if needed to restore volume after multiple uses
-Store in a glass jar out of direct light; stable for 1 year

Table A.2 Weigert's Resorcin-Fuchsin stain recipe

Ingredients	Amount	Product Details
Basic fuchsin	2.0 g	Fisher Scientific Co., Fairlawn, NJ; Cat. No.: F98-10
Resorcinol	4.0 g	Mallinckrodt Chemical Works, St. Louis, MO; Cat. No.: 7236
Deionized water	200.0 mL	N/A
29% Ferric chloride	25.0 mL	Sigman Chemical Co., St. Louis, MO; Cat. No.: F-2877
95% Ethanol	200 mL	Pharmco-APPER, Brookfield, CT; Cat. No.: 11100090
Hydrochloric acid	4.0 mL	Fisher Scientific Co., Fairlawn, NJ; Cat. No. 7647-01-0
Acid Alcohol		
Hydrochloric acid	1.0 mL	See above
50% Ethanol	17.5 mL	See above (dilute from 95% ethanol)

Instructions for Weigert's Resorcin-Fushsin stain recipe (Romeis 1968)

- In a 500 ml beaker, mix basic fuchsin, resorcinol and deionized water and bring to a strong boil under a fume hood.
- Add 25.0 mL 29% ferric chloride.
- Stir and continue to boil for 2-5 minutes under a fume hood.
- Cool the solution to room temperature, and then filter it (Fisherbrand P8 Grade filter paper; Fisher Scientific, Co., Pittsburgh, PA; Cat. No.: 09-795-H).
- Discard the filtrate.
- Dry the precipitate and the filter paper (this can be done quickly in an oven at 250°C, or left to dry overnight at room temperature).
- Return the precipitate (with the filter paper) to a 500 mL beaker.
- Add 200 mL 95% ethanol.
- Heat slowly and carefully (<100°C; do not boil) under a fume hood, stirring constantly, until the precipitate dissolves.
- Remove the filter paper from the solution.
- Cool the solution to room temperature, then filter it.
- Restore the volume of the filtrate to 200 mL by adding 95% ethanol.
- Add 4.0 mL hydrochloric acid.
- Mix well in a glass container and let stand overnight at room temperature.

Weigert's Iron Hematoxylin (Romeis 1968)

-Stable for 1 week; for best results, mix and use immediately

-Filter before use if a precipitate forms

Table A.3. Weigert's Iron Hematoxylin stain recipe

Ingredients	Amount	Product Details
Stock solution A (stable for 1 year)		
Hematoxylin	5.0 g	Eastman Kodak Co., Rochester, NY; Cat. No.: P309A
95% Ethanol	500.0 mL	Pharmco-APPER, Brookfield, CT; Cat. No.: 11100090
Stock solution B (stable for 1 year)		
29% Ferric chloride	20.0 mL	Sigma Chemical Co., St. Louis, MO; Cat. No. F-2877
Deionized water	475.0 mL	N/A
Hydrochloric acid	5.0 mL	Fisher Scientific Co., Fairlawn, NJ; Cat. No. 7647-01-0
Working solution (stable for 1 week)		
Stock solution A	50%	
Stock solution B	50%	

Instructions for Weigert's Iron Hematoxylin stain recipe

- In a 500 mL beaker, add the ingredients for stock solution A and mix well; transfer to a glass container for storage at room temperature.
- In another 500 mL beaker add the ingredients for stock solution B and mix well; transfer to a glass container for storage at room temperature.
- For the working solution, mix equal parts of stock solution A and stock solution B; mix and use immediately for each staining session; discard after use.

Van Gieson's Stain (Romeis 1968)

-Stable for 1 month, but can be refreshed by adding a 3-4 drops of 1% acid fuchsin to the solution)

Table A.4. Van Gieson's stain recipe

Ingredients	Amount	Product Details
1% Acid fuchsin	1.0 mL	Sigma Chemical Co., St. Louis, MO; Cat. No.: F97-25
Picric acid, saturated	45.0 mL	Sigma Chemical Co., St. Louis, MO; Cat. No.: SP9200

Instructions for Van Gieson's stain recipe (see Table [Letter].4.):

- In a 50 mL beaker, mix 1% acid fuchsin and saturated picric acid.

- Transfer the solution to a glass container and let stand overnight at room temperature.

<u>Weigert's Resorcin-Fuchsin Staining Procedure (modified from Romeis to omit the Van Gieson's counter stain):</u>

- Deparaffinize sections in two changes of clearing agent (Histochoice®), then hydrate them to water or Posphate Buffered Saline (PBS) in a descending series of ethanol concentrations: 100% ethanol (2 changes), 95% ethanol (2 changes), 70% ethanol, 50% ethanol, Phosphate Buffered Saline (see Table [Letter].i.5.).

- Stain sections with Weigert's Iron Hematoxylin (working solution)…….15 minutes.

- Wash slides in tap water……………………………………………………….10 minutes.

- Rinse slides in deionized water (1-2 dips)

- Stain sections with Weigert's Resorcin-Fuchsin………………………..3-4 hours.
  - o Place slides in a glass dish with the stain and microwave (high power; 1100 watts) for 30 seconds; the glass container should be hot to the touch (not warm). Microwave at 10 second intervals to prevent the stain from bubbling over.
  - o Let slides stand in the stain at room temperature …………………..1.5-2 hours
  - o Repeat steps a and b.

- Rinse slides in running tap water.

- Rinse slides in 95% ethanol to remove any excess stain (3-5 dips in two changes).

- If the collagen fibers are stained too dark, use a few drops of acid alcohol (check under a dissection microscope to make sure that the stained collagen fibers do not obscure the stained elastic fibers).

- Rinse slides in running tap water.

- Rinse slides in deionized water (1-3 dips).

135

- Counter-stain sections with Van Gieson's stain ……..……………….5 minutes
  - (Counter-stain can be omitted—elastic fibers are much more prominent without this stain).
  - Rinse slides in deionized water (1-3 dips).
  - Rinse slides rapidly in 70% ethanol (1-2 quick dips).
- Dehydrate slides quickly to Histochoice® (from 70% ethanol if counterstained with Van Gieson's stain; from 95% if not counterstained with Van Gieson's stain).
- Coverslip with mounting medium (i.e., Polymount®).

Table A.5. Hydration/Dehydration using Tissue-Tek® slide staining set**

	Chemical and Concentration	Time	Product Details
Ascending/ Dehydration	Histochoice® (2 changes)	3 min each change	Fisher Scientific Co., Fairlawn, NJ; Cat. No.: H103-4L
	100% Ethanol (2 changes)	3 min each change	Pharmco-APPER, Brookfield, CT; Cat. No.: 111000100
	95% Ethanol (2 changes)	3 min each change	Dilute from 100%
	70% Ethanol	3 min	Dilute from 100%
	50% Ethanol	3 min	Dilute from 100%
Descending/ Hydration	Phosphate buffered saline	3 min	Fisher Scientific Co., Fairlawn, NJ; Cat. No. 7647-01-0
	Polymount® Mounting medium		Polysciences, Inc., Warrington, PA; Cat. No. 08381-120

**Tissue-Tek® slide staining set containing propylene solution wells deep enough for total immersions of 1x3''microscope slides; Electron Microscopy Sciences, Hatfield, PA; Cat. No. 62540-01

136

Appendix B
Harris Hematoxylin & Eosin Y Stain

Table B.1. Results

Tissue	Color
Elastic fibers	Orange-pink; refractile
Collagen fibers	Dark Pink
Nuclei	Blue
Other (i.e., muscle, living epidermis, etc.)	Light purple

Table B.2. Harris Hematoxylin & Eosin Y staining recipe

Stain	Product Details
Harris Modified Hematoxylin (ready to use)	Fischer Scientific Co., Fairlawn, NJ; Cat. No.: SH30-500D
Eosin Y Yellowish Solution (1% solution in water; ready to use)	Fischer Scientific Co., Fairlawn, NJ ; Cat. No.: SE23-500D

Harris Hematoxylin & Eosin Y staining procedure (Benjamin D. Dubansky, personal communication):

1. Deparaffinize sections in 2 changes of clearing agent (Histochoice®), then hydrate them to water or Phosphate-Buffered Saline (PBS) in a descending series of ethanol concentrations: 100% ethanol (2 changes), 95% ethanol (2 changes), 70% ethanol, 50% ethanol, Phosphate Buffered Saline (see Table [Letter].i.5).

2. Stain sections with Harris Modified Hematoxylin (or any hematoxylin)………45 seconds

3. Rinse slides in running tap water until Hematoxylin has turned blue and excess stain is removed from slide (i.e., only the specimen is stained and there is no residual hematoxylin on the slide).

4. Dehydrate sections in an ascending series of ethanol concentrations to 70% ethanol: PBS, 50% ethanol, 70% ethanol.

5. Stain sections with Eosin Y…………………………………………..……….2 minutes

137

6. Dip slides in 95% ethanol until only the sections contain the stain (i.e., remove excess Eosin from the slide), then finish the dehydration series to 100% ethanol: 95% ethanol (2 changes), and 100% ethanol (2 changes); 1 dip each.

7. Two changes in Histochoice® clearing agent

8. Coverslip with mounting medium (i.e., Polymount® Polysciences, Inc., Warrington, PA; Cat. No.: 08381-120)

Table C.1. Results

Tissue	Color
Collagen fibers	Bluish
Nuclei	Dark Blue
Lipids	Red

Table C.2. Oil Red-O stain recipe

Ingredients	Amount	Product Details
Oil Red O Stock Solution (Stable for 1 year)		
Oil Red O	0.5 g	Sigma-Aldrich, Inc., St. Louis, MO; Cat. No.: O0625-25G
70% Isopropanol	100.0 mL	Department store grade; Cumberland Swan, Smyrna, TN
Oil Red O Working Solution (Stable for 2 days)		
Stock Solution	30 mL	
Deionized water	20 mL	

Instructions for Oil Red O Stock solution recipe (Lucas & Stettenheim 1972):

- Dissolve Oil Red O stain in isopropanol on low heat.

Instructions for Oil Red O working stain recipe (Lucas & Stettenheim 1972):

- Dilute 30 mL of stock solution in 20 mL of deionized water
- Filter into a Coplin jar, cover immediately, and let stand at room temperature for 10 minutes.

Oil Red O staining procedure for frozen sections:

1. Cut sections on freezing microtome 8-10 μm thick.
2. Transfer sections to poly-L-lysine coated slides.

139

3. Allow sections to dry completely on the slide; a hotplate set to low heat can increase drying time.
4. Rinse sections with 70% isopropanol.
5. Stain with Oil Red O working solution for 15-20 minutes (longer staining time for thicker sections).
6. Rinse in 70% isopropanol until only the sections contain the stain (i.e., remove excess stain from the slide).
7. Rinse in deionized water.
8. 1 dip in Harris Modified Hematoxylin (counterstain optional).
9. Wash in running tap water until hematoxylin turns blue.
10. Rinse in deionized water.
11. Coverslip with aqueous mounting medium.

Vita

Brooke Hopkins Dubansky was born in Little Rock, Arkansas, in 1982, to Jess A. Hopkins and Kathy A. Tilmon Hopkins. She completed high school in Dardanelle, Arkansas, in May 2000. In August 2000 she came to Louisiana State University in Baton Rouge to study pre-veterinary medicine. She chose to major in biological sciences and began undergraduate research in anatomy under Dr. Dominique G. Homberger. Upon receiving her Bachelor of Science degree in August 2004, she decided to pursue a doctorate in biological sciences under the guidance of Dr. Homberger at LSU and a minor in veterinary anatomy under the guidance of Drs. Daniel J. Hillmann and Hermann H. Bragulla.